Fundamentals and applications of electrocatalytic oxidation of NADH at chemically modified electrodes

Persson, Björn

1990

Document Version:
Publisher's PDF, also known as Version of record

FUNDAMENTALS AND APPLICATIONS OF ELECTROCATALYTIC OXIDATION OF NADH AT CHEMICALLY MODIFIED ELECTRODES

BJÖRN PERSSON

LUND 1990

FUNDAMENTALS AND APPLICATIONS OF ELECTROCATALYTIC OXIDATION OF NADH AT CHEMICALLY MODIFIED ELECTRODES

by

BJÖRN PERSSON

Akademisk avhandling som med vederbörligt tillstånd av matematisk-naturvetenskapliga fakulteten i Lund för avläggande av filosofie doktorsexamen kommer att offentligen försvaras å Kemicentrum, Sölvegatan 39, hörsal F, fredagen den 8 juni 1990, kl. 10.15.

Organization LUND UNIVERSITY	Document name DOCTORAL DISSERTATION
	Date of issue June 1990
Department of Analytical Chemistry	CODEN: LUNKDL/(NKAK-1017)/1- 164(1990)
Author(s) Björn Persson	Sponsoring organization

Title and subtitle

Fundamentals and Applications of Electrocatalytic Oxidation of NADH at Chemically Modified Electrodes

Abstract

Derivatives of dialkylamino-benzophenoxazinium, -phenoxazinium, -phenothiazinium and -phenazinium compounds were further substituted by the addition of aromatics substituents. The new structures constituted the basis for preparation of chemically modified electrodes (CMEs) by adsorption on graphite. The electrochemical properties of the adsorbed compounds were studied with cyclic voltammetry. The mediator properties for the electrocatalytic oxidation of 1,4 dihydronicotinamide adenine dinucleotide (NADH) at the CMEs are presented. Kinetic investigations with a rotating disk electrode gave evidence for the formation of an intermediate charge transfer complex in the catalytic reaction at the modified electrode surface.

The behaviours of the CMEs as NADH sensors in flow systems showed improved properties compared with previously studied CMEs in terms of alkaline stability, decreased pH dependence of the response factor for NADH, and long term stability. A compact amperometric glucose sensor was constructed by chemical modification of carbon paste with glucose dehydrogenase, NAD^+, and a phenoxazine mediator. Increased stability and selectivity were obtained by further modification of the electrode surface by the deposition of a cation-exchange membrane.

The possibilities to use carbohydrates as fuel in energy production with a regenerative biofuel cell anode is demonstrated. A flow system of an anode halfcell, incorporating an enzyme reactor containing immobilized glucose dehydrogenase, utilizing NADH as the charge carrier between glucose and a rotating phenoxazine CME, is described. An additional study of the use of porous flow-through electrodes as anode material was made with emphasis on the adsorption characteristics of the phenoxazine mediator.

Key words

Classification system and/or index terms (if any)

Supplementary bibliographical information

Language
English

ISSN and key title

ISBN

Recipient's notes

Number of pages
164

Price

Security classification

Distribution by (name and address) Björn Persson, Department of Analytical Chemistry, University of Lund, P.O.Box 124, S-221 00 Lund, Sweden

Signature Björn Persson Date 1990-05-08

List of Papers

This thesis is based on the following papers, referred to in the text by their Roman numerals

I Catalytic Oxidation of Reduced Nicotinamide Coenzyme at Chemically Modified Electrodes Prepared with a New Phenoxazine Mediator
B. Persson, L. Gorton and G. Johansson
Proceed. 2nd Int. Meeting on Chem. Sens.,
Bordeaux, 1986, (6-20) 584

II Chemically Modified Electrodes for the Electrocatalytic Oxidation of NADH
L. Gorton, B. Persson, M. Polasek and G. Johansson
Proceed. ElectroFinnAnalysis Conference, 1988
Plenum Publ. Co., in press

III A Chemically Modified Graphite Electrode for Electrocatalytic Oxidation of Reduced Nicotinamide Adenine Dinucleotide based on a Phenothiazine Derivative, 3-ß-Naphthoyl-Toluidine Blue O
B. Persson
J. Electroanal. Chem., in press

IV A Comparative Study of Some 3,7-Diamino Derivatives of Phenoxazines and Related Compounds for Electrocatalytic Oxidation of NADH
B. Persson and L. Gorton
J. Electroanal. Chem., accepted

V An Amperometric Glucose Electrode Based on Carbon Paste, Chemically Modified with Glucose Dehydrogenase, Nicotinamide Adenine Dinucleotide and a Phenoxazine Mediator, Coated with a Poly(Ester-Sulfonic Acid) Cation-Exchanger
G. Bremle, B. Persson and L. Gorton
Electroanalysis, submitted

VI Biofuel Anode Based on D-Glucose Dehydrogenase, Nicotinamide Adenine Dinucleotide and a Modified Electrode.
B. Persson, L. Gorton, G. Johansson and A. Torstensson
Enzyme Microb. Technol. 7 (1985) 549

VII A Biofuel Anode for Cell Reactions Involving Nicotinamide Adenine Dinucleotide as a Charge Carrier
B. Persson, L. Gorton and G. Johansson
Bioelectrochem. Bioenerg. 16 (1986) 479

CONTENTS

1. INTRODUCTION

In biological systems, the class of enzymes denoted oxidoreductases [1] catalyze chemical redox reactions. All oxidoreductases depend on a redox compound, a cofactor, for activity, e.g. flavine nucleotides, protohemines, iron-sulphur clusters, or pyridine nucleotides. The cofactor is generally permanently bound to the enzyme but in the case of the pyridine nucleotide dependent dehydrogenases it acts as a soluble cosubstrate. The general reaction can be depicted

substrate + cofactor (ox) $\rightleftharpoons$ **product + cofactor (red)** (1)

The dehydrogenase subgroup of the oxidoreductases is of special interest because this group consists of a very large number of different enzymes. More than 400 have been described today. The enzymes are often substrate specific or group specific, and many of them are commercially available by the major chemical manufacturers [2]. These dehydrogenases generally depend on a nicotinamide cofactor for activity (Fig. 1), either NAD^+ or $NADP^+$, acting as the charge carrier in the enzymatic reaction

substrate + **$NAD(P)^+$** $\rightleftharpoons$ **product** + **$NAD(P)H + H^+$** (2)

Some of the enzymes are active with both NAD^+ or $NADP^+$, whereas others are specific for either of the cofactors.

The pyridine nucleotides per se are of fundamental importance in biological systems, where they play a central role in the energy transport, e.g. in the respiratory chain (NADH), and as a reductive source in the anabolism (NADPH) of the living cell. The general chemical aspects of the pyridine nucleotides have recently been thoroughly reviewed [3,4].

The inherent nature of the general reaction (1) i.e. an electron transfer, makes it natural to couple these enzymatic reactions to electrochemical methods. The transfer of the electron(s) from a substrate to an electrode (or the reverse) may then take place via electrochemical redox reactions of the cofactors or the cosubstrates. The utility of combining enzymes and electrochemical methods was predicted by Clark and Lyons [5] in electroanalysis by an enzyme electrode (biosensor), and by Shaw [6] in energy production by a biofuel cell anode, in the early 1960s.

For analytical purposes [*paper V*] reactions catalyzed by oxidoreductases have shown to be of great value [7-11]. There are many groups of analytes, e.g. carbohydrates and amino acids, that lack physical or chemical properties that make them easily and selectively detected by common analytical techniques. By the use of suitable dehydrogenase(s), the analysis of such analytes can be based on their indirect determination by the measurement of either the production or the consumption of $NAD(P)^+$ or NAD(P)H. From an electrochemical point of view, an inherent sensitivity exists by the participation of two electrons in the $NAD(P)^+$/NAD(P)H redox reaction (Fig. 1). The dehydrogenase reaction may also be applied in biosynthesis [4] and, as already stated, in energy production [*papers VI,VII*], where regeneration of the cofactor to improve the economy of the process is of utmost importance.

The use of electrochemical reduction or oxidation of the nicotinamide cofactors in the applications mentioned above is dependent on the occurrence of a smooth redox reaction at an electrode. For amperometric measurements an inherent sensitivity exists by the participation of two electrons in the $NAD(P)^+$/NAD(P)H redox reaction (Fig. 1). However, both the reduction and the oxidation of the pyridine dinucleotides occur at high overpotentials at conventional electrode materials also resulting in fouling of the electrodes (Ch. 2). Furthermore, the high overpotential opens up a system for additional unwanted redox reactions. The concept of chemically modified electrodes (CMEs) [12,13] is one way to circumvent these problems.

This thesis will focus on the electrocatalytic oxidation of NADH. What is presented is also generally valid if not in detail for NADPH [14]. Electrochemical studies of graphite electrodes, whose surfaces have been modified by adsorption of derivatives of phenoxazines [*papers I-IV*], a phenothiazine [*papers III-IV*], and a phenazine [*paper IV*], are presented. The properties of the derivatives, as mediators for the oxidation of NADH with a decreased overpotential, are demonstrated. The combination of a dehydrogenase and phenoxazine CMEs in the applications [*papers V,VI*], follows the general concept illustrated in Fig. 2.

All potentials refer to the saturated calomel electrode (SCE), unless otherwise stated.

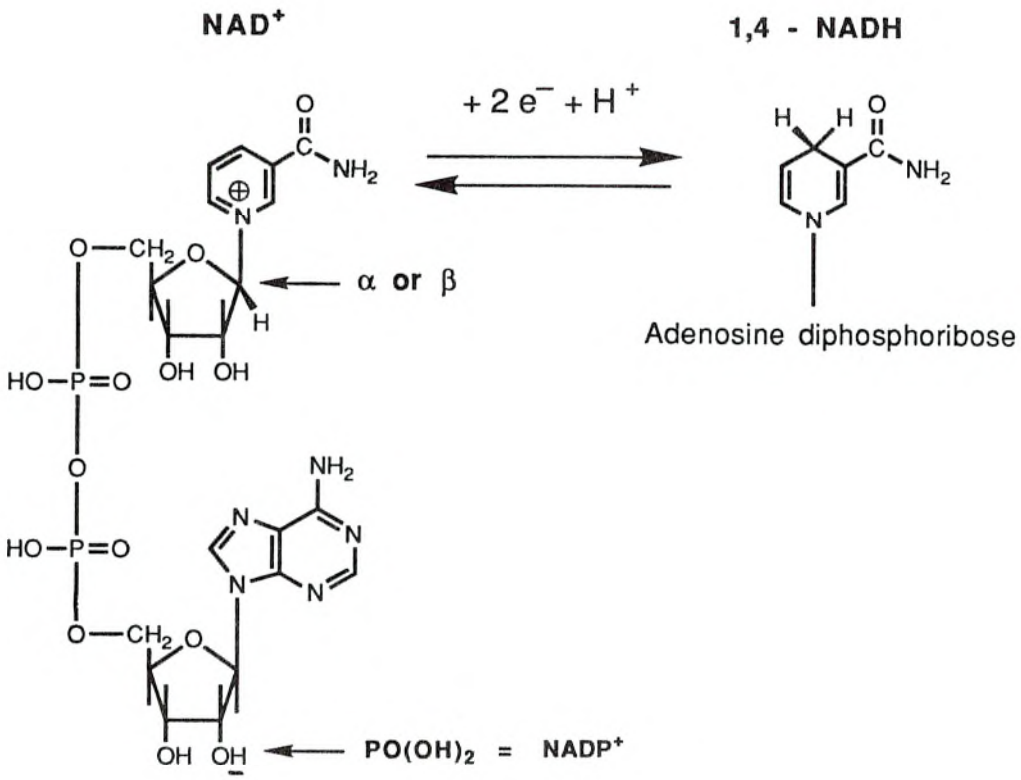

Fig. 1. *Structural formulae (β-form shown) and overall redox reaction of nicotinamide adenine dinucleotide, NAD^+, and its reduced form, the enzymatically active 1,4-NADH.*

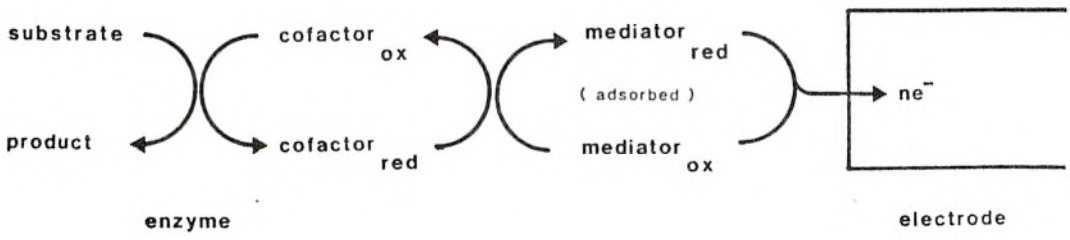

Fig. 2. *The reaction path of the electron transfer from the substrate to the electrode via the cofactor of the oxidoreductase and the mediator.*

2. ELECTROCHEMISTRY OF NAD^+ AND NADH

2.1 Introduction

A reaction catalysed by a dehydrogenase is reversible (eqn. 2) and involves the stereospecific net transfer of a hydride ion between the substrate and the C(4) of the pyridine ring of the coenzyme (Fig.1) and an exchange of a proton with the medium [1]. However, the exact mechanism of the reaction is not known. The central key role of the nicotinamide coenzymes in biological processes has encouraged numerous studies of the nonenzymatic redox behaviours of the NAD^+/NADH coenzymes and model compounds thereof. These studies have been made both in aqueous and organic solvents involving chemical, photochemical, and electrochemical redox reactions. The continued discussion will mainly focus on the electrochemical redox behaviours of NAD^+/NADH in aqueous solutions where neither the net oxidation of NADH to NAD^+ nor the net reduction of NAD^+ to NADH is electrochemically reversible.

2.2 Formal potential of NAD^+/NADH

The generally accepted formal potential, $E^{\circ\prime}$, of the redox couple NAD^+/NADH at pH 7.0 (25 °C) is -315 mV vs NHE (-560 mV vs SCE) [15]. From thermal data and the equilibrium constants of the ethanol/acetaldehyde and 2-propanol/acetone reactions catalyzed by alcohol dehydrogenase, Burton and Wilson calculated the value of -320 mV which was later recalculated to be -315 ± 5 mV vs NHE by Clark [15]. Through direct potentiometric titrations using several different mediators and xanthine oxidase as a catalyst, Rodkey [16,17] obtained an $E^{\circ\prime}$-value of -311 mV vs NHE (25 °C) and a temperature variation of the $E^{\circ\prime}$ of -1.31 mV/°C in the range of 20 to 40 °C. A variation of the $E^{\circ\prime}$ with pH of -30.3 mV/pH (30°C) was found, which is in good agreement with the theoretical value of -30.1 mV/pH.

2.3 Electrochemical reduction of NAD^+

The electrochemical reduction of NAD^+ in aqueous solutions is well documented including studies of the adsorption phenomena of products, intermediates, and NAD^+ itself on electrode surfaces [18-24]. Appropriate conditions had to be chosen to diminish the adsorption effects [18], ascribed to be mainly caused by the adenine moiety [20,21,23,25] of the species participating in the overall reduction of NAD^+. In an initial polarographic study by Kaye and Stonehill [26], the

reduction of NAD^+ at the mercury electrode was observed as a single wave, $E_{½} \approx$ -0.9 V, in neutral aqueous solution. Burnett and Underwood [18] resolved this single wave into two cathodic waves, a first one at $E_{½} \approx$ -1.1 V and a second one at $E_{½} \approx$ -1.7 V, by recording the polarogram in an alkaline buffer based on a tetra-alkylammonium salt, whereby adsorption of NAD^+ and related species were depressed.

The first wave corresponds to the addition of one electron to the nicotinamide ring to produce a radical. No dependence on pH of the reaction was observed above pH 5. The electron transfer appears reversible since the reoxidation of the produced radical can be observed by cyclic voltammetry at moderately fast scan rates [20,21]. The heterogeneous rate constant, k_s, of this reaction

$$NAD^+ + e^- \underset{}{\overset{k_s}{\rightleftharpoons}} NAD\cdot \qquad (3)$$

has been estimated to exceed 1 $cm \cdot s^{-1}$ and an $E^{o'}$ of -1.155 V at pH 9.1 (25°) was found for the $NAD^+/NAD\cdot$ couple [24]. The reversibility of eqn. (3) is virtual since it is coupled to a fast dimerization reaction

$$2\ NAD\cdot \xrightarrow{k_d} NAD_2 \qquad (4)$$

Different values of k_d have been given from electrochemical measurements, e.g., $3 \cdot 10^6$ [21], $8 \cdot 10^7$ [24], and $8 \cdot 10^6$ $(M\ s)^{-1}$ [27]. A value of $k_d = 8 \cdot 10^7$ $(M\ s)^{-1}$ [28] was obtained from pulse radiolysis and spectrophotometric measurements.

The dimer is not further reduced in the potential range down to -1.8 V (foot of the discharge current at mercury), but it can be oxidized to NAD^+ at a potential of $\approx$ -0.4 V [20]

$$NAD_2 \longrightarrow 2\ NAD^+ + 2\ e^- \qquad (5)$$

The formation of the dimer is not stereospecific [19,20,29]. Solutions of NAD^+, electrolyzed at -1.1 V with a mercury electrode produced a dimer mixture in 90% yield consisting of two sets of stereoisomers, 4,4'-dimers (90%) and 4,6'-dimers (10%), where each set consisted of three different stereoisomers [29]. The relative abundance of the dimers was independent of pH (7-10) and no 6,6'-dimers could be traced. When solutions of NAD^+ were reduced at -1.8 V i.e at the limiting current plateau of the second wave, the result was the formation of

1,4-NADH (50-60%), 1,6-NADH (15-30%), and dimers (10-20%) [20,29]. The obtained amount of 1,4-NADH increased when pH was decreased from 10 to 7 [29].

The reduction at the second polarographic wave, resulting in the formation of NADH from NAD^+ by the net transfer of two electrons and a proton, is not so well understood. This wave shows a slight pH dependence and is not observed in aprotic media [20]. The free radical, initially produced in the first wave is a very weak base and is not protonated at pH 0.4 [30]. However, the character of the proton donors (HX), e.g. water or ammonium ions, present in the solution seems to have an influence on the ease of the continued reduction to NADH and the following reaction sequence at the second wave has been suggested [22]

$$NAD\cdot + HX \rightleftharpoons [NAD\cdot\text{-}H\text{-}X] \xrightarrow{-e^-} [NADH\text{-}X^-] \xrightarrow{-X^-} NADH \quad (6)$$

2.4 Electrochemical oxidation of NADH

Studies of the electrochemical oxidation of NADH have been made using cyclic voltammetry (CV), potential step chronoamperometry, constant electrode potential coulometry, and the rotating disk electrode (RDE) methodology [31], usually with carbon electrodes, glassy carbon (GC) and pyrolytic graphite (PG) [32-42], but also with platinum (Pt) electrodes [34,37,39,41,43-47]. It was also recognized, as in the case of the reduction of NAD^+, that the electrochemical reaction results in electrode fouling, necessitating careful pretreatment and conditioning of the electrodes to obtain reproducible results between runs [33,37,43,47]. At both carbon and Pt electrodes adsorption of NAD^+ and possibly other unknown species occur at positive potentials [32-34,36-38,47], with indications of desorption of NAD^+ from GC electrodes at a potential of 0 V [36].

A poorly defined oxidation wave of NADH at a Pt electrode around 1 V was observed in an initial study by Burnett and Underwood [18], reflecting the large overvoltage of the electrochemical NADH oxidation. The electrode material has a significant effect on the overvoltage. The oxidation of NADH in aqueous solutions, seen as a single peak in CV, takes place at potentials of $\approx$ 0.4 , $\approx$ 0.7 and $\approx$ 1 V at carbon, platinum and gold electrodes, respectively [33,41]. CV often gives values of n close to the expected value of 2 (Fig. 1), while lower values

of n are usually found in coulometric studies [34]. In a continued coulometric study of the investigations of Coughlin et al. [45], Jaegfeldt et al. [46] found a recovery of 99.3% enzymatically active NAD^+, using low concentrations of the cofactor, a pretreated fast rotating platinum-gauze to minimize adsorption, and correcting for the decomposition of the coenzyme in solution.

An ECE mechanism for the electrochemical oxidation of NADH has been proposed in several studies [22,39,42,43,47-49]

$$\mathrm{NADH} \xrightarrow{-e^-} \mathrm{NADH}^{+\cdot} \rightleftharpoons \mathrm{NAD}\cdot \overset{-e^-}{\rightleftharpoons} \mathrm{NAD}^+ \qquad (7)$$

However, different views of the rate of the individual steps in the reaction mechanism as well as influences of concurrent reactions have been discussed.

Blaedel and Haas [43], oxidized NADH model compounds in acetonitrile and observed two main oxidation steps in the absence of a base clearly demonstrating the stepwise oxidation of NADH. When oxidizing NADH in aqueous solutions, no re-reduction of intermediates was observed in CV at fast sweeps (30 V/s) [34] indicating a high chemical irreversibility of the reaction. A potential variation (E_p or $E_{½}$) with pH for the overall electrochemical NADH oxidation of -30 mV/pH may be expected (Fig.1), but has not been observed. Various results have been reported such as, -17 [33], -11 [34], +35 mV/pH [44] and no pH dependence at all [48].

Kinetic studies of the electrochemical oxidation of NADH were presented by Moiroux and Elving [39], and by Jaegfeldt [47], almost simultaneously. Jaegfeldt reported the involvement of a second-order pH dependent reaction. Moiroux and Elving determined the rate constant of the second step in eqn.(7) to be 60 s^{-1} at NAD^+ covered GC electrodes, assuming the rate to be initially comparable with the overall rate limiting first step. All authors suggested the possibility of a dimerisation of NAD· radicals, followed by formation of NAD^+ from the oxidation of the dimers (eqn. (5)), and an extension of eqn.(7) by also taking the disproportionation reaction into account

$$\mathrm{NADH}^{+\cdot} + \mathrm{NAD}\cdot \rightleftharpoons \mathrm{NADH} + \mathrm{NAD}^+ \qquad (8)$$

Blankespoor and Miller [42] later reexamined the results and demonstrated that NAD^+ is an inhibitor of the oxidation process, and

that the oxidation is first order in NADH in the presence of a large excess of NAD^+. Investigations by pulse radiolysis [50] indicated a deprotonation rate of the second step greater than 10^6 s^{-1}. A chemical one-electron oxidation of NADH by ferrocenium salts in buffered aqueous propanol [51,52] gave an estimated value of the formal potential for the $NADH^{+}$/NADH couple of 0.81 V. Although reaction (8) is highly energetically favourable ($E^{o'}$ NAD^+/NAD· = -1.16 V), Blankespoor and Miller referred to studies by Amatore and Savéant [53], who used relatively comparable parameters in a theoretical treatment of a concurrent ECE and disproportionation mechanism, suggesting that more than 95% of the product is formed through the ECE pathway.

In light of an initial rate limiting electron transfer and knowledge of the formal potential of the produced cation radical, its fast deprotonation rate [50,52] and its estimated high acidity, $pK_a \approx -4$ [54], a pH dependence of the oxidation of NADH should not be observed. Thus the reaction paths suggested by Elving et al. [39,40] assuming an ECE mechanism may be supplemented, see Fig. 3.

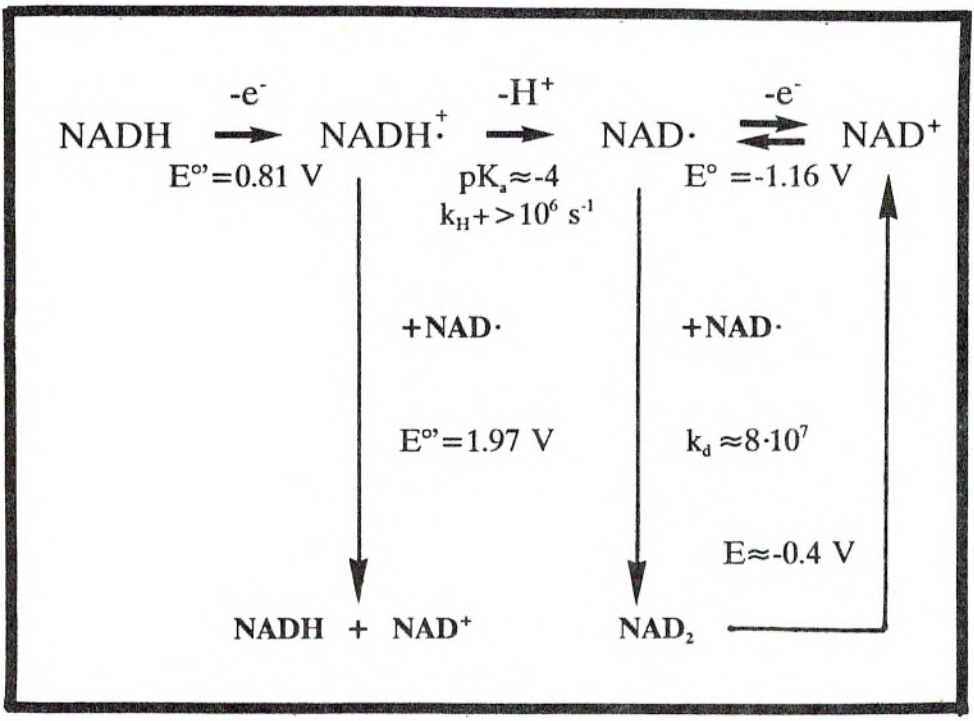

Fig. 3. Summary of the reaction paths for the electrochemical oxidation of NADH.

3. CHEMICALLY MODIFIED ELECTRODES (CMEs).

3.1 Introduction

Adsorption and precipitation at electrode surfaces affecting the potential, the current response or the available electrode area, were for a long time considered only as drawbacks in electrochemistry. In the mid-1970s, this view was changed by the deliberate immobilization of chemicals to the electrode surface with the intention that the electrode should not only reflect the properties of the conventional material used, but also those of the immobilized species. Such devices which were denoted chemically modified electrodes (CMEs) [55], have proven to benefit enhanced selectivity and sensitivity in electrochemistry. Lane and Hubbard [56] were among the first to study the redox properties of structures strongly adsorbed on electrodes, and since then, the topic of CMEs has continued to attract a high level of interest and activity reflected by the large number of published papers [57,58,59].

Some of the benefitial properties that may be obtained by electrode modification are listed below;

- electrocatalysis (mediated/promoted electron transfer) [60,61]
- selective molecular recognition (biosensors) [10]
- selective preconcentration [62]
  (by ion-exchange, complexation or covalent reactions)
- separation via permselectivity through membrane barriers [62]
  (occlusion and exclusion based on charge or size)
- electroreleasing properties [63]
- chromic properties [64]
- photogalvanic properties [65]
- combinations of the aspects mentioned above

3.2 Classification and preparation of CMEs

From the point of view of the transducer, CMEs can be divided into two groups, composite and surface modified electrodes. The composite modified electrode constitutes a solid combination of transducer and modifier exemplified by carbon paste electrodes [66, *paper V*] or pellets of conducting radical salts [67]. Surface modified electrodes either of the mono- or the multi-layer type, are obtained by immobilizing the modifier on the surface through covalent bonding, adsorption, dispersion, or polymer deposition. Most CMEs are based on the deliberate immobilization of an electrochemically active compound as a modifier. An intimate contact between the transducer and the modifier at the electrode surface usually favours a rapid electron transfer between the redox active compounds within the layer and the electrode. Surface modified electrodes, discussed below, are by far the most studied group [12,68,69]

Covalent immobilization - A linkage between the modifier and the electrode is introduced by producing functionalities such as hydroxylic groups from oxides on metal electrodes and carboxylic and ketonic groups on carbon electrodes by exposing the surface to strong acids, heat, plasma etching, or anodic oxidation. After the introduction of e.g. acid chlorides or organosilanes the modifier can be anchored to the surface, usually with an amide bond. The initially introduced oxygen functionalities can themselves be considered modifiers.

Adsorption - CMEs are rapidly and easily prepared by dipcoating. The success of a stable immobilization is based on the solubility of the modifiers in solution and the modifiers' tendency to adhere to the electrode surface. Carbon electrodes are especially effective when the modifier consists of a large aromatic system resulting in an extended π-bond interaction [*papers I-IV,VI,VII*].

Dispersion [70] - This type of modification refers to (metal) particle deposition onto the surface by, e.g. polishing [71] or vacuum sputtering [72].

Polymer deposition - Polymer deposition is obtained by applying preformed polymers on the electrode surface followed by evaporation of the solvent, by spin or dip coating, or bonding via covalent linking agents. Polymerization of monomers resulting in precipitation of the polymer on the electrode surface can take place through plasma discharge, or through chemical or electrochemical polymerization. The

redox active modifier may be part of the monomer or be entrapped in the polymer matrix. The polymer itself may be conducting or non-conducting. Polymers consisting of the equivalent of several thousands of monolayers are easily prepared while the other methods usually give active coverages from one to a few monolayers.

Three broad categories can be distinguished among the polymeric films, *electronically* (π-conjugated) *conducting*, *redox*, and *ion-exchange* polymers [73]. Electronically conducting polymers, e.g. polypyrrole [74], may be partially oxidized or reduced electrochemically. The charge transport in either configuration occurs in a metal like fashion. A conducting state can also be made by reductive or oxidative doping with chemical agents. Redox polymers, e.g polyvinylferrocene [75], conduct current by electron self-exchange reactions between neighbouring redox sites. Ion-exchange polymers, e.g. a protonated polyvinylpyridine film exchanging counterions for the redox active compounds [76], conduct current both by self-exchange reactions and ion diffusion. However, in the case of multilayer polymers, the control of the overall rate of the charge transfer is complex and involves contributions by the flow of solvent and reagents, the motion of redox centers, the rate of the redox reactions, and the diffusion of counterions to maintain electroneutrality within the polymeric layer [77]. Theoretical models of the electrochemistry of extended polymer films have been given where the contributions of the propagation of charge within the film are treated as diffusive processes [78,79,80].

The CMEs can also be divided into different types depending on the size and the configuration of the electrodes. Some examples are modified microelectrodes with diameters in the μm range [81] and transistors (CHEMFETs) [82]. Configurations such as array, sandwich and bilayer have also been described [73].

3.3 Electrochemistry of CMEs.

Surface analysis of electrodes modified with redox compounds is most commonly employed by different spectroscopic and electrochemical techniques [12,68,83]. Cyclic voltammetry in particular, offers a rapid picture of the surface state of an immobilized redox compound [12,31]. This subject will briefly be treated here with reference to CMEs based on adsorption of the modifier, and with coverages of less than or of only a few monolayers.

A theoretical treatment of the ideal case, obeying a Langmuir adsorption isotherm, has been given [84]. Adsorption and electrochemical reactions are assumed to be at equilibrium, all adsorption sites are considered equal, and no interactions between the asorbed species take place. Theory then predicts a variation of the anodic and cathodic peak currents, $i_{p,a}$ and $i_{p,c}$, with the sweep rate, v, according to the equation given in Fig. 4, a peak potential separation, ΔE_p, of zero, a peak width at half maximum, E_{FWHM}, of 90.6/n mV (25°C), and a formal potential of the adsorbed species given by

$$E^{o'}(ads) = E^{o} - \frac{RT}{nF} \ln(\frac{b_{ox}}{b_{red}}) \qquad (9)$$

where E° is the standard potential of the redox reaction in solution, and b_{ox} and b_{red} are the adsorption coefficients of the oxidized and the reduced form, respectively. Deviations from the ideal case are most common. This has been ascribed to interactions between the adsorbed molecules (ox-ox, ox-red, and red-red) giving broader and lower voltammetric waves for repulsive interactions and the opposite for attractive interactions [85]. Adsorption at different sites resulting in a spectrum of E°' values [86] or different activity coefficients varying with the surface coverage [87] have also been considered as reasons for these observations. Gerischer and Scherson [88] treated the deviations from the ideal case as a contribution from a surface potential, considering the modifiers as dipoles. A single parameter, γ, proportional to the difference between the effective dipole length of the reduced and oxidized species, then gives a modification of the Nernst equation with n replaced by $(n+\gamma)$. This will affect e.g. the value of E_{FWHM} and i_p , see equation given in Fig. 4, but not the determination of the surface coverage of the modifier.

A great deal of information can be obtained about an adsorbed redox compound from a single cyclic voltammogram. The electrochemical reversibility is reflected by the experimental values of ΔE_p, E_{FWHM}, $i_{p,a}$ and $i_{p,c}$. Kinetic limitations in the overall charge transfer reaction are indicated when an increased sweep rate results in a decrease in the peak current to sweep rate ratio, or an increase in the potential parameters. The formal potential of the adsorbed redox active compound is given by the average of the anodic and the cathodic peak potential. From the area under a peak, which is proportional to the amount of transferred charge, Q, The apparent surface coverage, Γ, can be determined from the area under a peak which is proportional to the

amount of transferred charge Q. The number of electrons, n, participating in the redox reaction and the electrode area, A, has to be known. A chemical reversibility of the redox reaction is suggested when the area under the anodic and the cathodic peaks are of equal magnitude with no appearance of new peaks in the voltammogram. Multiple scans easily demonstrate the stability of the adsorbed layer through the constancy of Γ.

The parameters i_p, E_p, ΔE_p, and E_{FWHM} may also be affected by factors such as coupled chemical reactions and rearrangements of the species on the electrode surface. The variation of the three first parameters with the sweep rate allows a semiqualitative determination of the rate of the redox reactions and of any coupled chemical reaction. Additional information such as the participation of protons in the redox reaction may also be obtained from a variation of E°' with pH of the contacting solution.

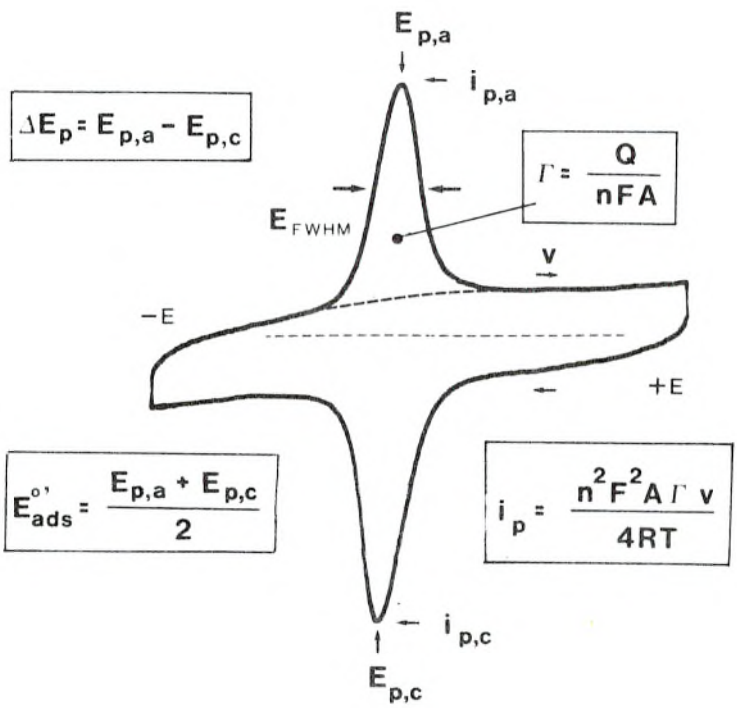

Fig. 4. *A cyclic voltammogram of a redox modified electrode also showing the characteristic parameters that can be obtained and studied with cyclic voltammtery.*

3.4 Electrocatalysis at CMEs.

Electron transfer (ET) between a redox compound and an electrode, although thermodynamically feasible, may be obstructed by a large kinetic barrier (overpotential) or steric hindrances. Only in a few cases a direct ET between the bound cofactor of an oxidoreductase and an electrode has been reported, e.g. [89-93]. Promoted electrocatalysis between bound cofactors and an electrode may be obtained by the immobilization on the electrode surface of compounds that facilitate a direct ET by diminishing the steric hindrances [61]. Mediated electrocatalysis, see Fig. 2, takes place by the use of a low molecular weight redox mediator acting as an electron shuttle between a compound in solution and the electrode [77]. Mediated electrocatalysis may overcome both steric hindrances and a large overpotential. The potential at which the mediated ET occurs between the substrate and the electrode will mainly be dictated by the E°' of the mediator.

The simplest case of mediated electrocatalysis at a surface modified electrode is when the current is limited only by the mass transport of a redox compound to the surface and/or the reaction rate between the compound and the mediator at the surface. The potential at which an anodic catalytic peak appears in CV, provided that the reaction rate is not too low, is then described by [13,94]

$$E_p = E^{o'} + \frac{RT}{nF}\left[0.78+\ln\left(\frac{D^{1/2}}{k_{obs}\Gamma}\right)+\ln\left(\frac{nFv}{RT}\right)\right]^{1/2} \qquad (10)$$

where D is the diffusion coefficient, ($cm^2\ s^{-1}$), of the compound in solution, and k_{obs} is the second order overall rate constant, $(M{\cdot}s)^{-1}$, of the reaction between the compound and the modifier at the surface. The difference in the peak potentials of the direct and the mediated electrochemical reactions is a measure of the decrease in the overpotential.

4. ELECTROCATALYTIC OXIDATION OF NADH AT CMEs

4.1 Introductory remarks

Electrocatalytic reduction of NAD^+ has rendered success than electrocatalytic oxidation of NADH, mostly due to the problem of dimer formation. However, mediated electrocatalysis has been reported using rhodium-bipyridyl complexes [95], and one-electron donors like

viologens with diaphorase as a catalyst for the donor-NAD^+ reaction [96,97].

It has been suggested that a contribution of mediated ET probably takes place at "unmodified" conventional electrode materials by the involvement of surface oxygen functionalities [41]. At carbon electrodes in particular, many different oxygen functionalities are easily introduced and observed [98]. Oxidative treatments of carbon surfaces [99-104], as the initial treatment for covalent immobilization of modifiers (Ch. 3.2), result in an improved oxidation of NADH with a decrease in the overpotential of a few 100 mV. Mediated catalysis by the introduction of quinone groups on the surface is believed to be the reason for this.

4.2 Claims on the CME

A CME for electrocatalytic oxidation of NADH must more or less fulfil the criteria listed below to make it more useful than an unmodified electrode as an amperometric sensor or an anode in a biofuel cell.

1. A decrease in the overpotential is essential.

2. Fast reactions and charge transfers
   a) between the immobilized mediator and the electrode.
   b) within the mediator layer.
   c) between the mediator and the contacting electrolyte, e.g. when acid-base reactions or counter-ion exchange take place in the mediator redox reaction.
   d) between the mediator and NADH in solution.

3. Stability
   a) irreversible immobilization of the mediator.
   b) chemical stability of the modifier against e.g. hydrolysis, light decomposition.
   c) electrochemical stability at every possible redox state i.e. no radical reactions leading to side products.
   d) in the presence of NADH, NAD^+ or intermediates i.e no side reactions should take place.

4. pH independent working potential, reaction rate and stability.

5. A selective electrocatalysis.

The demand on the size of the decrease in overvoltage is related to the intended use of the CME with emphasis on the working potential. For amperometric detection of NADH an optimum working potential range is around 0 mV where the background current at carbon electrodes changes signs and is therefore low. To obtain mainly the oxidized catalytic form of the mediator (Fig. 2) by an applied potential, E_{app}, of 0 mV, the E°' of the mediator must be lower than 0 mV. At a potential of 0 mV, several interfering compounds common in biological fluids, such as ascorbic acid, uric acid, bilirubin, neurotransmitters, oxygen etc., also subjected to large overpotentials [105], may give no or only a small contribution to the recorded response [13]. Thus the working potential in combination with a discriminating electrocatalysis are means to obtain an increased selectivity.

The same arguments should also hold true in regenerative biosynthesis whereas for a biofuel cell anode the E°' of the mediator should be as negative as possible since a high power output is related to the potential difference between the anode and the cathode. The use of a CME based on a mediator having a low formal potential (E°'=-360 mV at pH 7) as an anode in a biofuel cell is illustrated in Fig. 5 [106].

An $E_{app} >> E°'$ of the mediator ensures a rapid electrochemical reaction between the immobilized modifier and the electrode, and the overall rate of the chemical reaction between NADH and the modifier may be rate limiting. The latter reaction will then dictate the detection limit, the sensitivity and the linear range when using the CME as an NADH sensor [*paper III*], or the current output when using the CME as an anode in a biofuel cell [*papers VI,VII*]. However, investigations have shown that the E°' of quinoid type mediators and the overall reaction rate with NADH are strongly interconnected (Ch. 4.4) and therefore the structural elements of the mediators are of greatest importance.

4.3 Electrocatalytic structures

The use of mediators as "depolarization catalysts" [107] goes back to the beginning of this century. The electrocatalytic oxidation of NADH at electrodes intentionally modified is a concept that has been studied for a decade only [108]. Compilations [15,109-111] of mediators dissolved in aqueous solutions and used in electrochemical studies of biological compounds give guidelines of the great number of possible structures that may constitute the basis for the construction of CMEs for bioelectrocatalysis.

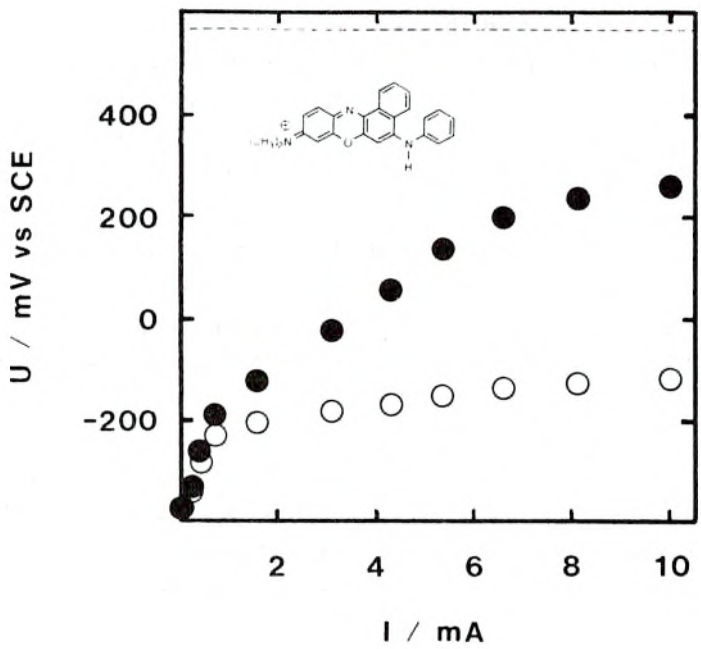

Fig. 5. *Loading characteristics of an anode halfcell showing the potential, U, at the front (●) and back (○) of the anode versus the current output, I. The experimental set-up was the same as in paper VII. The graphite felt anode was modified by adsorption of 3-anilino Meldola Blue. The anolyte was 0.64 mM NADH in 0.25 M phosphate buffer (pH 7.0) and the flow rate 3.8 ml·min^{-1}. A constant current of 3.7 mA was found for flow rates higher than 3 ml·min^{-1}in the range of 1.5 to 9 ml·min^{-1} with a load of 400 Ω. The conversion of NADH to NAD$^+$ was 18 % at a current output of 1.55 mA. (---) the potential of the simulated oxygen electrode ,+560 mV vs SCE.*

Redox compounds whose redox reactions involve two electrons and at least one proton, should be the most favourable mediators for electrocatalytic oxidation of NADH. A reaction path of a fast inner sphere hydride transfer [112] is then possible, at least theoretically. Quinones and paraphenylenediimines belong to this class of compounds some of which are known to react rapidly with NADH in aqueous solutions. Miller et al. [113,114] observed that the ortho compounds reacted faster than their corresponding para analogues and also that a charged (N,N-dimethyl) phenylenediimine was the most efficient structure among those studied.

CMEs for electrocatalytic oxidation of NADH are presented in Table 1. CMEs based on quinones can be made rather stable by themselves but their lifetimes are limited in the presence of NADH [108,115,116]. It has been suggested that the cause for the limited lifetime of such CMEs is a side-reaction between a semiquinone and an NAD· radical, intermediates in the reaction, resulting in a blocking of the electrode surface [120]. In the redox reaction of the phenylenediimines a liability of the intermediates to react with water is included, resulting in the formation of quinones [137]. Increased chemical and electrochemical stabilities are obtained by the incorporation of the basic phenylenediimine structure into a larger aromatic skeleton exemplified by the dye Meldola Blue in Table 1 (formula and ring numbering in *paper III*, p. 2).

CMEs based on Meldola Blue [14] showed promising properties for electrocatalytic oxidation of NADH at a low potential. This mediator exhibits a good chemical stability in neutral or acid solutions, and to the exposure to visible light in contrast to some other mediators, e.g. N-methylphenazine (NMP^+) [125].

CMEs with improved properties based on adsorption of mediators onto graphite electrodes can be made by derivatization of commercially available dyes similar to Meldola Blue in structure [127, *papers I-IV*]. Blocking of positions of the mediators subjected to nucleofile attack (positions 3 and 7) with a proper functionality, and a simultaneous extension of the number of aromatic rings of the mediator can give improved properties such as

i) alkaline stability of the mediator

ii) faster reaction rate with NADH

iii) increased adsorption strength resulting in a more pronounced irreversible immobilization of the mediator

The reported practical lifetime of such CMEs as sensors is increased from 1 day [138] (Meldola Blue) to 1-2 weeks [139] (3-ß-naphthoyl Nile Blue).

CMEs with catalytic properties for NADH oxidation can also be made from organic radical salts based on complexes of the radical anion tetracyanoquinodimethane $(TCNQ)^{\cdot -}$ with e.g tetra-thiafulvalinium (TTF^+) or NMP^+ [130,131,134]. CMEs of the aqueous insoluble radical

TABLE 1. Chemically modified electrodes for electrocatalytic oxidation of NADH

Mediator group	immobilization	$E^{o'}$ pH 7/ mV vs SCE	ref.
oxidized carbon		0 to +200	[100,101,103, 104]
orthoquinone	covalent	+170	[108]
orthoquinone	covalent	+170	[115]
orthoquinone	polymer	+160*	[116]
orthoquinone	polymer	+170	[117]
orthoquinone	polymer	+170	[118]
orthoquinone	adsorbed	+170	[119]
orthoquinone	adsorbed	+100	[120]
1,2-naphthoquinone	mixed with carbon	-150	[121]
chloranil	mixed with carbon	+ 50	[122]
mercaptoquinone	polymer		[123]
phenylenediimines	mixed with carbon	+100	[124]
N-methylphenazinium (NMP^+)	adsorbed	-160	[125,126]
N-ethylphenazinium	adsorbed	-210	[125]
Meldola Blue	adsorbed	-175	[14]
3-anilino-Meldola Blue	adsorbed	-360	[*paper IV*]
3-α-pyrenylidene-Nile Blue A	adsorbed	-190	[*paper I*]
bis(3,3-Nile Blue A)-terephthoyl	adsorbed	-220	[*paper II*]
3-ß-naphthoyl-Nile Blue A	adsorbed	-220	[127, *paper IV*]
3-ß-naphthoyl-Brilliant Cresyl Blue	adsorbed adsorbed	-180	[*paper IV*]
1,2-benzophenoxazine-7-one	adsorbed	-210	[128]
3-ß-naphthoyl-Toluidine Blue O	covalent	-135	[*papers III,IV*]
FAD		+200	[129]
NMP^+TCNQ (conducting radical salt)			[130,131,132]
TTF^+TCNQ			[133,134]
ferrocene and immobilized diaphorase	electrodeposited		[135]
$NaNiFe(III)(CN)_6$			[136]

*pH 6.35

salts can be prepared from pellets of the salt or by mixing the salt with a polymeric binder, e.g. PVC. NMP^+ is a well known catalyst for NADH oxidation [125] both in solution and as a modifier of electrodes. However, $TCNQ^-$ alone also oxidizes NADH in aqueous solutions with a decrease in the reaction rate with an increase in pH [140]. Kulys has suggested the cation to be the main catalytic component [133]. NMP-TCNQ CMEs are electrochemically stable in a potential range of -0.1 to +0.3 V, and throughout this range NADH is oxidized. A desorption of the outer crystal layer will expose a new fresh layer, and this can easily be made intentionally by applying a potential outside the stable potential range [131]. The rate of the electrocatalytic oxidation of NADH at these CMEs appears to be sufficient for practical uses as amperometric biosensors [132,133,141]. However, the catalytic nature of these radical salts does not seem to be selective for NADH oxidation, indicated by the electrochemical responses observed for ascorbic acid, uric acid and 6-mercaptopurine at TTF- and NMP-TCNQ CMEs [134].

4.4 Mechanisms of the catalytic NADH oxidation

4.4.1 In solution

Studies of the oxidation of NADH in aqueous solutions with phenazines, phenoxazines, or phenothiazines are scarce [142,143] while corresponding studies with quinones have rendered more attraction [113,114,144-146]. The Marcus theory [147] is commonly used to interpret the reaction mechanism of the NADH oxidation. The redox reaction of a quinone can be given as [105]

$$Q \overset{+e^-}{\rightleftharpoons} Q^{\cdot-} \overset{+H^+}{\rightleftharpoons} QH\cdot \overset{+e^-}{\rightleftharpoons} QH^- \overset{+H^+}{\rightleftharpoons} QH_2 \qquad (11)$$

Carlson and Miller [144] made studies in aqueous buffers and found two linear free energy relationships of the reaction rate between NADH and the hydroquinone anion, QH^-, one for the para and one for the ortho quinones, respectively. A single hydride transfer as the reaction mechanism was suggested from the following observations; the reaction was found to be of first order in concentration of NADH and of first order in concentration of quinone, no pH effect on the reaction rate was found in the pH range between 6 and 8, a deuterium isotope effect was observed, and by a comparison of the energetics and the rates obtained for one-electron transfer reactions using different ferrocenium salts [52]. However, in this study [52] and in an additional study [145]

of an NADH analogue in aqueous propanol, it was stated that a stepwise charge transfer within a complex could not be excluded. This was earlier proposed by Tanaka and co-workers [146] who studied the oxidation of dihydropyridine compounds in organic solvents with quinones, as well as with other oxidants, both one-electron and known hydride acceptors [148]. The formation of charge transfer complexes was observed and an electron-proton-electron mechanism within a complex was suggested. Other authors have given their support for a single hydride transfer as the mechanism for the NADH oxidation (see references in [148]). The reaction mechanism between NADH and quinoid structures is thus still an open question and much debated.

4.4.2 At CMEs based on phenoxazines and phenothiazines

The fundamental electrochemical and catalytic properties of CMEs based on phenoxazines are summarized in *paper II*. The reaction rate between an adsorbed phenoxazine derivative and NADH is largely a function of the E°'-value of the mediator. Two linear free energy relationships of the overall reaction rate between NADH and seven different adsorbed phenoxazine mediators at pH 7.0 have preliminary been indicated [13]. Any direct structural correlation between the two lines was not noted. For mediators derivatised with larger aromatic substituents in position 3, a general trend of an increased reaction rate with an increase in the E°'-value of the mediator is observed. However, an efficient reaction rate will cease at too low an E°'-value of the mediator.

Over a wide pH range, the acid-base properties of the mediator will influence the thermodynamic driving force of the catalytic reaction. The structural change caused by the acid-base reaction can influence both the intrinsic catalytic activity and the stability of the mediator [*paper IV*]. A constant thermodynamic driving force of the catalytic reaction at various pHs demands a variation of the E°' with pH of the mediator equal to that of the NAD^+/NADH couple, i.e. 30 mV/pH. Even when this condition is fulfilled, a pH dependence of the overall reaction rate has been observed [13].

Strong indications of the formation of charge transfer complexes, (CT), between mediators, M, and NADH have been found from electrochemical measurements [13,14,128, *papers III,IV*] and recently with a spectroelectrochemical investigation [149]. The reaction mechanism has been described analogous to Michaelis-Menten kinetics

$$NADH + M_{ox} \underset{k_{-1}}{\overset{k_{+1}}{\rightleftharpoons}} (CT) \xrightarrow{k_{+2}} NAD^+ + M_{red} \qquad (12)$$

where the reoxidation of the mediator is considered fast at $E_{app} >> E°'$, and the second step rate limiting [14]. The overall rate seen as the reoxidation of the mediator including the overall rate constant, k_{obs}, has been given as

$$d\Gamma/dt = k_{obs}\, \Gamma\, [NADH] \qquad (13)$$

with

$$k_{obs} = k_{+2} / (K_M + [NADH]) \qquad (14)$$

and with

$$K_M = (k_{-1} + k_{+2}) / k_{+1} \qquad (15)$$

At a constant pH, a low surface coverage, and a surplus of NADH at the electrode surface, this approximative model offers the advantage of a simple two parameter characterization, k_{+2} and K_M, of the mediator-NADH reaction.

The catalytic reaction eqn. (12), can be treated in terms of concentrations by the adoption of a reaction layer concept (thickness $\approx$ monolayer). If the free concentrations are used by correcting both the [NADH] and [M] for the [CT], then a steady state treatment (true at the RDE) gives

$$d[CT]/dt = k_{+1}\, ([M]-[CT])([NADH]-[CT]) - (k_{-1}+k_{+2})\, [CT] = 0 \qquad (16)$$

In the evaluation of eqn. (16) the $[CT]^2$ term can be neglected if the [CT] is small compared with the [NADH] and the [M]. With only the second step in eqn. (12) being rate limiting, it can be shown that [150]

$$k'_{obs} = k_{+2} / (K_M + [M] + [NADH]) \qquad (17)$$

A variation of k_{obs} with the surface coverage of the mediator [*paper IV*] can thus be explained if both the [M] and the [NADH] at the surface vary with the amount of charge transfer complex formed.

The mechanism given by eqn. (12) is not fully valid for all values of [NADH] and [M]. Deviations from this approximative model by use of eqn. (14) have been observed at low concentrations of NADH [*papers I, III, IV*]. The studies in this thesis cannot consistently account for these observations. A relatively large K_M-value may be a reason for a deviation at low NADH concentrations. The nature of the electrode surface may also have an influence. It has been observed that surface reactions at a smooth surface obeying a rate equation equivalent to eqn. (13) may at a nonuniform surface show a variation of the reaction rate with the square root of the right side in eqn. (13) [150]. Furthermore, a contribution of a direct electrochemical oxidation of the formed CT complex may also be a part of the overall mechanism. In a study of Nile Blue A ($E^{\circ\prime}$= -420 mV at pH 7) adsorbed on GC electrodes, an $E_p(CT) \approx 0$ mV at pH 7 was observed [149].

The orientation of the mediators on and their interaction with the electrode surface are subjects where much is unknown. Raman spectra of oxidized Nile Blue A adsorbed on a GC electrode indicated a change from an edgewise orientation at acid pHs to a flat orientation at more alkaline pHs [149]. A slightly folded configuration of an unsubstituted 10H-phenoxazine (reduced state) in solution has been suggested where the two outer rings to some extent are facing each other [151]. Although the oxidized form of a mediator is generally more water soluble than its reduced counterpart, a decrease in the $E^{\circ\prime}$-value of the mediator is observed when the state is changed from soluble to adsorbed (c.f eqn. (9)). A stronger interaction with the graphite surface for the oxidized rather than for the reduced form is thus suggested through a more extended planar configuration and a higher aromaticity [*paper IV*]. A speculative question is whether the adsorption of the mediators and the rate of the electrocatalysis are more efficient at the edge or the basal plane of the graphite.

4.5 Sensitivity and selectivity of NADH oxidation

The direct oxidation of NADH at unmodified electrodes has been used in a number of biosensor applications [152-154]. At low NADH concentrations the effect of electrode fouling is less noticeable [33]. By in situ laser treatment of a carbon surface between runs, reproducible responses for the direct oxidation of NADH have been reported [155]. Detection of NADH can also be based on the reduction of acid hydrolysed NADH at a mercury electrode, as demonstrated by Osteryoung et al. [156,157]. Square-wave voltammetry and a four-electron reduction gave a detection limit of less than 7 nM.

However, analysis of complex mixtures based on a direct oxidation or reduction of NADH calls for measures of precaution to avoid interfering redox reactions.

In a recent study of the direct oxidation of NADH at different carbon materials, it was concluded that spectrographic graphite (Ringsdorff, GFR) was a most favourable material [158]. At this material, the mediators studied in this thesis exhibit the strongest adsorption compared with e.g. at coal, GC or PG. The porosity of the material and the preparation of the electrodes by polishing on fine emery paper give an enhanced microsurface, see Fig. 6. An enhanced porous surface compared with a smooth surface is believed to be advantageous when using the CME as a sensor, giving a larger number of available mediator molecules for high surface coverages, and thereby an improved sensitivity. However, the enlarged surface may also cause the observed variation of the catalytic properties between otherwise equally prepared CMEs [*papers III, IV*]. With a phenothiazine CME used as an amperometric sensor in flow analysis, a detection limit of 0.2 μM NADH was found [*paper III*].

Appelqvist et al. [138] investigated the response for some possible interfering compounds in biological matrices such as ascorbic acid, catechol, and uric acid at a Meldola Blue ($E^{\circ\prime}$= -145 mV at pH 6) modified graphite electrode at pH 6. With the CME mounted in an amperometric flow-through detector of the wall-jet type and with an applied potential of +50 mV, only ascorbic acid interferred. The oxidation of ascorbic acid started already at -50 mV, both at the CME and at a naked electrode. Thus, although the mediator may selectively oxidize NADH electrocatalytically, the electrode material itself can prevent a selective detection. By the use of membrane exclusion of interfering compounds, an increased selectivity can be obtained [*paper V*]. Sample clean-up is another possible strategy. Selective analysis of carbohydrates in complex matrices based on amperometric detection with a phenoxazine CME in combination with sample clean-up, chromatographic separation, and enzyme reactors has been demonstrated by Marko-Varga et al. [159].

a

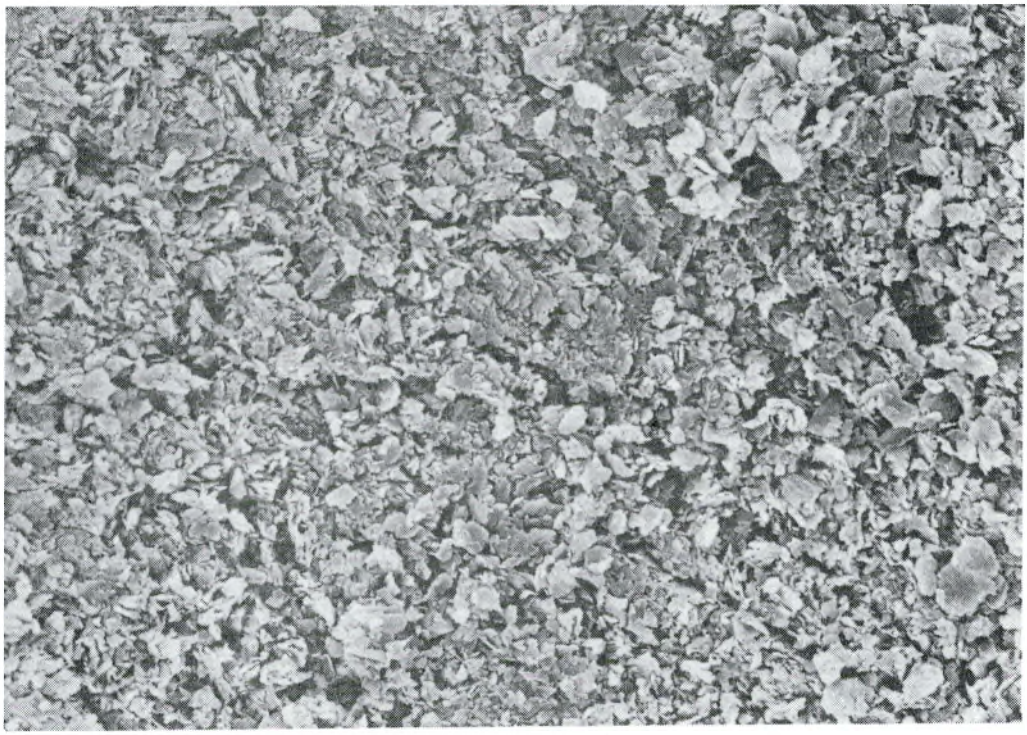

b

Fig. 6. *Scanning electron microscopy pictures showing the surface of a graphite electrode polished on fine emery paper. Magnifications (a) x500 and (b) x1500.*

5. CONCLUSIONS AND PERSPECTIVES

Adsorption of the mediating structures onto graphite, offers a simple and rapid technique to prepare CMEs for electrocatalytic oxidation of NADH. 3,7-diamino-derivatives of phenoxazines and phenothiazines, are mediating structures that give an efficient electrocatalytic oxidation of NADH with a large decrease in the overpotential. The formal potential of the mediators can be given a desirable value by proper derivatization of the basic phenoxazine or phenothiazine structures, a way to obtain suitable mediators for different purposes. Indications of a selective electrocatalysis have been observed, and this may be a consequence of a fastidious choice of these structures for NADH as counterpart in a charge transfer complex, preceding a mediated catalysis.

The usefulness of the CMEs in combination with enzymes for bioanalytical purposes, has been well documented at this laboratory [160, 161, 162]. For enzyme electrode preparations two main advantages may be obtained by modification of a carbon paste with the dehydrogenase, NAD^+, and a mediator; the close coupling of the enzymatic and the mediated reactions in the paste can drive infavourable equilibria of enzymatic reactions to the product side, and the cofactor does not have to be added to the analytical set-up thereby making it less expensive. The usefulness and possibilities of the CMEs as anodes in biofuel cells have been demonstrated in this thesis.

So far, the electrode materials used have been restricted to a few different kinds of graphite. The choice of electrode material has mainly been dictated by the adsorption properties of the mediators. Further improvements may be obtained by the preparation of phenoxazine or phenothiazine CMEs based on polymeric films. An increased stability of the layer of the modifier and a longer practical lifetime of the CMEs may thereby be achieved. Polymer deposition of the mediators may also make other types of electrode materials available.

ACKNOWLEDGEMENT

I want to express my gratitude to Professor Gillis Johansson for introducing me in the field of electrochemistry, for his continuous support and valuable discussions. I also want to express my sincere thanks to Dr. Lo Gorton for his devoted encouragement and support in my work, and for a stimulating and friendly cooperation. Special thanks are given to friends and colleagues within my group, Dr. György Marko-Varga, Dr.Elena Domínguez, Gunilla Pettersson, Jenny Emnéus and Elisabeth Csöregi for their interest in my work and much fun. I also want to express my gratitude to all my friends and collegues at the department of Analytical Chemistry, both present and former, for creating a friendly and stimulating atmosphere. A special thank is given to Dr. Roger Appelqvist for the recreational possibilities at the department. In addition I am very grateful to Annica Bergkvist for all help given during my time at the department. Special thanks are also given to my co-authors Dr. Arne Torstensson, Dr. Miroslav Polasek, and Gudrun Bremle for a fruitful cooperation. I also want to express my sincere thanks to Hannele, to whom I am indebted for great domestic support during the time of this thesis work.

Financial support from the Swedish Natural Research Council, the Swedish Board for Technical Development and the National Energy Administration is gratefully acknowledged. Permission by Butterworth Publishers, Elsevier Scientific Publishing Company, and Plenum Publishing Corporation to reproduce the papers being accepted for publication or originally appearing in Bioelectrochemistry an Bioenergetics, Enzyme and Microbial Technology, Journals of Electroanalytical Chemistry, and the Book of Proceedings of ElectroFinnAnalysis Conference, is gratefully acknowledged.

REFERENCES

1 *The Enzymes*, Vol. XII and XIII, P. D. Boyer (Ed.), Academic Press, New York, 1975-76.

2 *Biochemicals Organic Compounds for Research and Diagnostic Reagents*, Sigma Chemical Co., St. Louis, 1990.

3 D. Dolphin, R. Poulson and O. Avramovic' (Eds.), *Coenzymes and Cofactors*, Vol. II, John Wiley & Sons, New York, 1987.

4 H. C. Chenault and M. Whitesides, *Appl. Biochem. Biotechnol.*, 14 (1987) 147.

5 L. C. Clark, Jr. and C. Lyons, *Ann. N.Y. Acad. Sci.*, 102 (1962) 29.

6 M. Shaw, *Biochemical Fuel Cells*, Part 1., Proc. 17th Annual Power Sources Conf., 1963, pp. 53-56.

7 P. W. Carr and L. D. Bowers, *Immobilized Enzymes in Analytical and Clinical Chemistry*, John Wiley & Sons, New York, 1980.

8 G. G. Guilbault, *Analytical Uses of Immobilized Enzymes*, Marcel Dekker, New York, 1984.

9 F. W. Scheller, F. Schubert, R. Renneberg, H.-G. Müller, M. Jänchen and H. Weise, *Biosensors*, 1 (1985) 135.

10 A. P. F. Turner, I. Karube and G. S. Wilson (Eds.), *Biosensors, Fundamentals and Applications*, Oxford University Press, New York, 1987.

11 P. N. Bartlett and R. G. Whitaker, *Biosensors*, 3 (1987/88) 359.

12 R. W. Murray, in A. J. Bard (Ed.), *Electroanalytical Chemistry*, Vol. 13, Marcel Dekker, New York, 1984, pp. 191-368.

13 L. Gorton, *J. Chem. Soc., Faraday Trans.*, 1, 82 (1986) 1245.

14 L. Gorton, A. Torstensson, H. Jaegfeldt and G. Johansson, *J. Electroanal. Chem.*, 161 (1984) 103.

15 W. M. Clark, *Oxidation-Reduction Potentials of Organic Systems*, William and Wilkins, Baltimore, 1960.

16 F. L. Rodkey, *J. Biol. Chem.*, 213 (1955) 777.

17 F. L. Rodkey, *J. Biol. Chem.*, 234 (1959) 188.

18 J. N. Burnett and A. L. Underwood, *Biochem.*, 4 (1965) 2060.

19 A. L. Underwood and J. N. Burnett, in A. J. Bard (Ed.), *Electroanalytical Chemistry*, Vol. 6., Marcel Dekker, New York, 1973.

20 P. J. Elving, C. O. Schmakel and K. S. V. Santhanam, *Crit. Rev. Anal. Chem.*, 6 (1976) 1.

21 W. T. Bresnahan and P. J. Elving, *J. Am. Chem. Soc.*, 103 (1981) 2379.

22 P. J. Elving, W. T. Bresnahan, J. Moiroux and Z. Samec, *Bioelectrochem. Bioenerg.*, 9 (1982) 365.

23 M. A. Jensen, W. T. Bresnahan and P. J. Elving, *Bioelectrochem. Bioenerg.*, 11 (1983) 299.

24 M. A. Jensen and P. J. Elving, *Biochim. Biophys. Acta*, 764 (1984) 310.

25 J. Moiroux and S. Deycard, *J. Electroanal. Chem.*, 194 (1985) 99.

26 R. C. Kaye and H. I. Stonehill, *J. Chem. Soc.*, 56 (1952) 3244.

27 A. J. Cunningham and A. L. Underwood, *Biochem.*, 6 (1967) 266.

28 B. H. J. Bielski and P. C. Chan, *J. Am. Chem. Soc.*, 102 (1980) 1713.

29 H. Jaegfeldt, *Bioelectrochem. Bioenerg.*, 8 (1981) 355.

30 E. M. Kosower, A. Teuerstein, H. D. Burrows and A. J. Swallow, *J. Am. Chem. Soc.*, 100 (1978) 5185.

31 A. J. Bard and L. R. Faulkner, *Electrochemical Methods, Fundamentals and Applications*, Wiley & Sons, New York, 1980.

32 W. J. Blaedel and R. A. Jenkins, *Anal. Chem.*, 46 (1974) 1952.

33 W. J. Blaedel and R. A. Jenkins, *Anal. Chem.*, 47 (1975) 1337.

34 R. D. Braun, K. S. V. Santhanam and P. J. Elving, *J. Am. Chem. Soc.*, 97 (1975) 2591.

35 M. A. Jensen and P. J. Elving, *Bioelectrochem. Bioenerg.*, 5 (1978) 526.

36 J. Moiroux and P. J. Elving, *Anal. Chem.*, 50 (1978) 1056.

37 J. Moiroux and P. J. Elving, *Anal. Chem.*, 51 (1979) 346.

38 J. Moiroux and P. J. Elving, *J. Electroanal. Chem.*, 102 (1979) 93.

39 J. Moiroux and P. J. Elving, *J. Am. Chem. Soc.*, 102 (1980) 6533.

40 P. J. Elving, W.T. Bresnahan, J. Moiroiux and Z. Samec, *Bioelectrochem. Bioenerg.*, 9 (1982) 365.

41 Z. Samec and P. J. Elving, *J. Electroanal. Chem.*, 144 (1983) 217.

42 R. L. Blankespoor and L. L. Miller, *J. Electroanal. Chem.*, 171 (1984) 231.

43 W. J. Blaedel and R. G. Haas, *Anal. Chem.*, 42 (1070) 918.

44 M. Aizawa, R. W. Coughlin and M. Charles, *Biochim. Biophys. Acta*, 385 (1975) 362.

45 R. W. Coughlin, M. Aizawa, B. F. Alexander and M. Charles, *Biotechnol. Bioeng.*, 17 (1975) 515.

46 H. Jaegfeldt, A. Torstensson and G. Johansson, *Anal. Chim. Acta*, 97 (1978) 221.

47 H. Jaegfeldt, *J. Electroanal. Chem.*, 110 (1980) 295.

48 P. Leduc and D. Thevénot, *Bioelectrochem. Bioenerg.*, 1 (1974) 96.

49 J. Ludvik and J. Volke, *Anal. Chim. Acta*, 209 (1988) 69.

50 J. Grodkowski, P. Neta, B. W. Carlson and L. Miller, *J. Phys. Chem.*, 87 (1983) 3135.

51 B. W. Carlson and L. L. Miller, *J. Am. Chem. Soc.*, 105 (1983) 7453.

52 B. W. Carlson, L. L. Miller, P. Neta and J. Grodkowski, *J. Am. Chem. Soc.*, 106 (1984) 7233.

53 C. Amatore and J.-M. Savéant, *J. Electroanal. Chem.*, 123 (1981) 189.

54 F. M. Martens and J. W. Verhoeven, *Recl. Trav. Chim. Pays-Bas*, 100 (1981) 228.

55 P. R. Moses, L. Wier and R. W. Murray, *Anal. Chem.*, 47 (1975) 1882.

56 R. F. Lane and A. T. Hubbard, *J. Phys. Chem.*, 77 (1973) 1401.

57 M. D. Ryan and G. S. Wilson, *Anal. Chem.*, 54 (1982) 20R.

58 D. C. Johnson, M. D. Ryan and G. S. Wilson, *Anal. Chem.*, 58 (1986) 33R.

59 D. C. Johnson, M. D. Ryan and G. S. Wilson, *Anal. Chem.*, 60 (1988) 147R.

60 R. W. Murray, A. G. Ewing and R. A. Durst, *Anal. Chem.*, 59 (1987) 379A.

61 J.E. Frew and H. A. O. Hill, *Phil. Trans. R. Soc. Lond.*, B316 (1987) 95.

62 S. Dong and Y. Wang, *Electroanalysis*, 1 (1989) 99.

63 L. L. Miller, A. N. K. Lau and E. K. Miller, *J. Am. Chem. Soc.*, 104 (1982) 5242.

64 C. M. Elliott and J. G. Redepenning, *J. Electroanal. Chem.*, 197 (1986) 219.

65 W. R. Bowen, *Acta Chem. Scand.* A 34(6) (1980) 437.

66 G. Dryhurst and D. L. McAllister, in P. T. Kissinger and W. R. Heineman (Eds.), *Laboratory Techniques in Electroanalytical Chemistry*, Marcel Dekker, New York, 1984, pp. 294-301.

67 C. D. Jaeger and A. J. Bard, *J. Am. Chem. Soc.*, 102 (1980) 5435.

68 W. J. Albery and A. R. Hillman, *Ann. Rep. Prog. Chem.*, Vol. 78, 1981, Sec. C. Phys. Chem., R. Soc. Chem., pp. 377-437.

69 G. G. Wallace, in T. E. Edmonds (Ed.), *Chemical Sensors*, Blackie & Sons, Glasgow, 1988, pp. 132-154.

70 L. R. Faulkner, *Chem. Eng. News*, 62(9) (1984) 28.

71 J. Zak and T. Kuwana, *J. Electroanal. Chem.*, 150 (1983) 645.

72 L. Gorton, *Anal. Chim. Acta*, 178 (1985) 247.

73 C. E. D. Chidsey and R. W. Murray, *Science*, 231 (1986) 25.

74 A. Diaz, *Chem. Scr.*, 17 (1981) 145.

75 A. Merz and A. J. Bard, *J. Am. Chem. Soc.*, 100 (1978) 3223.

76 N. Oyama and F. C. Anson, *J. Electrochem. Soc.*, 127 (1980) 247.

77 R. A. Durst, *Anal. Chem. Symp. Ser.*, 22 (1985) 115.

78 W. J. Albery and A. R. Hillman, *J. Electroanal. Chem.*, 170 (1984) 27.

79 C. P. Andrieux, J. M. Dumas-Bouchiat and J. M. Savéant, *J. Electroanal. Chem.*, 169 (1984) 9.

80 C. P. Andrieux and J. M. Savéant, *J. Electroanal. Chem.*, 171 (1984) 65.

81 A. G. Ewing, B. J. Feldman and R. W. Murray, *J. Electroanal. Chem.*, 172 (1984) 145.

82 A. J. Sibbald, *Molecular Electronics*, 2 (1986) 51.

83 R. J. Gale (Ed.), *Spectroelectrochemistry, Theory and Practice*, Plenum Press, New York, 1988.

84 E. Laviron, in A. J. Bard (Ed.), *Electroanalytical Chemistry*, Vol. 12, Marcel Dekker, New York, 1982, 53-157.

85 E. Laviron, *J. Electroanal. Chem.*, 52 (1974) 355.

86 W. J. Albery, M. G. Boutelle, P. J. Colby and A. R. Hillman, *J. Electroanal. Chem.*, 133 (1982) 135.

87 A. P. Brown and F. C. Anson, *Anal. Chem.*, 49 (1977) 1589.

88 H. Gerischer and Scherson, *J. Electroanal. Chem.*, 188 (1985) 33.

89 F. Scheller, G. Strnad, B. Neumann, M. Kühn and W. Ostrowski, *Bioelectrochem. Bioenerg.*, 6 (1979) 117.

90 R. M. Ianiello, T. J. Lindsay and A. M. Yachynych, *Anal Chem.*, 54 (1982) 1098.

91 R. M. Ianiello, T. J. Lindsay and A. M. Yachynych, *Anal. Chim. Acta*, 141 (1982) 23.

92 R. M. Paddock and E. F. Bowden, *J. Electroanal. Chem.*, 260 (1989) 487.

93 G. Jönsson and L. Gorton, *Electroanalysis*, 1 (1989) 465.

94 C. Andrieux and J. M. Savéant, *J. Electroanal. Chem.*, 93 (1978) 163.

95 R. Ruppert, S. Herrman and E. Steckhan, *Tetrahedron Lett.*, 28 (1987) 6583.

96 T. Matsue, H.-C. Chang, I. Uchida and T. Osa, *Tetrahedron Lett.*, 29 (1988) 1551.

97 H.-C. Chang, T. Matsue, I. Uchida and T. Osa, *Chem. Lett.*, (1989) 1119.

98 K. Kinoshita, *Carbon. Electrochemical and Physicochemical Properties*, John Wiley & Sons, New York, 1988

99 J. F. Evans and T. Kuwana, *Anal. Chem.*, 49 (1977) 1635.

100 N. Čenas, J. Rozgite, A. Pocius and J. Kulys, *J. Electroanal. Chem.*, 154 (1983) 121.

101 L. Falat and H.-Y. Cheng, *J. Electroanal. Chem.*, 157 (1983) 393.

102 J. Scheurs, J. van den Berg, A. Wonders and E. Barendrecht, *Recl. Trav. Chim. Pays-Bas*, 103 (1984) 251.

103 K. Ravichandran and R. P. Baldwin, *Anal. Chem.*, 56 (1984) 1744.

104 N. K. Čenas, J. J. Kanapieniene and J. J. Kulys, *J. Electroanal. Chem.*, 189 (1985) 163.

105 G. Dryhurst, K. M. Kadish, F. Scheller and R. Renneberg, *Biological Electrochemistry*, Vol. I, Academic Press, New York, 1982.

106 E. Csöregi, B. Persson and G. Johansson, unpublished results.

107 R. Luther, *Z. Phys. Chem.*, 36 (1901) 385.

108 D. C.-S. Tse and T. Kuwana, *Anal. Chem.*, 50 (1978) 1315.

109 J. M. Ottaway, in E. Bishop (Ed.), *Indicators*, Pergamon Press, Oxford, 1972, pp. 469-684.

110 R. Szentrimay, P. Yeh and T. Kuwana, in D. T. Sawyer (Ed.), *Electrochemical Studies of Biological Systems*, ACS Symp. Ser. 38, Washington DC, 1977, pp. 143-169.

111 M. L. Fultz and R. A. Durst, *Anal. Chim. Acta*, 140 (1982) 1.

112 L. Eberson, *Electon Transfer Reactions in Organic Chemistry*, Springer-Verlag, Berlin, 1987.

113 A. Kitani and L. L. Miller, *J. Am. Chem. Soc.*, 103 (1981) 3595.

114 A. Kitani, Y.-H. So and L. L Miller, *J. Am. Chem. Soc.*, 103 (1981) 7636.

115 C. Ueda, D. C.-S. Tse and T. Kuwana, *Anal. Chem.*, 54 (1982) 850.

116 C. Degrand and L. L. Miller, *J. Am. Chem. Soc.*, 102 (1980) 5728.

117 M. Fukui, A. Kitani, C. Degrand and L. L. Miller, *J. Am. Chem. Soc.*, 104 (1982) 28.

118 N. K. Lau and L. L. Miller, *J. Am. Chem. Soc.*, 105 (1983) 5271.

119 H. Jaegfeldt, A. B. C. Torstensson, L. G. O. Gorton and G. Johansson, *Anal. Chem.*, 53 (1981) 1979.

120 H. Jaegfeldt, T. Kuwana and G. Johansson, *J. Am. Chem. Soc.*, 105 (1983) 1805.

121 K. Ravichandran and R. P. Baldwin, *J. Electroanal. Chem.*, 126 (1981) 293.

122 H. Huck and H.-L. Schmidt, *Angew. Chem.*, 93 (1981) 421.

123 G. Arai, M. Matsushita, and I. Yasumori, *Nippon Kagaku Kaishi*, 5 (1985) 894

124 K. Ravichandran and R. P. Baldwin, *Anal. Chem.*, 55 (1983) 1586.

125 A. Torstensson and L. Gorton, *J. Electroanal. Chem.*,130 (1981) 199.

126 Y. Kimura and K. Niki, *Anal. Sci.*, 1 (1985) 271.

127 H. Huck, *Fresenius' Z. Anal. Chem.*, 313 (1982) 548.

128 L. Gorton, G. Johansson and A. Torstensson, *J. Electroanal. Chem.*, 196 (1985) 81.

129 O. Miyawaki and L. B. Wingard, Jr, *Biochim. Biophys. Acta*, 838 (1985) 60.

130 J. J. Kulys, *Enzyme Microb. Technol.*, 3 (1981) 344.

131 W. J. Albery and P. N. Bartlett, *J. Chem. Soc., Chem. Commun.*, (1984) 234.

132 S. Todoriki, T. Ikeda, M. Senda and G. S. Wilson, *Agric. Biol. Chem.*, 53 (1989) 3055.

133 J. J. Kulys, *Biosensors*, 2 (1986) 3.

134 K. McKenna, S. E. Boyette and A. Brajter-Toth, *Anal. Chim. Acta*, 206 (1988) 75.

135 A. P. F. Turner, *Biotech'85(Europe)* (Online Publications, Plenar), 1985, p. 181

136 B. F. Y. Yon Hin and C. R. Lowe, *Anal. Chem.*, 59 (1987) 2111.

137 R. N. Adams, *Electrochemistry at Solid Electrodes*, Marcel Dekker, New York, 1969, pp. 356-360.

138 R. Appelqvist, G. Marko-Varga, L. Gorton, A. Torstensson and G. Johansson, *Anal. Chim. Acta*, 169 (1985) 237.

139 H. Huck, A. Schelter-Graf and H.-L. Schmidt, *Bioelectrochem. Bioenerg.*, 13 (1984) 199.

140 N. K. Čenas, J. J. Kanapieniene and J. J. Kulys, *Biochim. Biophys. Acta*, 767 (1984) 108.

141 W. J. Albery, P. N. Bartlett and A. E. G. Cass, *Phil. Trans. R. Soc. Lond. B 316*, (1987) 107.

142 H. P. Bennetto, J. L. Stirling and K. Tanaka, *Chem. Ind. (London)*, 20 (1985) 695.

143 T. Yomo, H. Sawai, I. Urabe, Y. Yamada and H. Okada, *Eur. J. Biochem.*, 179 (1989) 293.

144 B. W. Carlson and L. L. Miller, *J. Am. Chem. Soc.*, 107 (1985) 479.

145 L. L. Miller and J. R. Valentine, *J. Am. Chem. Soc.*, 110 (1988) 3982.

146 S. Fukuzumi, N. Nishizawa and T. Tanaka, *J. Org. Chem.*, 49 (1984) 3571.

147 R. A. Marcus, *J. Chem. Phys.*, 43 (1965) 679.

148 S. Fukuzumi, S. Koumitsu, K. Hironaka and T. Tanaka, *J. Am. Chem. Soc.*, 109 (1987) 305.

149 F. Ni, H. Feng, L. Gorton, and T. M. Cotton, *Langmuir*, 6 (1990) 66.

150 K. J. Laidler, *Chemical Kinetics*, McGraw-Hill, New York, 1950.

151 M. Ionescu and H. Mantsch, in A. R. Katritzky and A. J. Boulton (Eds.), *Advances in Heterocyclic Chemistry*, Vol. 8, Academic Press, New York, 1967, pp. 91-92.

152 W. J. Blaedel and R. C. Engstrom, *Anal. Chem.*, 52 (1980) 1691.

153 H. M. Eggers, H. B Halsall and W. R. Heineman, *Clin. Chim.*, 28 (1982) 1848.

154 J. M. Laval and C. Bourdillon, *J. Electroanal. Chem.*, 152 (1983) 125.

155 M. Poon and R. L. McCreery, *Anal. Chem.*, 58 (1986) 2745.

156 A. Webber, M. Shah and J. Osteryoung, *Anal. Chim. Acta*, 157 (1984) 1.

157 A. Webber and J. Osteryoung, *Anal. Chim. Acta*, 157 (1984) 17.

158 G. Palleschi, H. S. Rathore and M. Mascini, *Electroanalysis*, 1 (1989) 199.

159 G. Marko-Varga, E. Dominguez, B. Hahn-Hägerdal and L. Gorton, *J. Chromatogr.*, in press.

160 R. Appelqvist, *Bioelectrochemical Determinations of Carbohydrates in Flow Systems*, doctoral Thesis, University of Lund, Sweden, 1987.

161 G. Marko-Varga, *Carbohydrate Determinations in LC and FIA Using Immobilized Enzymes and Electrochemical Detection - Extension of Selectivity and Sensitivity*, doctoral Thesis, University of Lund, Sweden, 1988.

162 T. Buch-Rasmussen, *Development of Biosensors Based on Dehydrogenase Enzymes and Electrochemical Detection*, Thesis, Radiometer Medical A/S, Denmark and University of Lund, Sweden, 1989.

Proc. of the 2nd int. meeting on chemical sensors, BORDEAUX 1986
6 - 20

CATALYTIC OXIDATION OF REDUCED NICOTINAMIDE COENZYME AT CHEMICALLY MODIFIED ELECTRODES PREPARED WITH A NEW PHENOXAZINE MEDIATOR

B. Persson, L. Gorton and G. Johansson
Department of Analytical Chemistry, University of Lund
P.O.Box 124, S-221 00 Lund, Sweden

Abstract

A new phenoxazine derivative, obtained by reacting 3-amino-7-diethylamino-1,2-benzophenoxazinium and 1-pyrenecarboxaldehyde to form a Schiffs base, strongly adsorbs on graphite to give chemically modified electrodes with an $E^{o'}$ of -0.19 V vs SCE at pH 7.0. The adsorbed phenoxazine mediated the electron transfer in the electrocatalytic oxidation of NADH, with an all over rate constant of $2 \cdot 10^4$ M^{-1} s^{-1} at pH 7.0, evaluated from experiments with a rotating disc electrode. As a sensor, the phenoxazine modified electrodes, responded strictly linearly to NADH concentrations between 10 uM - 0.5 mM, and with a detection limit of less than 1 uM.

1-Introduction

Chemically modified electrodes (CME), based on the adsorption of phenoxazine mediators on graphite, have shown promising properties as amperometric sensors for NADH [1,2]. At the electrode surface NADH is oxidized in a chemical step by the adsorbed mediator defined by the rate constant k_1 ($M^{-1}s^{-1}$), whereby NAD^+ and the reduced form of the mediator are produced.

$$\text{NADH} + \text{oxidized mediator} \xrightarrow{k_1} \text{NAD}^+ + \text{reduced mediator} \qquad (1)$$

The mediator is then reoxidized electrochemically.

$$\text{reduced mediator} \longrightarrow \text{oxidized mediator} + 2e^- + xH^+ \qquad (2)$$

where the number of protons, x, depends on the phenoxazine structure [3]. The decrease in overvoltage, compared to the direct electrochemical oxidation of NADH, is larger the lower the formal potential ($E^{o'}$) of the mediator is. The reaction rate with NADH, however, is larger for mediators with higher $E^{o'}$ [3]. An optimal $E^{o'}$, with respect to these properties, seems to be around -0.20 - -0.15 V vs SCE, at pH 7.0 [3]. An applied potential of 0 V vs SCE can thus be applied to the electrode when operating as a NADH sensor, i.e. in the range where the background current switches signs and where most common interferents are not expected to interfere. 7-dimethylamino-1,2-benzophenoxazinium, Meldola Blue ($E^{o'}$ = -0.18 V vs SCE, at pH 7.0) serves well as a mediator with a rate constant with NADH of $3\ 10^4$ $M^{-1}s^{-1}$ at pH 7.0 [4]. Due to its limited number of aromatic rings it slowly desorbs from the electrode surface resulting in a decrease in the response of the CME with time. A new mediator with an increased number of aromatic rings was therefore synthesized by reacting 3-amino-7-diethylamino 1,2-benzophenoxazinium with 1-pyrenecarboxaldehyde to form a Schiffs base (I). Some fundamental properties of this new mediator are presented.

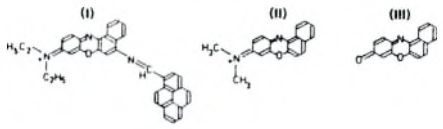

2-Experimental

Graphite electrodes were prepared from graphite rods, type RWO, diam. 3.1 mm, Ringsdorff Werke GmbH. They were cut, polished and mounted into teflon holders so that only the flat circular end could contact the solution [5].

Measurements of electrode properties were made either with triangular sweep voltammetry or at a stationary potential when mounted in a rotating disc assembly (Tacussel EDI), with a SCE as reference and a Pt-foil as counter electrode. Adsorption of mediator was made through dipping the electrode into a stirred solution containing the mediator for various times depending on the amount of aquired surface coating.

The coverage, Γ(mol cm^{-2}), was evaluated by integration of the area under a voltammetric wave.

When used as a sensor for NADH the modified electrode was mounted in a flow through cell in a wall jet arrangement with an Ag/AgCl (0.1 M KCl) as reference and a Pt-wire as counter electrode [5] connected to a three-electrode potentiostat. The cell was connected to a single line flow injection analysis (FIA) system. Samples (50 ul) were injected with a pneumatically operated valve into a carrier consisting of a deaerated 0.1 M phosphate buffer. Connections between various parts were made with teflon tubing (0.5 mm i.d.).

Equal molar amounts of 1-pyrenecarboxaldehyde and 3-amino-7-diethylamino-1,2-benzophenoxazinium, Nile Blue, were dissolved in aqueous-free ethanol supplied with dried K_2CO_3. The reaction mixture was purged with argon and allowed to react overnight at boiling temperature. The new mediator (I) was purified by HPLC on a C18 u-Bondapac column (Waters Assoc.) with 65% ethanol, 34% 0.1 M phosphate buffer pH 5.0 and 1% triethylamine as the mobile phase. Total identification of the mediator is under way at this laboratory.

3-Results and discussion

The separation of the anodic and cathodic peaks of cyclic voltammograms obtained for electrodes modified with I, was 5-25 mV at scan rates 50-300 mV s^{-1} for Γ up to 1 10^{-9} mole cm^{-2}. A fast electrochemical charge transfer between the graphite and the adsorbed mediator is thus shown. The charge transfer rate constant was evaluated to be around 10 s^{-1} [6]. $E^{o'}$, taken as the mean value between the anodic and cathodic peak potentials, was -0.16 and -0.19 V vs SCE at pH 6.0 and 7.0 respectively.

For evaluation of kinetic data between NADH and adsorbed I, the CME was mounted in the rotating device. The potentials applied to the CME were set to 0 V at pH 7.0 and 0.05 V at pH 6.0 to speed up the reoxidation of the mediator, eqn.(2). The limiting reaction rate, k_1, of the catalytic reaction can be evaluated from the intercept of $1/i_{cat}$ versus $1/w^{1/2}$ plot (Koutechy-Levich plot) [7]. The Koutechy-Levich equation is

$$1/i_{cat} = 1/n\ F\ A\ k_1\ \Gamma\ c + (1.61\ v^{1/6}/n\ F\ A\ D^{2/3}\ c)\ 1/w^{1/2} \quad (3)$$

where c is the bulk concentration of NADH, D is the diffusion coefficient of NADH, v is the hydrodynamic viscosity, w is the rotational speed and all other parameters have their usual significancies. Values for k_1 were evaluated from the intercepts of such plots, c.f. Fig. 1, and were found to vary with c, similarly to the results obtained for electrodes modified with Meldola Blue (II) [4] and 1,2-benzophenoxazine-7-one (III) [8]. A charge transfer complex, CT, was postulated to be formed between NADH and the mediator changing eqn.(1) to;

$$\text{NADH} + \text{ox. mediator} \underset{k_{-1}}{\overset{k_{+1}}{\rightleftharpoons}} \text{CT} \xrightarrow{k_{+2}} \text{NAD}^+ + \text{red. mediator} \quad (4)$$

Combining k_{+1}, k_{-1} and k_{+2} give

$$K_M = (k_{-1} + k_{+2})/k_{+1} \quad (5)$$

which means that k_1 can be expressed as

$$k_1 = k_{+2}/(K_M + c) \quad (6)$$

If this holds true eqn.(3) can be rewritten as

$$1/i_{cat} = 1/nFA\, k_{+2}\Gamma + (K_M/nFA\, k_{+2}\Gamma + (1.61\, v^{1/6}/nFA\, D^{2/3}\, w^{1/2}))\,1/c \quad (7)$$

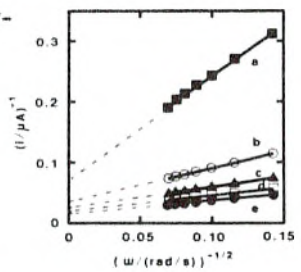

Fig. 1. Koutechy-Levich plots. [NADH]; a=0.16 b=0.47, c=0.77 d=1.06, e=1.36 mM

Γ=0.4 nmole/cm^2

0.25 M phosphate buffer pH 7.0

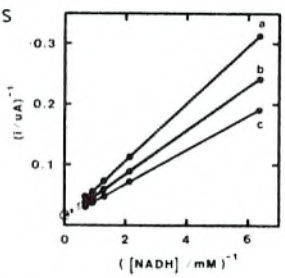

Fig. 2. 1/i vs 1/c plots, eqn.(7) Rotational speeds; a=49 b=101, c=204 rad s^{-1}

Γ=0.4 nmole/cm^2

0.25 M phosphate buffer pH 7.0

Plotting $1/i_{cat}$ versus 1/c should give straight lines with a common intercept, irrespective of the rotational speed. A plot of $1/k_1$ versus c should also result in a straight line, i.e. inversion of eqn.(6);

$$1/k_1 = K_M/k_{+2} + c/k_{+2} \quad (8)$$

Fig. 2 shows that plots according to eqn.(7) give strictly linear curves with a single common intercept. A plot of $1/k_1$ vs c was, however, not found to result in a straight line, see Fig. 3, contrary to the corresponding plots obtained for electrodes modified with II and III [4,8]. Analogous results were obtained at pH 6.0, with the exception that higher currents were obtained for otherwise equal conditions, indicating a higher reaction rate at this pH, in line with the results from experiments with II and III. The complex variation of the rate constants of adsorbed phenoxazine mediators and NADH [3,8] with pH was taken as an impact to support a more

elaborate reaction mechanism [9] than that which is presented by eqn.(4). The bent curve in Fig. 3, indicating a dependence on k_{+2} of the concentration of NADH, also supports this. Only approximative values of k_{+2} and K_M can thus be evaluated from the common intercept and the slopes of the $1/i_{cat}$ vs 1/c plots, eqn.(7). At pH 7.0 k_{+2} and K_M were found to be 15 s^{-1} and 0.8 mM respectively, yielding a k_1 (for c=0) of 2 10^4 M^{-1} s^{-1}. This slightly lower rate constant than that of II, 3 10^4 M^{-1} s^{-1}, is expected as the E^0 of I is 15-20 mV more negative than that of II [3,4].

Fig. 3. $1/k_1$ vs c plot, eqn.(8), k_1 evaluated from intercepts in Fig. 1, c.f. eqn.(3)

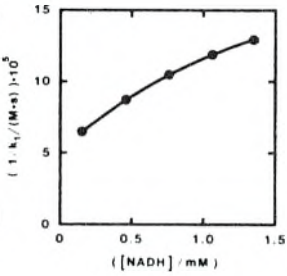

Fig. 4. Current response of an electrode modified with I, for consecutive injections of various NADH-samples.

$\Gamma \equiv 2$ nmole/cm^2, flow rate: 0.85 ml min^{-1}

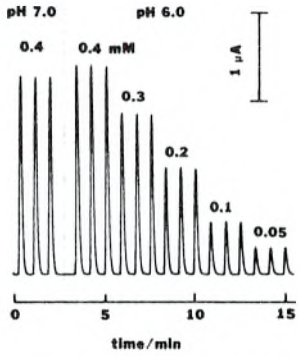

Fig. 4 shows the current response for consecutive injections of various NADH samples in the FIA-system. The lower reaction rate at pH 7.0 than at pH 6.0 is reflected by a somewhat lower response. In the investigated concentration range 0.5 uM (the detection limit) -0.5 mM, strictly linear calibration curves were obtained from 10 uM and upwards in concentration. A log-log plot of the linear part of the calibration curve gave a slope of 0.997.

For all the experiments, Γ was evaluated before and after the CME had been in contact with NADH either in the FIA system or with the rotational device. Only a very minute decrease in Γ could be found.

References

1 - L. Gorton, H. Jaegfeldt, A. Torstensson and G. Johansson - Patent No. 82/SE 59 A1(8203729)(pub. 821028)
2 - H. Huck - Fresenius' Z. Anal. Chem., 313, 548 (1982)
3 - L. Gorton - J. Chem. Soc., Faraday Trans., 1, in press.
4 - L. Gorton, A. Torstensson, H. Jaegfeldt and G. Johansson - J. Electroanal. Chem., 161, 103 (1984)
5 - R. Appelqvist, G. Marko-Varga, L. Gorton, A. Torstensson and G. Johansson - Anal. Chim. Acta, 169, 237 (1985)
6 - E. Laviron, J. Electroanal. Chem., 101, 19 (1979)
7 - R.W. Murray - in "Electroanalytical Chemistry", vol. 13, Dekker, p. 191 (1984)
8 - L. Gorton, G. Johansson and A. Torstensson - J. Electroanal. Chem., 196, 81 (1985)
9 - S. Fukuzumi, N. Nishizawa and T. Tanaka - J. Org. Chem., 49, 3571 (1984)

II

CHEMICALLY MODIFIED ELECTRODES FOR THE ELECTROCATALYTIC OXIDATION OF NADH

L. Gorton[1], B. Persson[1], M. Polasek[2] and G. Johansson[1]

1. *Dept. of Analytical Chemistry,*
   University of Lund,
   P.O.Box 124 S-221 00 Lund, Sweden
2. *Analytical Chemistry Dept.,*
   Faculty of Pharmacy,
   CS-50165 Hradec Kralove, Czechoslovakia

Introduction

The development of chemically modified electrodes, CMEs, has now reached a level of maturity which allows the inclusion of such electrochemical cells into various sensing devices.[1] Special interest has been focused on the electron transfer or rather the hindrances for electron transfer during bioelectrochemical reactions. Studies of the oxidation of the reduced form of the nicotinamide coenzymes NADH and NADPH are attractive because a single electrochemical transducer reaction can be combined with any of the great number of dehydrogenases to give a sensor with the desired selectivity.

Direct electrochemical oxidation of coenzymes NADH and NADPH is possible at a high overvoltage, but it may result in electrode fouling.[2,3] Immobilization of mediating functionalities (catalysts) on an electrode surface can reduce the overvoltage and overcome difficulties encountered with unmodified electrodes.[4] We have found that mediators of the phenoxazine type, Fig.1, incorporating a paraphenylene-diimine moiety are particularly attractive because they seem to be selective for the NADH-catalysis.[5] Graphite and a number of other carbon electrode materials are easily modified with phenoxazine dyes by just dipping the electrode into a solution containing the mediator. The resulting coverage depends on the concentration of the dissolved mediator and the time allowed for adsorption. Very large coverages ($\Gamma > 10^{-8}$ mol cm^{-2}) can be obtained within a few minutes.

The stability of the modified layer towards desorption is mainly governed by the number of conjugated aromatic rings, so that a mediator containing a large number of rings makes a more stable CME than one with a low number of rings. The strong interaction between the carboneous surface and the phenoxazine (π-electron overlapping) results in a very fast charge transfer between the electrode proper and the modifier. This is demonstrated by the small peak separation, ΔE_p, between the peaks of the oxidation and reduction waves in cyclic voltammetry.[6,7] For coverages below 10^{-9} mole cm^{-2} the ΔE_p usually takes a value of about 5–20 mV, for scan rates up to about 400 mV s^{-1}. At higher coverages and for faster scan rates larger ΔE_p-values are obtained.[6] The oxidation and reduction waves are almost mirror images allowing the formal potential, $E^{0\prime}$, of the adsorbed species to be evaluated as the mean value of the peak potentials of the oxidation and reduction waves.[8]

Protons are invovled in the redox conversion of the mediator and the $E^{0\prime}$, will therefore move with a change of pH in the contacting solution. Phenoxazine dyes (see Fig.2) in solution undergo a $2e^-$ redox conversion. Depending on the number of protons also taking part in the redox process, the $E^{0\prime}$ will move with 90 mV/pH ($3H^+$), 60 mV/pH ($2H^+$) or 30 mV/pH ($1H^+$). The number of electrons, n, taking part in the redox conversion for a mediator immobilized on the electrode, is reflected by the width of the voltammetric wave at half peak

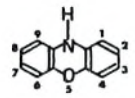

phenoxazine

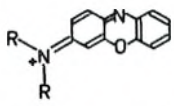

phenoxazine incorporating
a paraphenylenediimine functionality

Fig.1. Structural formulae of phenoxazine and of a phenoxazine with a paraphenylene diimino functionality.

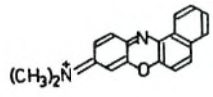

Meldola Blue

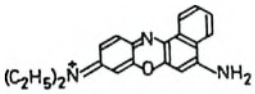

Nile Blue

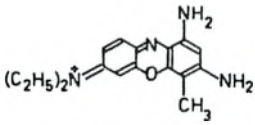

Brilliant Cresyl Blue

Fig.2. Structural formulae of Meldola Blue, Nile Blue, and Brilliant Cresyl Blue.

height $\delta_{0.5}$, which theoretically should equal 90.5/n mV.[8] The number n can also be obtained from the straight line obtained when plotting the peak current, i_p, versus the scan rate,

$$i_p = (n^2F^2/4RT)A\Gamma v \tag{1}$$

Most adsorbed phenoxazine derivatives give slightly broader peaks than what is theoretically stipulated for a Langmuirian adsorption process. The number n, whether evaluated from the $\delta_{0.5}$ or from eqn.(1), is usually somewhat lower than two, reflecting interactions between the adsorbed molecules.[8] The immobilization process may strongly influence the properties of the adsorbed species, which is clearly revealed for Nile Blue in Fig.3. Both the energy level, as well as the various pK_a-values of the oxidized and the reduced forms, are changed on adsorption.[9–11]

Mediators

The phenoxazines can mediate the electron transfer from NADH in solution to the electrode. The reaction sequence can be summarized according to the following:

$$\mathrm{NADH} + M_{ox} \xrightarrow{k_{obs}} \mathrm{NAD^+} + M_{red} \tag{2}$$

In the first step NADH reduces the oxidized form of the mediator, M_{ox}, whereby the reduced form, M_{red}, and NAD^+ are produced. In the next step M_{red} is reoxidized to form

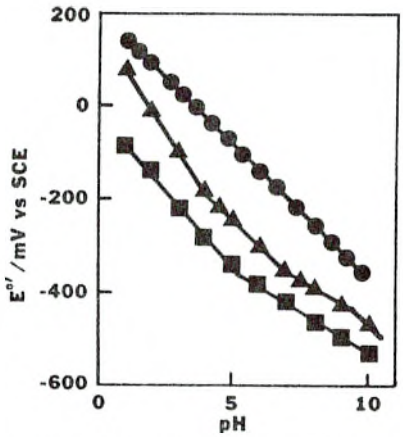

Fig.3. Variation of $E^{0\prime}$ with pH for Nile Blue adsorbed on graphite (-□-□-), Nile Blue dissolved in aqueous solution (-△-△-), bis (benzophenoxazinyl) derivative of terephthaloic acid adsorbed on graphite (-○-○-).

the active mediator. When a potential, E_{appl}, more positive than the $E^{0\prime}$, is applied to the CME, the following reaction will take place.

$$M_{red} \overset{E_{appl} > E^{0\prime}}{\longrightarrow} M_{ox} + H^+ + 2e^- \tag{3}$$

The actual number of protons taking part in the reduction and oxidation of the mediator depends on the structural elements of the phenoxazine.[4,11]

In a previous work we found that the reaction rate k_{obs} between NADH in solution and the adsorbed phenoxazine mediator depends on a number of factors. To obtain kinetic data the phenoxazine-CME was mounted in a rotating device and experiments were run and evaluated according to Levich and Koutecky.[12]

The highest reaction rates were obtained for the mediators with the most oxidative $E^{0\prime}$-values. A linear correlation was found when plotting the logarithm of the rate coefficients versus the $E^{0\prime}$-values.[4] The commercially available phenoxazine Meldola Blue, with an $E^{0\prime}$-value at pH 7.0 of -185 mV vs SCE was found to be the most efficient one having a rate constant of $3 \times 10^4 M^{-1}s^{-1}$ at this pH.[4]

The various structural elements of the mediator are also of great importance. Introducing other redox active groups, may drastically lower the reaction rate expected from the linear log k_{obs} vs $E^{0\prime}$-relationship stated above.[4] Exchanging a charged iminogroup, Fig.1, for an uncharged or a ketogroup has been stated to decrease the reaction rate with NADH.[13,14]

Different values of the rate coefficient, k_{obs}, were obtained when the NADH-concentration was varied.[2,6,7] This observation was found for all the various phenoxazine mediators investigated. A formation of a complex between NADH and the adsorbed mediator could explain this behaviour. The reaction can be described (rewriting eq.(2)) to take place according to the following:

$$\mathrm{NADH} + M_{ox} \underset{k_{-1}}{\overset{k_{+1}}{\rightleftharpoons}} complex \overset{k_{+2}}{\rightarrow} \mathrm{NAD^+} + M_{red} \tag{3}$$

The overal reaction rate, k_{obs}, can thus be described as:

$$k_{obs} = k_{+2} / (K_M + [NADH]) \tag{4}$$

where

$$K_M = (k_{-1} + k_{+2}) / k_{+1} \tag{5}$$

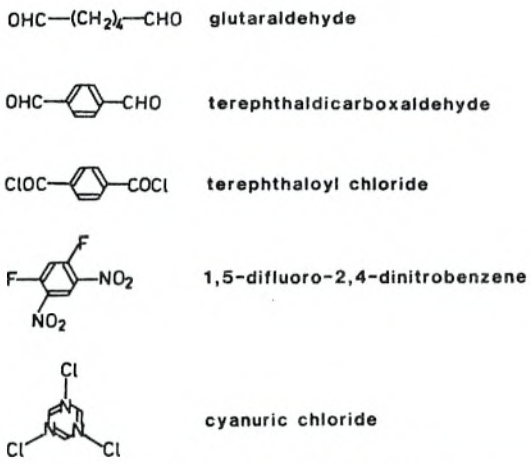

Fig. 4. Structural formulae of some bi- and trifunctional reagents.

The various rate coefficients, k_{obs}, k_{+2} and K_M can be evaluated from rotating disk electrode experiments.[4,6,7]

The reaction mechanism, eq.(3) will cause the current response to a constant NADH-concentration to increase linearly with surface coverage for small values of Γ and to level off towards a constant plateau for high values of Γ.[6] Thus once the coverage has reached a certain minimal value, the current response will virtually be unaffected by the coverage.[5]

The pH of the contacting solution has a profound effect on the reaction rate of eqn.(3). Under otherwise constant conditions, k_{obs} will decrease with an increase in pH. This effect seems to be common to all phenoxazine mediators.[4,7,15,16] For Meldola Blue, k_{obs} reached almost a value of 10^5 M^{-1} s^{-1} at pH 6.0.[4] A virtually mass controlled current could thus be obtained at this pH with this CME working as an NADH sensor in a FIA-setup.[5]

Straight calibration curves for NADH over at least three orders of magnitude were obtained between pH 6 and 9 with phenoxazine CMEs as sensors in flow systems despite the decreasing reaction rate. As long as the effective NADH-concentration at the electrode-solution interface is well below the K_M-value a linear response characteristic is expected. K_M-values in the millimolar level have been obtained for most phenoxazines.[4] When using phenoxazine-CME as sensors in FIA-systems with normal dispersion factors[17] of about 10 the upper linear response range is expected around 10–30 mM.

A high pH can also have a detrimental effect on the mediator. Phenoxazines, like Meldola Blue, which are derivatized in position 3 or 7, will decompose at pH-values higher than 7.[18,19] However, if they are derivatized in both these positions they will become alkaline-stable. The stability towards desorption of a phenoxazine-CME depends largely on the number of aromatic rings of the phenoxazine structure. The drawbacks of the restricted stability of electrodes modified with Meldola Blue, having only 4 rings and being alkaline instable, were partly overcome by reacting the amine function in position 3 of Nile Blue, whereby the aromatic ring system could be increased with either a naphthalene[10] or a pyrene moiety.[15]

Mediators with Several Aromatic Centra

Polyfunctional molecules including more than one catalytically active phenoxazine part can be synthesized by coupling the original phenoxazine dye with bi- or trifunctional reagents, see Fig.4. Such a coupling can overcome several problems encountered with simple phenoxazines. The desorption of the polyfunctional mediators, see e.g. Fig.5, seems to be very small due to the large number of aromatic rings. A Nile Blue derivative of terephthaloyl chloride, Fig.5, can be produced if the bifunctional reagent is reacted either with the reduced form of Nile Blue or with the imino form of oxidized Nile Blue, see Fig.6. Electrodes modified with this derivative could be used for a month, even in flowing solution, without noticeable

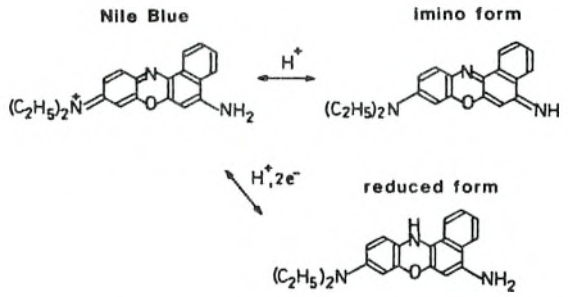

Fig.5. Structural formulae of Nile Blue, its imino and reduced forms.

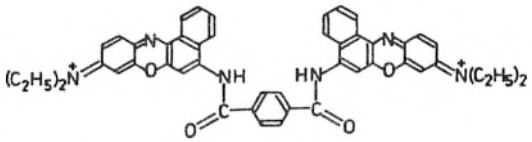

Fig.6. Proposed formula of a bis(benzophenoxazinyl) derivative obtained when reacting Nile Blue with terephthaloyl chloride.

indications of desorption, when followed by surface coverage measurements. The coupling increases the $E^{0\prime}$-value of adsorbed Nile Blue from -430 to -200 mV vs SCE at pH 7.0, see Fig.3. The alkaline stability of the compound permits the CME to be used at pH 9.0, which is about 2 pH-units higher than the upper pH-range for Meldola Blue.[6] The somewhat lower $E^{0\prime}$-value compared to Meldola Blue results in lower rate coefficients for the NADH oxidation, c.f. eqn.(3). preliminary values, $k_{+2} = 40\ s^{-1}$ and $K_M = 2 \times 10^{-3}$ M (pH 7.0) with a resulting $k_{obs(NADH=O)} = 2 \times 10^4\ M^{-1}\ s^{-1}$ (pH 7.0) were evaluated by rotating disk electrode measurements at various NADH-concentrations. The lower reaction rates compared to Meldola Blue implies that the electrode response is under partial kinetic rather than under full mass transfer control.

Fig.7 shows a series of cyclic voltammograms obtained at various pHs for one electrode modified with this Nile Blue derivative (Fig.6). It can be seen that the shapes of the waves will vary both with pH and with buffer constituents.[6] The variation of $E^{0\prime}$ with pH for this compound is depicted in Fig.3 and shows a single linear pH dependence, 60 mV/pH, through the whole pH range investigated, pH 1–9. This indicates that equal numbers of protons and electrons take part in the redox conversion of the adsorbed species.

An increased value of $E^{0\prime}$ of the adsorbed phenoxazine is expected to increase the reaction rate with NADH[4]. If it is large enough ($k_{obs} > 10^5\ M^{-1}\ s^{-1}$ at all pHs) it should be possible to produce a virtually pH insensitive NADH sensor. A number of other phenoxazines (e.g. Brilliant Cresyl Blue, Fig.2) and other coupling reagents (Fig.4) are therefore under study at present.

Two examples may be given, by reacting the reduced form of Nile Blue with 1,5-dichloro-2,5-dinitrobenzene, one compound could be obtained with an $E^{0\prime}$-value of -135 mV vs SCE (pH 7.0), and by reacting the iminoform of Brilliant Cresyl Blue with terephthaloyl chloride a compound could be obtained with an $E^{0\prime}$-value of -55 mV vs SCE (pH 7.0). They were both found to be catalytically active for NADH-oxidation. No kinetic data are available yet, however. Purification and identification of both the commercially available phenoxazines (usually with a purity of 50–90 %) and of the reaction products are far from straightforward.

The basic understanding of phenoxazines as mediators for NADH-oxidation and as modifiers for preparation of stable CMEs are demonstrated by the work discussed above. The prospects seem therefore to be good to make optimal phenoxazine mediators with high

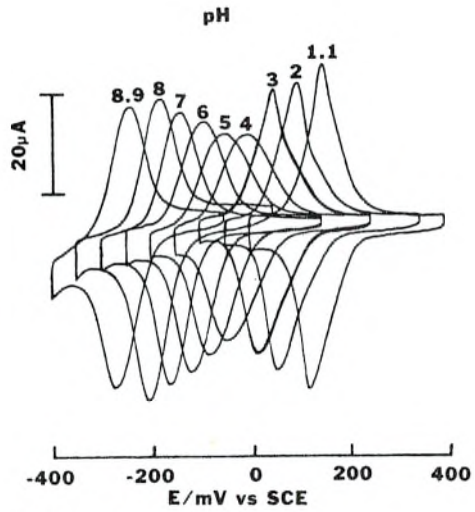

Fig.7. Cyclic voltammograms of a graphite electrode modified with the substance depicted in Fig.6. The surface coverage was 2.7×10^{-9} mole cm^{-2} and the scan rate was 50 mV s^{-1}. The buffers used were 0.1 M HCl (pH 1.1), 0.25 M phosphate buffer (pH 2–8) and 0.15 M pyrophosphate (pH 8.9).

reaction rates at all pHs, alkaline stability and desirable adsorption properties.

Acknowledgements

This work was granted by supports of the Swedish National Reserach Council (NFR), The Swedish Board for Tecnical Development (STUF) and the National Energy Research Board (STEV).

References

1. R.W. Murray, A.G. Ewing and R.A. Durst, Anal. Chem., **59** (1987) 379A.
2. Z. Samec and P.J. Elving, J. Electroanal. Chem., **144** (1983) 217.
3. J. Moiroux and P.J. Elving, J. Am. Chem. Soc., **102** (1980) 6533.
4. L. Gorton, J. Chem. Soc., Faraday Trans., I, **82** (1986) 1245.
5. R. Appelqvist, G. Marko-Varga, L. Gorton, A. Torstensson and G. Johansson, Anal. Chim. Acta, **169** (1985) 237.
6. L. Gorton, A. Torstensson, H. Jaegfeldt and G. Johansson, J. Electroanal. Chem., **161** (1984) 103.
7. L. Gorton, G. Johansson and A. Torstensson, J. Electroanal. Chem., **196** (1985) 81.
8. E. Laviron, in: "Electroanalytical Chemistry", A.J. Bard (Ed.), Vol. **12**, Marcel Dekker, New York, pp. 53-157 (1982).
9. H. Huck, Ber. Bunsenges. Phys. Chem., **87** (1983) 945.
10. H. Huck, Fresenius' Z. Anal. Chem., **313** (1982) 548.
11. J.M. Ottaway, in: "Indicators", E. Bishop (Ed.), Pergamon Press, Oxford, pp. 498-503 (1972).
12. A.J. Bard and L.R. Faulkner, in: "Electrochemical Methods, Fundamentals and Applications", Wiley, New York, 1980.
13. A. Kitani and L.L. Miller, J. Am. Chem. Soc., **103** (1981) 3595.
14. A. Kitani, Y.H. So and L.L. Miller, J. Am. Chem. Soc., **103** (1981) 7636.
15. B. Persson, L. Gorton and G. Johansson, in: "Proc. 2nd Int. Meeting on Chemical Sensors", J-L. Aucouturier, J.-S. Cauhapé, M. Destriau, P. Hagenmuller, C. Lucat, F.

Menil, J. Portier and J. Salardenne (Eds), Imprimerie Biscaye, Bordeaux, pp. 584-587 (1986).
16. M. Polasek, L. Gorton, R. Appelqvist, G. Marko-Varga and G. Johansson, in: "Thesis", R. Appelqvist, Lund University, 1987.
17. J. Růžička and E. Hansen, in: "Flow Injection Analysis", Wiley, New York, 1981.
18. M. Kotouček, J. Tomášová and S. Durčáková, Collect. Czech. Chem. Commun., **34** (1969) 212.
19. M. Kotouček and J. Zavadilová, Collect. Czech. Chem. Commun., **37** (1972) 3212.

III

J. Electroanal. Chem., 00 (1990) JEC00885
Elsevier Sequoia S.A., Lausanne – Printed in The Netherlands

A chemically modified graphite electrode for electrocatalytic oxidation of reduced nicotinamide adenine dinucleotide based on a phenothiazine derivative, 3-β-naphthoyl-toluidine blue O

Björn Persson

Department of Analytical Chemistry, University of Lund, P.O. Box 124, S-221 00 Lund (Sweden)

(Received 13 November 1989; in revised form 5 February 1990)

ABSTRACT

The 7-dimethylamino-2-methyl-3-naphthamido-phenothiazinium salt (3-NTB) was obtained by reacting Toluidine Blue O (TBO) and 2-naphthoyl chloride. It was adsorbed on graphite to give a chemically modified electrode (CME) with a formal redox potential of −135 mV (vs. SCE) at pH 7. The 3-NTB CME catalyses the electrochemical oxidation of the reduced co-enzyme nicotinamide adenine dinucleotide (NADH). The reaction rate between 3-NTB and NADH was evaluated from rotating disk electrode measurements. The 3-NTB CME was also mounted in a flow-through amperometric cell in a single-channel FIA system and tested as a sensor for NADH. The calibration graph was linear over almost three decades of concentration at pH 9 with a sensitivity of 13.8 mA M^{-1} and a detection limit of 0.2 μM NADH with an injection volume of 50 μl. The NADH sensor showed good stability in alkaline solutions and an improved response in terms of a decrease in pH dependence compared with previously studied sensors based on graphite electrodes modified with phenoxazine derivatives.

INTRODUCTION

Methods that combine the selectivity of enzymes with the sensitivity of amperometric detection are in progress in analytical chemistry [1]. The oxidation of the reduced nicotinamide co-enzymes (NADH and NADPH) is particularly important because they are produced in reactions catalysed by more than 300 dehydrogenases. NADH is oxidized directly at different bare electrode materials only with high overvoltages of the order of 1 V [2]. A decrease in the large overvoltage can be obtained by the immobilization of functionalities on the electrode surface which mediate the electron transfer from NADH to the electrode [3–8].

Studies, at this laboratory, of chemically modified electrodes (CMEs) based on the irreversible adsorption of commercial phenoxazine derivatives on graphite electrodes indicated very promising features. A mediator with sufficient stability in the acid region, a low formal potential, and a high reaction rate with NADH was

0022-0728/90/$03.50

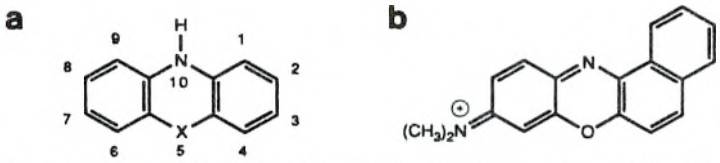

Fig. 1. (a) Structural formulae of phenoxazine (X = O) and phenothiazine (X = S). (b) Structural formula of 7-dimethylamino-1,2-benzophenoxazinium (Meldola Blue), incorporating a paraphenylenediimine functionality within the molecular structure.

found in Meldola Blue [9], and analytical systems based on the combination of enzymes and amperometric detection for determination of carbohydrates could be developed for practical applications [10–12].

Mediators stable at higher pHs are of interest because many dehydrogenases have their pH optima in the alkaline region. Since 7-amino-benzophenoxazine derivatives with no or small substituents in position 3 (e.g. Meldola Blue, see Fig. 1) are subjected to nucleophile attack [13,14], increased alkaline stability was obtained by reacting aromatic aldehydes and acid chlorides with Nile Blue A, an analogue of Meldola Blue with an amino group in position 3 and a diethylamino group in position 7. The derivatization of position 3 increased the formal redox potential, $E^{\circ\prime}$, of the new mediator by about 200 mV compared with the parent compound [15–17]. Furthermore, by introducing several aromatic rings, the stability of the modified layer increased towards desorption owing to enhanced π-electron overlapping with the carbonaceous surface.

The reaction rate between NADH and the adsorbed mediator depends to a large extent on the structural elements and the formal redox potential of the phenoxazine derivatives, where a general trend was found of an increased reaction rate at more oxidative $E^{\circ\prime}$ values of the mediator [18]. The pH of the contacting solution also has a profound effect on the reaction rate between phenoxazine derivatives and NADH, the rate decreasing with increasing pH [19]. The mediators mentioned above have $E^{\circ\prime}$ values at pH 7.0 of around -200 mV (vs. SCE) and rate coefficients with NADH of the order of $2\text{-}3 \times 10^4$ ($M\ s^{-1}$). The reaction rate is almost sufficient to give a response which is independent of the pH in the acid region, since the response is close to mass transfer-controlled [9,10]. A mediator with a more positive $E^{\circ\prime}$ value may result in a reaction rate with NADH high enough to give a sensor with a virtually mass transfer-controlled response in a flow system at higher pHs. However, the $E^{\circ\prime}$ value should not exceed the optimum potential range for detection around 0 mV (vs. SCE), where the background and noise level are at a minimum and electrochemical interference from several other oxidizing or reduction reactions is excluded.

In general, the $E^{\circ\prime}$ value in solution for comparable derivatives of phenoxazines and benzophenoxanines is slightly higher for the former [20], which suggests the use of a three-ring derivative to obtain a mediator with a more positive $E^{\circ\prime}$ value. The phenoxazine derivatives also seem to be less sensitive to replacement of substituents

[21]. The 3,7-diamino-derivatives of phenoxazines and phenothiazines possess, in many aspects, chemical properties in common [22]. Members of the phenothiazine group have so far not been considered to be suitable mediators owing to a low reaction rate with NADH both in solution [23] and when adsorbed on graphite electrodes. Modification of 3,7-diaminophenothiazine derivatives may alter this and introduce a new group of potential mediators for catalytic NADH oxidation.

This paper reports on the making of a CME based on a phenothiazine derivative, rather than on a phenoxazine derivative, with a formal potential of −135 mV (vs. SCE) at pH 7.0. The electrochemical properties of the CME and its performance as an NADH sensor are reported.

EXPERIMENTAL

Synthesis and purification of 3-β-naphthoyl-Toluidine Blue O

7-Dimethylamino-2-methyl-3-β-naphthamido-phenothiazinium chloride (3-NTB) was synthesized from 2-naphthoyl chloride and 3-amino-7-dimethylamino-2-methyl-phenothiazinium chloride (Toluidine Blue O).

To a solution of 1.5 g (4.2 mmol) of Toluidine Blue O (Aldrich-Chemie, Cat. No. 19.816-1) in 100 ml of anhydrous pyridine was added 1 ml (5.7 mmol) of *N,N*-diisopropylethylamine (Aldrich, Cat. No. 29.896-4), whereupon the colour of the mixture changed from blue to red-violet. After 5 min stirring, the remaining solids were filtered off and 0.9 g (4.7 mmol) of 2-naphthoyl chloride (Fluka, Cat. No. 70680) was added. The colour of the reaction mixture changed to violet within 1 min of adding the acid chloride. The mixture was stirred at room temperature for another 30 min. After that, the solvent was removed by evaporation, giving a blackish-blue residue.

The crude product was purified by column chromatography. Columns (i.e. 1 cm) were packed with a slurry of Silica gel 60 (Merck, Art. 9385) in 1,4-dioxan, to a depth of 10 cm. Pyridine solutions saturated with the crude product were applied to the top of the columns. The columns were eluted with 1,4-dioxan followed by 1,4-dioxan containing 2% (v/v) *N,N*-diisopropylethylamine.

For the structural analysis of the main product, further purification was necessary. Collected fractions containing the main product were diluted with dichloromethane and transferred to a separation funnel. The solution was washed re-

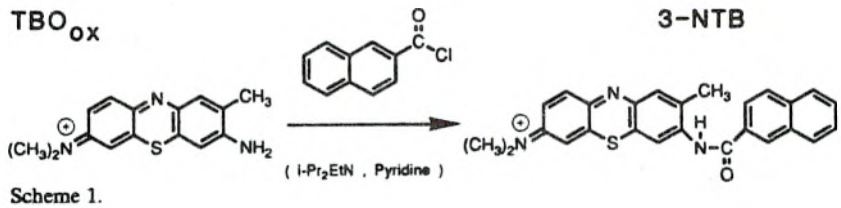

Scheme 1.

peatedly, first with 5 mM HCl and then with water. After evaporation of the organic solvent, the product was dried in a desiccator over phosphorus pentoxide.

^{1}H-NMR spectra were recorded using a Varian XL 300 instrument with the main product dissolved in d_6-acetone (Janssen Chimica, Cat. No. 16.622.35).

Preparation and study of chemically modified electrodes

Graphite rods (RW001, Ringsdorff-Werke, GmbH) were polished on wet fine emergy paper (Tufbak Durite, P1200) and washed thoroughly with deionized water. The electrodes were press fitted into a Teflon holder so that a flat circular surface ($A = 0.0731$ cm^2) contacted the solution. Modification of the electrode surface was performed by dipping the electrode into a solution containing the modifier for various times (10 s–2 min), depending on the desired coverage.

Cyclic voltammetry was employed using a Pt gauze as the counter-electrode and a saturated calomel electrode (SCE) equipped with a Luggin capillary as the reference. The surface coverage (Γ) of the modifier was evaluated from the integrated anodic peak of a single linear scan (from -500 to $+200$ mV vs. SCE, at 50 mV s^{-1}), corrected for the background current. The measurements were done in a buffer solution of the same composition as the buffer into which the electrode was transferred for further experiments. The formal potential, $E°'$, of the adsorbed species was evaluated by taking the mean value of the anodic and cathodic peak potentials of a cyclic voltammogram [24].

Rotating disk electrode (Tacussel, model EDI) experiments were carried out at 23 ± 1°C with a stationary applied potential of 0 mV (vs. SCE). The surface coverages of the 3-NTS modified graphite electrodes were 0.75–0.85 nmol cm^{-2} and the rotational speed was veried between 50 and 200 rad s^{-1}. In this range, the background currents were less than 0.1 μA and any correction could therefore be omitted.

The supporting electrolytes were 0.25 M phosphate buffers at pH 2–10 and 0.1 M HCl at pH 1.1. Measurements were made in solutions deaerated by nitrogen bubbling.

Modification of graphite electrodes with Toluidine Blue O (TBO) was performed in a solution obtained by HPLC purification of the commercial dye. The purification was performed on a C_{18} μ-Bondapak column (Water Associates, i.d. 0.5 cm, length 18 cm) with a mobile phase (1 ml min^{-1}) consisting of 60% (v/v) ethanol, 39% 0.1 M phosphate buffer and 1% triethylamine, and adjusted to pH 5.0. The eluted TBO fraction was stored in a refrigerator until needed, and then diluted with 99% ethanol prior to use.

Preparation of 3-NTB CMEs was performed in a solution consisting of 20% (v/v) freshly column-chromatographed 3-NTB, 70% acetone and 10% anhydrous acetic acid. When surface coverages less than 1 nmol cm^{-2} were desired, the solution was diluted further with acetone. The solution was stable for some hours. Degradation was then observed as decolourization and a decrease in available mediator. However, the addition of both acetone and acetic acid to the violet

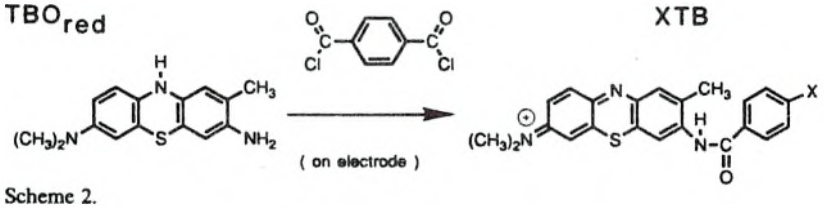

Scheme 2.

fraction did not only improve the tendency towards adsorption onto the graphite surface of the modifier, but also sharpened the peaks and decreased the peak separation as seen by cyclic voltammetry.

An alternative way to prepare CMEs of phenothiazinium derivatives, XTB, was by the reductive coupling of TBO and terephthaloyl chloride, TPC (Sigma Chemical Co., Cat. No. T-1390), directly on the electrode surface.

A 4 μl drop of a freshly prepared acetone solution saturated with TPC was applied on a TBO CME. The electrode was then subjected to cyclic voltammetry in phosphate buffers at various pHs (4–9), and the potential was swept at 50 mV s^{-1} in the negative direction from a starting potential of 0 mV (vs. SCE), followed by repeated cycling between -500 and $+300$ mV.

Flow injection analysis experiments

The flow injection system consisted of a peristaltic pump (Gilson Minipuls 2), a pneumatically operated injection valve (Cheminert, type SVA) and a flow-through amperometric cell of the wall-jet type [10] under three-electrode potentiostatic control using a Princeton Applied Research (model 174A) instrument. Knotted micro-line tubing (Cole Parmer, i.d. 0.51 mm, volume 100 μl) was used as the connector between the injector and the inlet of the amperometric cell. All other connections were made of Teflon tubing (i.d. 0.5 mm).

The outlet jet–electrode distance was set to 1.8 mm [10]. The applied potential was 0 mV (vs. an Ag/AgCl/0.1 M KCl reference electrode), with a Pt wire as the counter-electrode. After the potential had been applied to the CME, the background current was allowed to decay to a stable value in a continuous flow (40–60 min). The noise was of the order of 0.5 nA with a potentiostat time constant of 1 s.

The carriers, 0.1 M deaerated phosphate buffers of pH 6.0–10.0 unless otherwise stated, were pumped at a flow rate of 0.85 ml min^{-1}. Samples of NADH dissolved in the same buffer as the carrier were injected with a 50 μl injection loop. All the response values reported are the peak currents of the FIA recordings, unless otherwise stated.

1,4-Dihydronicotinamide adenine dinucleotide (NADH) was obtained from Sigma Chemical Co. (Cat. No. N-8129). The concentrations of the co-enzyme solutions were calculated from spectrophotometric assays at 340 nm using a molar absorptivity of 6220 $(M\ cm)^{-1}$.

RESULTS AND DISCUSSION

Derivatives of Toluidine Blue O

Toluidine Blue O can exist in different chemical forms (see Fig. 2). The ability of the amino group to react with aromatic acid chlorides is strongly affected by the pH and by the redox state of the molecule.

The oxidized form of TBO reacted slowly with 2-naphthoyl chloride, with a poor yield of coupling product at room temperature. This is due to the resonance stabilization of the molecule and the possible delocalization of the positive charge on the amino group (see Fig. 2).

The red imino form of oxidized TBO reacted rapidly with 2-napthoyl chloride, giving a high yield of reaction product. Purification of the reaction mixture by column chromatography gave a first red fraction when eluting with 1,4-dioxan, leaving a violet band at the top of the column. A second fraction was eluted with 1,4-dioxan containing 2% (v/v) *N*,*N*-diisopropylethylamine as a violet tailing band. A blue band remained at the top of the column. The two fractions obtained were examined by electrode modification and cyclic voltammetry at pH 7.0.

The red fraction contained electrochemically active compounds in the potential range +100 to +200 mV (vs. SCE). Commercial TBO has been shown to contain 2-methyl-thionine and *N*-methyl homologues thereof [25]. A preliminary study at this laboratory resulted in a compound in this potential range by reacting thionine with 2-naphthoyl chloride. Dimerization of phenothizine derivatives has also been demonstrated to give electrochemically active compounds in the same potential range at carbon electrodes [26,27].

The violet fraction contained only one electrochemically active compound (see Fig. 3c). Samples of the violet fraction were investigated by TLC on both aluminium oxide and silica, with ethanol, acetone and tetrahydrofuran as the mobile phase. In all cases, a single spot was found. The ^{1}H-NMR spectrum of the compound in the

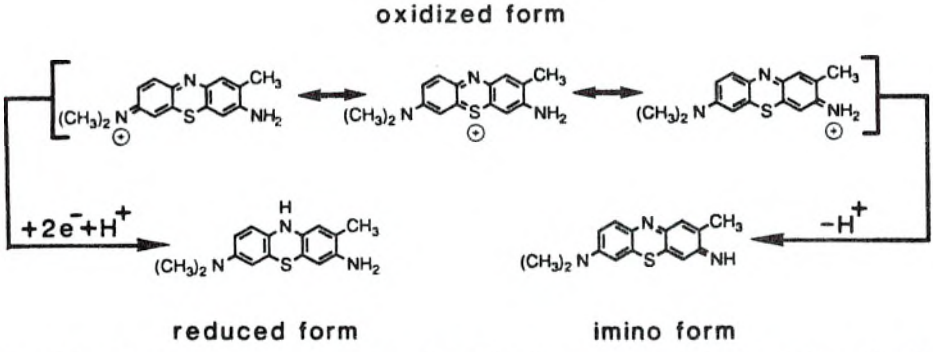

Fig. 2. Structural formulae of Toluidine Blue O showing the resonance stabilization of the oxidized form, its imino form and the reduced form.

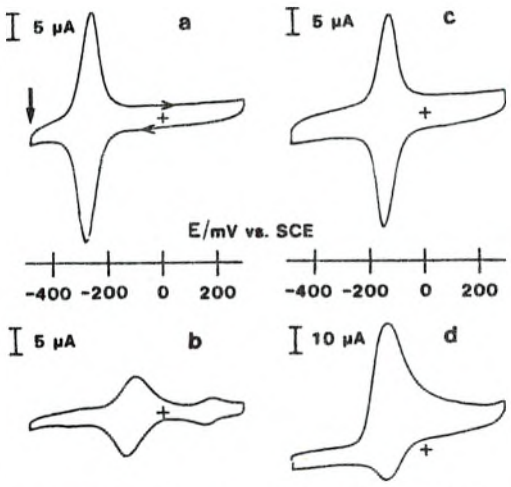

Fig. 3. Cyclic voltammograms of modified graphite electrodes in deaerated 0.25 M phosphate buffer at pH 7.0 obtained by a single scan with a sweep rate of 50 mV s^{-1}. (a) TBO-modified electrode (T = 4.2 nmol cm^{-2}); (b) the TBO-modified electrode after reductive coupling on the electrode surface with terephthaloyl chloride; (c) 3-NTB-modified electrode (T = 3.7 nmol cm^{-2}); (d) the same 3-NTB-modified electrode in the presence of 3.7 mM NADH. The crosses indicate zero current and potential, and the arrow the starting potential of a scan.

violet fractions was in accordance with the proposed formula of 3-NTS. Thus, the conversion of an amino group to a naphthamide group in TBO results in an increase of the $E^{\circ\prime}$ value of the adsorbed species from −285 to −135 mV (vs. SCE) at pH 7.0 (cf. Figs. 3a and 3c).

The reduced form of TBO adsorbed on graphite electrodes can be produced electrochemically as seen in Fig. 3a. With terephthaloyl chloride present on the electrode surface, chemical reactions were found to take place. When the potential was swept from 0 mV (vs. SCE) in the negative direction, traces of a new compound could be detected just below −100 mV followed by the positively-shifted reduction peak of TBO at about −200 mV. After reversing the sweep at −500 mV, only mirror or no traces of the oxidation peak of TBO were found while two new peaks with formal potentials of about −120 mV and +170 mV appeared. Repeated cycling gave no indications of further reactions on the surface. A typical final result is shown in Fig. 3b. Changing the reaction conditions by varying the pH (4–9) in the contacting solution did not change the final result significantly. Both peaks were able to oxidize NADH electrocatalytically. A peak width at half height of 120 mV was normally found for the main peak at −120 mV (vs. SCE).

When reduced TBO reacts with the bifunctional reagent terephthaloyl chloride, the result can be several products (XTB) depending on the reaction of the opposite acid chloride group. The outcome may be a bis derivative with two TBO functionalities, a carboxylic acid derivative, or covalent immobilization at the electrode surface, depending on whether the acid chloride group reacts with another molecule of TBO,

water, or surface functionalities on the electrode, respectively. If the peak at −120 mV is the result of several TBO derivatives, peak broadening is likely. The method demonstrates the possibility of an alternative way to produce CMEs with improved catalytic properties for catalytic NADH oxidation.

Electrochemistry of adsorbed 3-NTB

Figure 3c shows a cyclic voltammogram of a 3-NTB-modified graphite electrode recorded in a buffer solution with no soluble 3-NTB present. The cyclic voltammogram is well behaved with the anodic and cathodic waves almost mirror-images of each other. The peak potential separation, ΔE_p, is moderate as expected for a surface-immobilized redox species [26]. Typical values of 10–40 mV were obtained for surface coverages, Γ, ranging between 0.5 and 7 nmol cm^{-2}. Theory predicts a ΔE_p of zero for the ideal case if the charge-transfer exchange rate is very fast between the electrode and the modifier [24].

The peak width at half height, E_{fwhm}, was typically found to be 70 mV. For the ideal case where there are no interactions between the adsorbed molecules and all adsorption sites are equal, the expected E_{fwhm} value is equal to $(90.6/n)$ mV, where n is the number of electrons taking part in the redox conversion [28]. However, deviations from the ideal values of ΔE_p and E_{fwhm} seem to be normal for redox-modified electrodes, even at low coverages and sweep rates [29,30].

The relation between the peak current, i_p, vs. the sweep rate is ideally given for a redox-modified electrode by

$$i_p = \left[n^2F^2/4RT\right]\Gamma A v \qquad (1)$$

where A is the surface area, Γ is the coverage, v is the sweep rate and the other symbols have their usual meaning [31]. A plot of i_p vs. v for a 3-NTB-modified electrode (Fig. 4) shows a linear relation up to about 200 mV s^{-1}, as expected from eqn. (1). At sweep rates higher than 300 mV s^{-1} a linear relationship was found only when i was plotted against $v^{1/2}$, indicating a limiting diffusional step [32]. Similar behaviour has been reported previously for other modified electrodes based on adsorbed phenoxazine compounds where protons take part in the redox conversion of the modifier [9,18,19].

The number of electrons participating in the redox reaction can be calculated either from the E_{fwhm} value or from the slope of the linear part in Fig. 4, according to eqn. (1), and was found to be 1.6 for coverages between 0.9 and 1.9 nmol cm^{-2}. n value of two is given by other studies of phenothiazine derivatives in aqueous solution [20]. From previous experiments with similar compounds adsorbed on graphite a somewhat lower number than two is usually found. If interactions occur between the adsorbed molecules, it is assumed that the n value should deviate from the calculated theoretical value [28,29]. It is therefore reasonable to assume on n value of two for the adsorbed phenothiazine derivative.

The small ΔE value indicates that the redox conversion of the adsorbed 3-NTB is fast. The apparent electron-transfer rate, k_{app}, can be calculated by a method

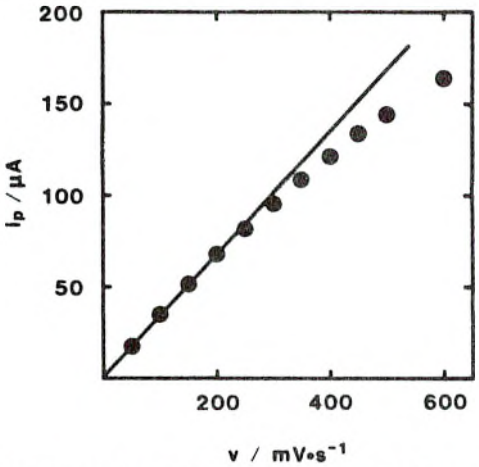

Fig. 4. Variation of the anodic peak current, i_p, with the sweep rate, v, in 0.25 M phosphate buffer at pH 7.0 for a 3-NTB-modified electrode. Surface coverage: 1.9 nmol cm^{-2}. The solid line is drawn through the linear segment.

based on mathematical formulation of the variation of $(n \cdot \Delta E)$ with v [33]. With this method, k_{app} was estimated to 8 s^{-1} at pH 7.0, at sweep rates between 20 and 400 mV s^{-1}, resulting in $(n \cdot \Delta E) < 200$ mV, and with a coverage of 2.4 nmol cm^{-2}, assuming a transfer coefficient (α) of 0.5. For adsorbed Meldola Blue under otherwise equal conditions, a k value of 6 ± 2 s^{-1} at pH 7.0 has been reported [9]. It can therefore be concluded that, in general, the adsorbed phenothiazine derivative possesses similar electrochemical properties to those of the adsorbed phenoxazine derivatives [9,15–19].

The pH dependence of the formal redox potential, $E°'$, for both adsorbed TBO and 3-NTB was investigated by cyclic voltammetry (see Fig. 5). A pK_a value of 4.0 for the reduced TBO was found from the intersection of the two straight lines with slopes of -75 mV pH^{-1} in the acid region and -39 mV pH^{-1} in the more alkaline region. The study of adsorbed 3-NTB resulted in a pK_a value of 4.5 and slopes of -62 and -36 mV pH^{-1}, below and above pH 4.5, respectively. The observation of slope values larger than the theoretical values, -60 and -30 mV pH^{-1}, could not be explained, but such results have been obtained earlier where related compounds were adsorbed on graphite electrodes [34]. For reasons of mass and charge balance an integer value of the protons participating in the redox reaction is expected. The observed pH dependence for 3-NTB is then best fitted by the reaction scheme 3.

In potentiometric studies of TBO dissolved in aqueous solution, two pK_as for the reduced form, pK_rs, and one for the oxidized form, pK_o, were found [35,36]. The values reported for pK_{r1}, pK_{r2} and pK_{o1} were 4.81, 5.41 and 11.04, respectively. A comparison of the dissociation constants in both water and organic solvents for different amino substituents shows that the pK_a for a dimethylamino group is greater than that for an amino group [37]. It is therefore reasonable to assume that

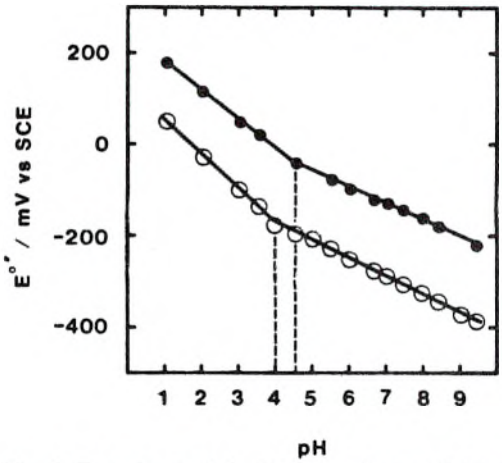

Fig. 5. Formal potential, $E°'$, for adsorbed Toluidine Blue O (○) and its derivative 3-β-naphthoyl-Toluidine Blue O (●) as a function of the pH. The dotted lines indicate the pK values of the reduced form.

the pk_{r2} value of 5.41 for dissolved TBO can be ascribed to the dimethylamino group and the pK_{r1} of 4.81 to the amino group.

Since TBO in the dissolved state shows two pK_rs, while in the adsorbed state only one pK_r is found, this suggests that one of the substituents in the TBO molecule interacts strongly with the graphite surface. Similar behaviour can be observed for Nile Blue A [15,17].

Adsorbed 3-NTB shows a single pK_a value for the reduced form at pH 4.5. A single dissociation, assigned to the dimethylamino group, is expected, since the resulting amide group, when coupling TBO and 2-naphthoyl chloride, should have a

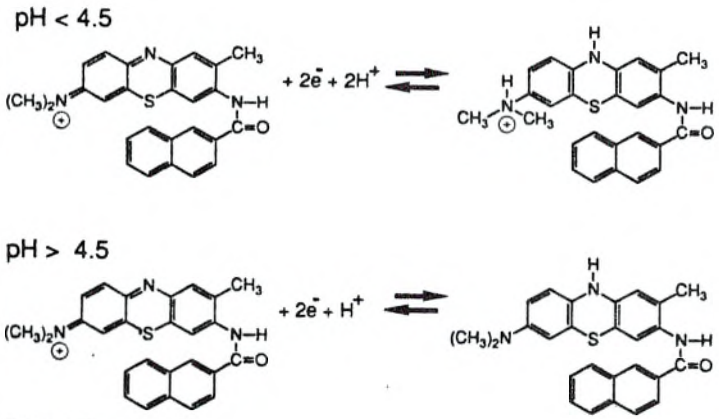

Scheme 3.

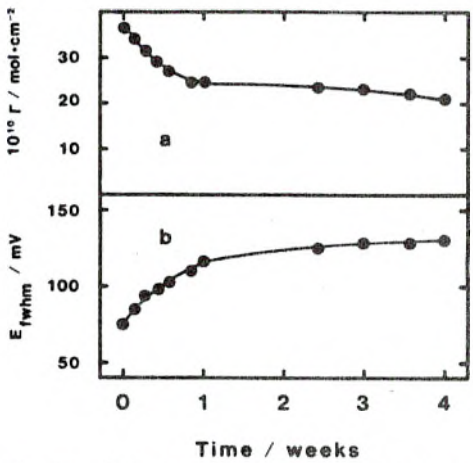

Fig. 6. (a) Variation of the apparent surface coverage, Γ, with the time that a 3-NTB modified electrode was stored at ambient temperature in 0.25 M phosphate buffer, pH 7.0. (b) Variation of the full width at half maximum, E_{fwhm}, of the oxidation peak of 3-NTB with time under the same conditions.

pK_a above 10 [38] and would therefore not be seen. A decrease in the pK_a of the dimethylamino group of 0.9 pH units compared with the parent molecule TBO dissolved in water is thus the result of the derivatization of position 3 and adsorption onto graphite. Likewise, an increase in the $E^{\circ\prime}$ value at pH 7.0 from -210 mV [20] to -135 mV (vs. SCE) is found. The derivatization gives an increased localization of the positive charge on the dimethylamino group of the oxidized 3-NTB. Since it is believed that a charged rather than an uncharged paraphenylenediimine structure is the more efficient catalytic structure [18,39], this is of importance for the properties of 3-NTB to oxidize NADH electrocatalytically.

The chemical stability of adsorbed 3-NTB was studied by storing an electrode at room temperature with the flat circular surface dipped into a buffer solution at pH 7.0. The electrode was periodically transferred to a measuring cell for determination of the apparent surface coverage and E_{fwhm} (see Fig. 6). The surface coverage decreased for the first week and then attained an almost stable value. This behaviour can be explained if it is assumed that the mediator moves inwards to unoccupied adsorption sites in the pores of the graphite where it is less accessible. The observed peak broadening and the increase in ΔE_p that occurred simultaneously could be due to an increased current contribution from molecules in narrow pores where proton gradients and uncompensated resistances will be larger. No new peaks were observed on the aged electrode in the range -500 to $+300$ mV (vs. SCE). Desorption and chemical degradation of 3-NTB cannot be excluded as part of the explanation. It was noted in separate experiments that the surface coverage decreased rapidly if the electrode was transferred repeatedly between acid and alkaline solutions.

Electrocatalytic oxidation of NADH

The cyclic voltammogram in Fig. 3d demonstrates the electrocatalytic properties of adsorbed 3-NTB in a buffer solution containing 3.7 mM NADH. Compared with a cyclic voltammogram obtained in the absence of NADH (curve c), it can be seen that there is a great increase in the anodic peak current (from 32 to 86 μA). The behaviour can be explained by assuming that the NADH diffuses up to the electrode surface and reduces oxidized 3-NTB$^+$ in a chemical reaction. The reduced form of the mediator is then electrochemically reoxidized during the scan. For the same reason, the cathodic current is lower in the presence of NADH as the reduced form of the mediator (3-NTBH) is produced simultaneously in both a chemical and an electrochemical reaction. The apparent reaction thus proceeds as follows.

$$\text{3-NTBH} \rightleftharpoons \text{3-NTB}^+ + 2\,e^- + H^+ \quad (2)$$

$$\text{NADH} + \text{3-NTB}^+ \xrightarrow{k_1} \text{NAD}^+ + \text{3-NTBH} \quad (3)$$

$$\text{NADH} \rightarrow \text{NAD}^+ + 2\,e^- + H^+ \quad (4)$$

The chemical rate limiting step is given in eqn. (3) with a rate constant k_1. The back reaction of eqn. (3) should be negligible for thermodynamic reasons and because the reduced form of the mediator is rapidly reoxidized. The overall oxidation of NADH is given in eqn. (4).

The fact that the oxidation of NADH at the 3-NTB-modified electrode gives a peak at -130 mV (vs. SCE), i.e. very close to the $E^{\circ\prime}$ of the mediator itself (-135 mV), indicates a fast reaction rate between NADH and the adsorbed mediator. The result is a decrease in overvoltage by about 500 mV compared with the direct oxidation of NADH at unmodified graphite electrodes, which occurs at about $+400$ mV [9,40]. A hydrodynamic voltammogram was obtained by rotating the electrode in Fig. 3c with a rotational speed of 100 rad s^{-1} and sweeping the potential from -500 mV with a rate of 5 mV s^{-1}. The limiting catalytic current plateau was reached at -50 mV (vs. SCE).

The existence of a charge-transfer complex between nicotinamide co-enzymes and phenoxazine derivatives on chemically modified electrodes has been indicated by electrochemical methods [9,18] and also demonstrated to occur with a spectroscopic method [41]. It is believed that such a charge-transfer complex (CT), initially formed between the reactants, decomposes in a rate-limiting step for the entire reaction, analogous to kinetics of the Michaelis–Menten type, e.g.

$$\text{NADH} + \text{M}_{ox} \underset{k_{-1}}{\overset{k_{+1}}{\rightleftharpoons}} \text{CT} \xrightarrow{k_{+2}} \text{NAD}^+ + \text{M}_{red} \quad (5)$$

where M denotes the mediator. At a constant pH, the overall rate constant, k_1 (cf. eqn. 3), can then be expressed as

$$k_1 = k_{+2}/(K_M + [\text{NADH}]) \quad (6)$$

$$1/k_1 = K_M/k_{+2} + [\text{NADH}]/k_{+2} \quad (7)$$

where $K_M = (k_{-1} + k_{+2})/k_{+1}$. The mechanism may be more complicated than indicated by reaction (5), since it was also found that the reaction rate varies with the pH in the contacting solution [16–19].

The catalytic current, as seen by the rotating disk method, for a mediated catalytic reaction with a limiting chemical step is given by

$$i_{cat} = \frac{nFAk_1\Gamma^* c^* D^{2/3}\omega^{1/2}}{D^{2/3}\omega^{1/2} + 1.61\nu^{1/6}k_1\Gamma^*} \tag{8}$$

where c' is the bulk concentration (in mol cm^{-3}), ω is the rotational speed (in rad s^{-1}), D is the diffusion coefficient (in cm^2 s^{-1}) and ν is the hydrodynamic viscosity (in cm^2 s^{-1}) [42,43]. All the other parameters have their usual meaning. Inversion of eqn. (8) gives the derived Koutecký–Levich equation

$$\frac{1}{i_{cat}} = \frac{1}{nFAk_1\Gamma^* c^*} + \frac{1}{0.620nFA\nu^{-1/6}D^{2/3}c^*} \cdot \frac{1}{\omega^{1/2}} \tag{9}$$

where the first term represents the reciprocal current in the absence of any mass-transfer effects [44]. An alternative equation which relates the reciprocal current to the reciprocal bulk concentration is obtained by combining eqn. (9) with eqn. (6):

$$\frac{1}{i_{cat}} = \frac{1}{nFAk_{+2}\Gamma^*} + \left[\frac{K_M}{nFAk_{+2}\Gamma^*} + \frac{1.61\nu^{1/6}}{nFAD^{2/3}\omega^{1/2}}\right] \cdot \frac{1}{c^*} \tag{10}$$

The electrocatalytic current of the NADH oxidation increased with increasing rotational speed and showed a curvature in plots of i vs. $\omega^{1/2}$ (Levich plot). Strictly linear plots were obtained when eqn. (9) (Koutecky–Levich plot) was used, yielding intercepts that differed from zero for the various concentrations of NADH. The apparent k_1 can be calculated from the intercept if the surface coverage and the concentration of NADH are known.

Figure 7 shows a typical result of a plot of the reciprocal apparent k_1 vs. the corresponding NADH concentration (eqn. 7) for an electrode modified with 3-NTB. A linear relation was only found at higher concentrations of NADH. This behaviour was observed for each individual electrode studied. By extrapolation of the linear part of the curves to an NADH concentration of zero, as indicated in Fig. 7, a rate constant $k_{1(c=0)}$ of $1.4 \pm 0.2 \times 10^4$ $(M\ s)^{-1}$ (SD, $n = 5$) was found. From the extrapolated lines the constants k_{+2} and K_M in eqn. (7) were calculated to be $34 \pm 1\ s^{-1}$ and 2.5 ± 0.3 mM, respectively.

The deviation from linearity occurred at an NADH concentration just below the calculated K_M value. The K_M value found for the phenothiazine derivative is higher than for most of the previously studied phenoxazine derivatives (0.2–1.1 mM) [9,16–18]. A curved rather than a straight line has been observed earlier with a derivative of Nile Blue A and 1-pyrenecarboxaldehyde [16].

When all the data in the concentration range investigated were used, a plot of $1/i$ vs. 1/[NADH] for a fixed rotational speed (eqn. 10) also resulted in discrepancy from a linear relationship, although less pronounced. When the data from the linear

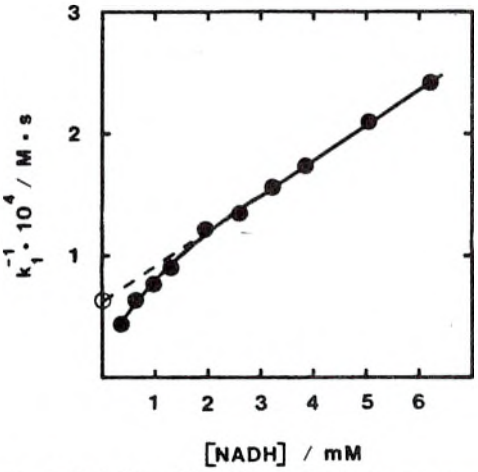

Fig. 7. Variation of the reciprocal apparent rate constant, $(k)^{-1}$, with the concentration of NADH for an electrode modified with 3-NTB. 0.25 M phosphate buffer, pH 7.0; surface coverage: 0.78 nmol cm^{-2}; applied voltage: 0 mV (vs. SCE).

part of Fig. 7 were used in the evaluation, regression analysis gave strictly linear plots. The lines, corresponding to different rotational speeds, intersected at a common intercept as postulated by eqn. (10).

Figure 8 illustrates the variation of the catalytic current with the surface coverage of 3-NTB when the NADH concentration and the rotational speed are kept

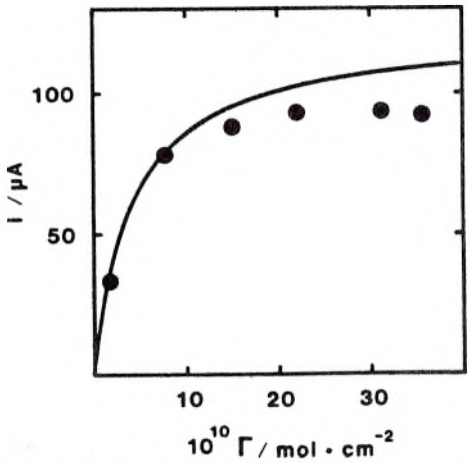

Fig. 8. Variation of the catalytic current, i, with the surface coverage, Γ, of 3-NTB in 0.25 M phosphate buffer, pH 7.0, containing 3.6 mM NADH. Rotational speed: 100 rad s^{-1}; applied voltage: 0 mV (vs. SCE). The solid curve was calculated from the kinetic data.

constant. The response is almost independent of the coverage above 2 nmol cm^{-2}. The solid curve in the figure shows the theoretical response based on the model of a charge-transfer complex. This curve was calculated by combining eqn. (6) with eqn. (8) and using a diffusion coefficient for NADH of 2.4×10^{-6} cm^2 s^{-1} [40] and the rate constants k_{+2} and K_M reported above. The deviation between the calculated and the measured response at higher coverages may be the result of diminished access for NADH to the mediator when a monolayer or multilayers are formed, or of slow charge transport in the mediator multilayer film [42,44,45].

The 3-NTB-modified electrode as an NADH sensor

The sensor properties of electrodes modified with 3-β-naphthoyl-Toluidine Blue O were investigated by flow injection analysis (FIA). Normal surface coverages were 4–8 nmol cm^{-2} when the electrodes were mounted in a flow-through amperometric cell of the confined wall–jet type [10].

Figure 9 demonstrates the linear current response for consecutive injections of some NADH samples in the FIA system. When the effective surface concentration of NADH is below K_M, pseudo-first-order reaction kinetics are expected if the apparent rate constant, k, and the pH can be considered constant (cf. eqn. 6). In such a case, a linear variation of the current response with the concentration should be the result. With an injection volume of 50 μl, the dispersion coefficient [46] was 1.3 at a flow rate of 0.85 ml min^{-1}, allowing a sample throughput of 150 h^{-1}.

The response of the 3-NTB-modified electrodes, in 0.1 M phosphate buffer at pH 7.0 and in 0.15 M pyrophosphate buffer at pH 9.0, was investigated in the

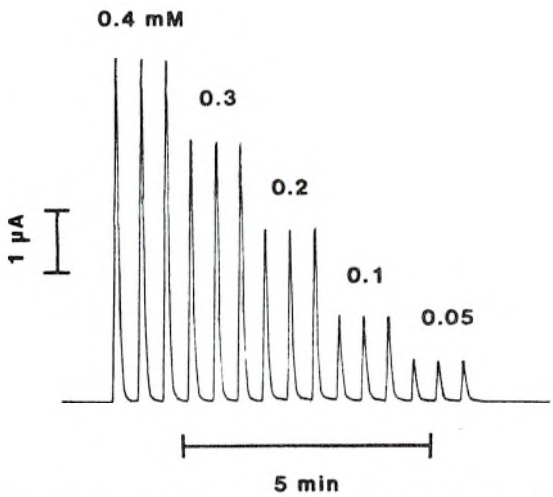

Fig. 9. Response of a 3-NTB-modified electrode mounted in the FIA system for consecutive 50 μl injections of NADH samples. Carrier: 0.1 M phosphate buffer, pH 7.0; flow rate: 0.85 ml min^{-1}; surface coverage: 4.7 nmol cm^{-2}; applied voltage: 0 mV (vs. Ag/AgCl/0.1 M KCl.

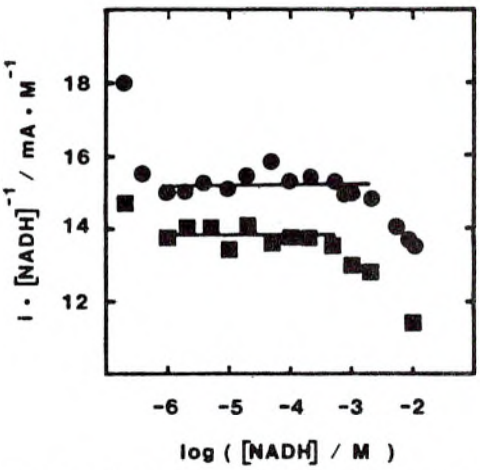

Fig. 10. Calibration data from FIA measurements showing the variation of the sensitivity, $i \cdot [NADH]^{-1}$, with the logarithm of the NADH concentration for two 3-NTB modified electrodes in buffers of different pHs. (●) In 0.1 M phosphate buffer, pH 7.0 ($\Gamma = 5.2$ nmol cm^{-2}); (■) in 0.15 M pyrophosphate buffer, pH 9.0 ($\Gamma = 6.5$ nmol cm^{-2}). The solid lines indicate the linear range and the average sensitivity. FIA conditions as in Fig. 9.

concentration range 0.01 μM to 10 mM NADH. The result is presented in Fig. 10, from which the linear range and the average sensitivity were evaluated (see Table 1). Strictly linear calibration graphs were obtained from 1 μM to 2 mM at pH 7.0 ($r = 0.99996$) and from 1 μM to 0.5 mM at pH 9.0 ($r = 0.999998$). The upper linear limit can easily be extended by reducing the injection volume. The repeatability was 0.2–1.0% RSD ($n = 6$ at each concentration) at both pHs, where the larger value applies to the lower part of the linear range where the S/N ratio is lower. Blank injections of buffer only gave rise to transients of about 2 nA. The detection limit was set as twice the current response of a blank injection. Different electrodes with various coverages yielded a response of 15 ± 1 mA M^{-1} (SD, $n = 4$) at pH 7.0.

The pH dependence for the NADH response is shown in Fig. 11. It can be seen that the response decreases as the pH increases. Increasing the NADH concentration from 100 μM to 1 mM gave an almost identical sensitivity at each pH

TABLE 1

Calibration data of 3-NTB-modified electrodes at pH 7 and pH 9 based on 12 and 9 NADH concentrations, respectively

pH	Average sensitivity/ mA M^{-1} (SD)	Slope of log–log plot (95% confidence level)	Detection limit/μM	Upper linear limit/mM
7.0	15.2 ± 0.3	1.001 ± 0.006	0.2	2
9.0	13.8 ± 0.2	0.997 ± 0.007	0.2	0.5

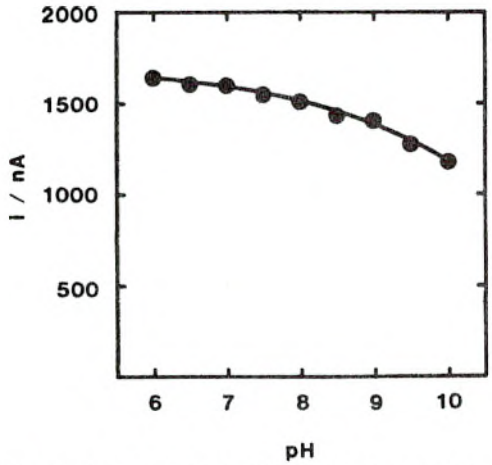

Fig. 11. Response of a 3-NTB-modified electrode in 0.1 M phosphate buffers of different pHs. NADH concentration: 100 μM; surface coverage: 7.5 nmol cm^{-2}. FIA conditions as in Fig. 9.

investigated. Similar results were also found with the rotating disk device with a rotational speed of 100 rad s^{-1} at high coverage and low NADH concentrations. The sensitivity decreased somewhat more at high pHs for a rotational speed of 200 rad s^{-1}. A pH-dependent response indicates that the reaction at the surface of the CME is under partial kinetic rather than under full mass-transfer control. The pH dependence is much less, 15%, than that of the previously described stable alkaline derivative of Nile Blue A and terephthaloyl chloride [47], where the response decreased by 60% from pH 6 to pH 9. The 3-NTB-modified electrode is thus in terms of pH sensitivity the most ideal sensor for NADH oxidation up to now.

A comparison was made between the responses to 100 μM solutions of different pHs at a naked electrode held at a potential of +400 mV (vs. Ag/AgCl/0.1 M KCl) and a 3-NTB CME held at 0 mV. The NADH solutions were pumped continuously through the FIA system to obtain a steady-state current. The limiting current plateau is reached at +400 mV for the naked electrode [10]. No electrode fouling [2,40] of the naked graphite electrode was noticed for this NADH concentration over the experimental time period of 5 min. At the 3-NTB CME, 99 and 95% of the limiting currents at the naked graphite electrode were obtained at pH 6.0 and 7.0, respectively. An almost mass transfer-controlled response current is thus indicated at acid pHs for the 3-NTB-modified electrode in this flow system and at low concentrations of NADH.

A comparison was also made with a Meldola Blue-modified electrode [9,10] with a coverage of 6.9 nmol cm^{-2}. Injection of various NADH samples gave a sensitivity of 16.5 mA M^{-1} at pH 7.0. The comparable sensitivities of Meldola Blue and 3-NTB at pH 7.0 and the variation of k_1 for 3-NTB with the NADH concentration (cf. Fig. 7) suggest that the rate constants (k_1) for the mediators are of the same order at low NADH concentrations.

The chemical and electrochemical stabilities of a 3-NTB CME in an alkaline solution were studied by continuously operating the electrode in 0.15 M pyrophosphate at pH 9.0 for 3.5 h. The initial response when 50 μl of a 170 μM NADH sample was injected every 60 s was 14.7 mA M^{-1} (0.5% RSD, $n = 20$). 1 h and 2 h later, the responses were 14.2 mA M^{-1} (0.6% RSD, $n = 20$) and 14.1 mA M^{-1} (0.4% RSD, $n = 20$), respectively. The initial and final coverages were 6.4 and 5.8 nmol cm^{-2}, respectively. No decomposition of NADH in the stock solution could be detected by spectrophotometric measurement after 2.5 h.

CONCLUSION

The 3-NTB-modified electrode could be considered to be the most suitable choice for the indirect detection of substrates when combined with dehydrogenases having pH optima in the alkaline region. The adsorbed 3-NTB mediator combines stability in the alkaline region (pH 7–10) with a high reaction rate with NADH. It gives a sensor with a linear response over nearly three decades in NADH concentration and its response is almost mass transfer-limited at pH 6. The pH dependence of the NADH sensor is much reduced compared with the sensors based on phenoxazine derivatives described before.

Graphite electrodes chemically modified by adsorbed phenoxazine or phenothiazine derivatives exhibit the same basic electrochemical properties. However, two main differences in the electrocatalytic oxidation of NADH appear compared with the phenoxazine derivatives studied earlier. First, the assumed rate-limiting decomposition of the charge-transfer complex shows a less pronounced dependence on the pH in the contacting solution. This might be the consequence of both energetic and steric effects. A comparably high $E^{\circ\prime}$ value reflects an increase in the electron acceptor properties for the new mediator, which should favour the formation of the complex and the subsequent decomposition wherby the overall reaction rate will be increased [48]. A possible steric effect can be the result of a different orientation of the mediator on the electrode surface [41] or of a different conformation of the NADH–mediator complex. The second difference is the observed deviation from the kinetic model of the Michaelis–Menten type at low concentrations of NADH. The relatively high K_M value may be the reason for this. These differences will be the subject of future studies.

ACKNOWLEDGEMENTS

The author thanks Dr. L. Gorton and Professor G. Johansson for valuable discussions concerning this paper. Financial support from the Swedish Board for Technical Development (STUF) is gratefully acknowledged.

REFERENCES

1 T. Yao in D.L. Wise (Ed.), Applied Biosensors (Biotechnology series 12), Butterworths, Boston, 1989, pp. 321–348.

2 J. Moiroux and P.J. Elving, J. Anal. Chem., 50 (1978) 1056.
3 D.C.-S. Tse and T. Kuwana, Anal. Chem., 50 (1978) 1315.
4 C. Degrand and L.L. Miller, J. Am. Chem. Soc., 102 (1980) 5728.
5 A. Torstensson and L. Gorton, J. Electroanal. Chem., 130 (1981) 199.
6 H. Jaegfeldt, T. Kuwana and G. Johansson, J. Am. Chem. Soc., 105 (1983) 1805.
7 L.L. Miller, B. Zinger and C. Degrand, J. Electroanal. Chem., 178 (1984) 87.
8 K. McKenna, S.E. Boyette and A. Brajter-Toth, Anal. Chim. Acta, 206 (1988) 75.
9 L. Gorton, A. Torstensson, H. Jaegfeldt and G. Johansson, J. Electroanal. Chem., 161 (1984) 103.
10 R. Appelqvist, G. Marko-Varga, L. Gorton, A. Torstensson and G. Johansson, Anal. Chim. Acta, 169 (1985) 237.
11 G. Marko-Varga, R. Appelqvist and L. Gorton, Anal. Chim. Acta, 179 (1986) 371.
12 J. Emneús, R. Appelqvist, G. Marko-Varga, L. Gorton and G. Johansson, Anal. Chim. Acta, 180 (1986) 3.
13 M. Kotoucek and J. Tomásová and S. Durcáková, Collect. Czech. Chem. Commun., 34 (1969) 212.
14 M. Kotoucek and J. Zavadilova, Collect. Czech. Chem. Commun., 37 (1972) 3212.
15 H. Huck, Fresenius' Z. Anal. Chem., 313 (1982) 548.
16 B. Persson, L. Gorton and G. Johansson in J.-L. Aucouturier, J.-S. Cautrape, M. Destriau, P. Hagenmuller, C. Lucat, F. Menil, J. Portier and J. Salardenne (Eds.), Proc. 2nd Int. "Meeting on Chemical Sensors", Imprimerie Biscaye, Bordeaux, 1986, p. 584.
17 L. Gorton, B. Persson, M. Polasek and G. Johansson, Proceedings of ElectroFinnAnalysis Conference, Plenum Press, New York, in press.
18 L. Gorton, J. Chem. Soc., Faraday Trans. 1, 82 (1986) 1245.
19 L. Gorton, G. Johansson and A. Torstensson, J. Electroanal. Chem., 196 (1985) 81.
20 J.M. Ottaway in E. Bishop (Ed.), Indicators, Pergamon Press, Oxford, 1972, pp. 498–503.
21 J.F. Thorpe, J. Chem. Soc., 91 (1907) 324.
22 H.T. Howard and G.R. Ramage in E.H. Rodd (Ed.), Chemistry of Carbon Compounds, Vol. 4c, Heterocyclic Compounds, Elsevier, Amsterdam, 1960, pp. 1544–1553.
23 H.P. Bennetto, J.L. Stirling and K. Tanaka, Chem. Ind. (London), 20 (1985) 695.
24 E. Laviron, J. Electroanal. Chem., 52 (1974) 355.
25 M.R. McKamey and L.A. Spitznagle, J. Pharm. Sic., 64 (1975) 1456.
26 A.J. McQuillan and M.R. Reid, J. Electroanal. Chem., 194 (1985) 237.
27 M.E.G. Lyons, H.G. Fay, C. Mitchell and D.E. McCormack, Anal. Chem. Symp. Ser., 25 (1986) 285.
28 E. Laviron in A.J. Bard (Ed.), Electroanalytical Chemistry, Vol. 12, Marcel Dekker, New York, 1982, pp. 53–157.
29 R.W. Murray in A.J. Bard (Ed.), Electroanalytical Chemistry, Vol. 13, Marcel Dekker, New York, 1984, pp. 191–368.
30 R.W. Murray, Acc. Chem. Res., 13 (1980) 135.
31 E. Laviron, J. Electroanal. Chem., 52 (1974) 395.
32 A.J. Bard and L.R. Faulkner, Electrochemical Methods, Fundamentals and Applications, Wiley, New York, 1980, pp. 521–522.
33 E. Laviron, J. Electroanal. Chem., 101 (1979) 19.
34 H. Huck, Ber. Bunsenges. Phys. Chem., 87 (1983) 945.
35 B.P. Nikolskii and V.V. Palchevskii, Bull. Acad. Sci. U.S.S.R., Div. Chem. Sci., (1957) 547.
36 B.P. Nikolskii and V.V. Palchevskii, Zh. Fiz. Chim., 32 (1958) 1280.
37 H.K. Hall, Jr., J. Phys. Chem., 60 (1956) 63.
38 J.D. Roberts and M.C. Caserio, Basic Principles of Organic Chemistry, 2nd ed., W.A. Benjamin, Massachusetts, 1981.
39 A. Kitani and L.L. Miller, J. Am. Chem. Soc., 103 (1981) 7636.
40 J. Moiroux and P.J. Elving, J. Am. Chem. Soc., 102 (1980) 6533.
41 Ni Fang, H. Feng, L. Gorton and T.M. Cotton, Langmuir, in press.
42 C.P. Andrieux, J.M. Dumas-Bouchiat and J.M. Savéant, J. Electroanal. Chem., 114 (1980) 159.
43 C.P. Andrieux, J.M., Dumas-Bouchiat and J.M. Savéant, J. Electroanal. Chem., 123 (1981) 171.

44 R.W. Murray, Philos. Trans. R. Soc. London, Ser. A, 302 (1981) 253.
45 F.C. Anson, J.M. Savéant and K. Shigehara, J. Phys. Chem., 87 (1983) 214.
46 J. Ruzicka and E.H. Hansen in P.J. Elving and J.D. Winefordner (Eds.), Flow Injection Analysis, Wiley, New York, 1981, pp. 15–17.
47 M. Polasek, L. Gorton, R. Appelqvist, G. Marko-Varga and G. Johansson, Paper in doctoral thesis, Roger Appelqvist, University of Lund, 1987.
48 S. Fukuzumi, N. Nishizawa and T. Tanaka, J. Org. Chem., 49 (1984) 3571.

ERRATA IN FIRST PROOF.

page	line	written	corrected
3	13	Cat. No. 29.896-4	D. 12.580-6
4	22	3-NTS	3-NTB
9	5	a k value	a k_{app} value
16	4	r=0.999998	r=0.99998
18	3	3.5 h	2.5 h

IV

A comparative Study of Some 3,7-Diaminophenoxazine Derivatives and Related Compounds for Electrocatalytic Oxidation of NADH.

Björn Persson and Lo Gorton

Dept. of Analytical Chemistry, University of Lund, P.O. Box 124, S-221 00 Sweden

ABSTRACT

The electrocatalytic oxidation of reduced nicotinamide adenine dinucleotide (NADH) at chemically modified electrodes (CMEs) based on some enlarged heterocyclic aromatic structures is investigated. On the basis of a phenoxazinium structure, the influences of different amino substituents in position 3 and 7, the hetero-atom in position 5, and of a benzene ring in the 1,2 position, on the electrocatalysis are documented. From the parent molecules Neutral Red (I), Toluidine Blue O (II), Brilliant Cresyl Blue (III), and Nile Blue A (IV), the homologous series consisting of the 7-dimethylamino-2-methyl-3-ß-naphthamido-phenazinium (VI), -phenothiazinium (VII), and -phenoxazinium (VIII) ions as well as the 7-diethylamino-3-ß-naphthamido-1,2-benzophenoxazinium (IX) ion were obtained by reacting the amine group in position 3 of the parent molecules with 2-naphthoyl chloride. By amination of Meldola Blue (V) with aniline the 3-anilino-7-dimethylamino-1,2-benzophenoxazinium (X) ion was obtained. The compounds (I-X) were adsorbed on graphite to give CMEs having formal redox potentials, E°', ranging from -630 to -135 mV vs SCE at pH 7. The acid-base properties of the adsorbed compounds were investigated by cyclic voltammetry in 0.25 M phosphate buffers in the pH range 2-11. The reaction rate of the electrocatalytic oxidation of NADH for compounds (VII-X) were evaluated from rotating disk electrode experiments. The dependence of the reaction rate on pH between the adsorbed compounds (VII-X) and NADH was studied in a single channel flow system with the CMEs mounted in a flow-through amperometric cell. The formation of a neutral imino structure of the derivatives at higher pHs, is shown to be the main limiting factor to obtain CMEs both with a stable and with a high sensitivity for NADH.

INTRODUCTION

The direct oxidation of reduced nicotinamide adenine dinucleotide (NADH) at conventional electrode materials is highly irreversible and coupled to fouling reactions, and the mechanism of the reaction has been thoroughly investigated in a series of publications [1-12]. The large overvoltage of about 1 V [7] faced for the direct oxidation, can be reduced to a large extent by the immobilization of electron mediating structures on the electrode surface [13-34]. A mediated electron transfer is achieved at chemically modified electrodes (CMEs) based on ortho-quinones [13-19], para-quinones [20], phenylenediimines [21], 5-alkylphenazines [22,23], phenoxazines [24-29], phenothiazines [30], 5-methylphenazinium- or tetrathiafulvalene-tetracyanoquinodimethane radical salts [31-33], and on nickel electrodeposited hexacyanoferrate [34]. The decrease in the overvoltage is mainly dictated by the formal potential, $E^{o'}$, of the mediator [35], and electrode fouling and interfering reactions may be prevented [36-38].

CMEs based on adsorption of phenoxazines onto graphite [24,25], indicated special features in terms of stability and a high reaction rate with NADH at low potentials with promising properties as sensors for NADH in conjugation with enzymatic analysis [37-39]. The continued strategy to improve the sensor properties of these CMEs has been based on the derivatization of commercial phenoxazine dyes [24]. A bis phenoxazine derivative was obtained by reacting 7-diethyl-3-amino-benzophenoxazinium, Nile Blue A, with terephthaloyl chloride [29,40]. This derivative showed an increased stability towards desorption caused by an enlargement of the aromatic structure, an increased alkaline stability since both positions 3 and 7 are hindered for nucleophilic attack [41-43] and an increased reaction rate with NADH due to an increase of the $E^{o'}$ of the new mediator compared with the parent compound. However, a pronounced decrease of the reaction rate between NADH and the mediator was observed at higher pHs which is a drawback for sensor making. A much less dependence on the reaction rate with pH was found in a recent study of a phenothiazine derivative, 3-ß-naphthoyl-Toluidine Blue O [30].

It is assumed that the basic catalytic structure of these derivatives is the charged paraphenylenediimine contained within the phenoxazines and the phenothiazines [27,30,44-46]. In order to further improve the mediator properties and to elucidate the mechanisms of the electrocatalytic oxidation of NADH at the CME, an extended knowledge of the influence of different substituent at different positions in the

Table 1. *The structural formulae, roman numbers, names, and abbreviations of the studied parent compounds and the 3-amino derivatives.*

Parent compounds	3-amino derivatives
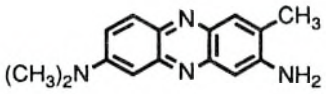	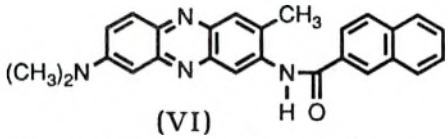
(I)	(VI)
Neutral Red	3-ß-Naphthoyl-Neutral Red
NR	3-NNR
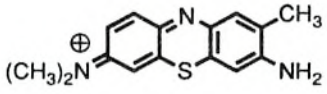	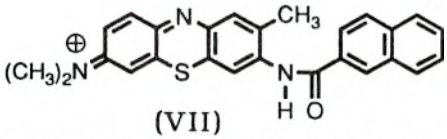
(II)	(VII)
Toluidine Blue O	3-ß-Naphthoyl-Toluidine Blue O
TBO	3-NTB
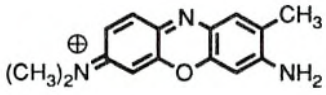	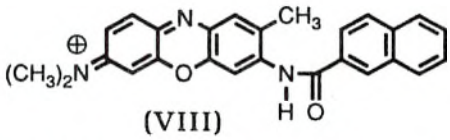
(III)	(VIII)
Brilliant Cresyl Blue	3-ß-Naphthoyl-Brilliant Cresyl Blue
BCB	3-NBCB
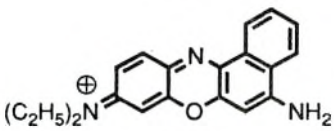	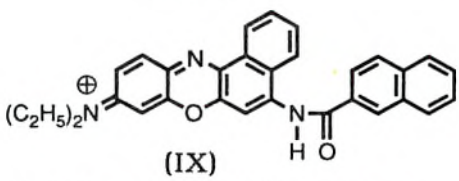
(IV)	(IX)
Nile Blue A	3-ß-Naphthoyl-Nile Blue A
NB	3-NNB
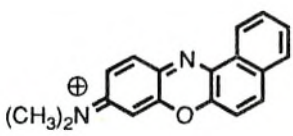	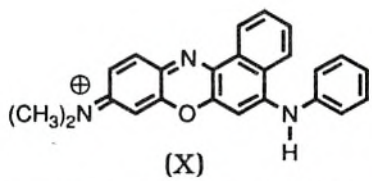
(V)	(X)
Meldola Blue	3-Anilino-Meldola Blue
MB	3-AMB

molecules is needed. In this paper a comparison is made of the electrocatalytic properties between three different adsorbed 3,7-diamino phenoxazine derivatives and of a homologous series of a phenazine, a phenoxazine and a phenothiazine derivative. The 3,7-diamino structures studied are summarized in Table 1.

EXPERIMENTAL

Synthesis and purification of the mediators

The derivatives (VI-X) were all prepared by reaction at position 3 of the commercial parent compounds (I-V), see Table 1. The derivatives (VI-IX) were synthesised by acylation. The syntesis of compound (X) was performed by amination of Meldola Blue (V) with aniline [47-49]. The obtained derivatives were all stored as the crystalline crude product in a dessicator over phosphorus pentoxide and were prior to use purified by column chromatography.

Neutral Red (Sigma, Cat. No. N-7005), Toluidine Blue O (Aldrich, Cat. No. 19.816-1), Brilliant Cresyl Blue (BDH, Cat. No. 34207 2Q), and Nile Blue A (Janssen, Cat. No. 20.696.359) were all reacted with 2-naphthoyl chloride (Fluka, Cat. No. 70680) in anhydrous pyridine in the presence of a molar excess of N,N-diisopropylethylamine (Aldrich, Cat. No. D12.580-6), a hindered non-nucleophilic base. The method, earlier described in the synthesis, purification, and identification of 3-NTB [30], is based on the procedure used by Huck [24] in the synthesis of 3-NNB with ethanol as solvent and K2CO3 as base. The procedure used is examplified by the preparation of 3-NBCB.

<u>7-dimethylamino-2-methyl-3-ß-naphthamido-phenoxazinium chloride, 3-NBCB</u>

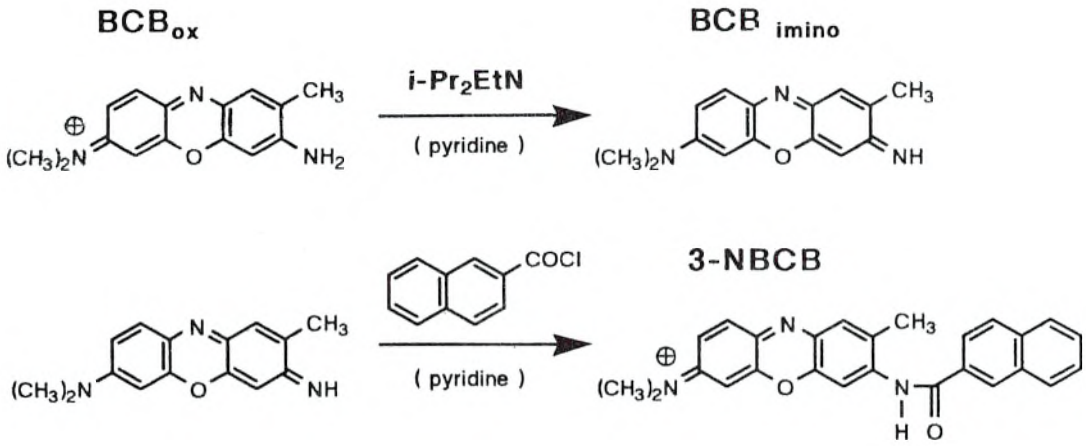

To a solution of 1 g (1.3 mmole) of Brilliant Cresyl Blue in 100 ml of anhydrous pyridine an amount of 0.5 ml (2.8 mmole) of N,N-diisopropyl-ethylamine was added. No colour change was observed. After 5 min stirring the remaining solids were filtered of and an amount of 0.3 g (1.6 mmole) of 2-naphthoyl chloride was added to the mixture. The colour of the solution changed from blue to blue-violet within one minute. The mixture was stirred at room temperature for another 30 min before the greater part of the pyridine was removed by evaporation. The residue of the mixture was diluted with dichloromethane and transferred to a separating funnel. The mixture was washed repeatedly, first with 5 mM HCl and then with water. After evaporation of the organic solvent the crude product was dried in a dessicator over phosphorus pentoxide.

In the syntheses of the other three derivatives some observations were made that differed from that observed when synthesising 3-NBCB. The solubility of NB was poor in pyridine. The addition of the base caused a colour change of the mixtures, which was for NR, from red to red-amber with yellow fluorescence, and for TBO and NB, from blue to red-violet. The colour change after the addition of the acid chloride was in the case of NR to red, and in the other two cases to violet or blue-violet. In general, the exclusion of the washing step resulted in a failure to obtain crystalline crude products. In the case of NR the yield was moderate and the washing procedure was performed with water only to avoid losses of the product.

3-Anilino-7-dimethylamino-1,2-benzophenoxazinium chloride, 3-AMB

A mixture consisting of 0.5 g (1.6 mmole) of Meldola Blue (Boehringer Mannheim, Cat. No. 258 504) and an amount of 1 ml (11 mmole) of freshly destilled aniline (Fluka, Cat. No. 10400) was heated on a water-bath under stirring for 30 min. After the addition of 20 ml of ethanol (99.5%), the blue-green mixture was allowed to stand at room temperature for another 30 min. The addition of 20 ml of alkaline ethanol (NaOH) caused a precipitation of the brown base. After removal by filtration, the product was twice recrystallized from 30 ml of acidic ethanol yielding 0.15 g of a green solid.

Purification of the crude products were performed on columns (i.d. 1 cm) packed with a slurry of Silica gel 60 (Merck, Art. 9385) in 1,4-dioxan or acetone to a depth of about 10 cm. Saturated solutions of the crude products were applied on top of the columns. The derivatives were then purified by the following procedures.

3-NNR was dissolved in acetone. The column was eluted with acetone giving the main product in an orange tailing band with a yellow front. 3-NTB was dissolved in pyridine and 3-NBCB in 1,4-dioxan. In both cases, a first red fraction was eluted with 1,4-dioxan, leaving a violet band on top of the column. The main product was then eluted as a violet tailing band with 1,4-dioxan containing 2% (v/v) N,N-diisopropyl-ethylamine. A blue band remained on top of the column in both cases. 3-NNB and 3-AMB were both dissolved in acetone. In both cases a weak red-violet tailing band containing the main product was eluted with acetone. A more concentrated fraction of the main product as a violet tailing band was obtained by a second elution with acetone containing 2% (v/v) N,N-diisopropylethylamine. For both compounds a weak blue band remained on top of the column.

7-diethylamino-1,2-benzophenoxazin-3-one, Nile Red, was obtained from Aldrich (Cat. No. 29.839-5). 3-benzoyl-Nile Blue A was obtained according to the method described by Huck [24] by reacting Nile Blue A with benzoyl chlorid (Aldrich, Cat. No. 25.995-0) and purified by the washing step only.

Electrochemical studies of the adsorbed mediators

Spectrographic graphite rods (RW001, Ringsdorff-Werke, GmbH) were polished on wet fine emery paper (Tufbak Durite, P1200). The flat circular surface of 0.0731 cm^2 was washed with a jet of deionized water before and after the pressfitting of the electrodes into a Teflon holder. Modification of the electrode surface with compounds (I-V) was made by dipping the electrode into an alcoholic solution containing 0.1 - 1 mM of the commercial dye used as purchased. Modification of the electrode surface with the synthesised derivatives (VI-X) was performed by dipping the electrode into a solution consisting of 20% (v/v) of freshly column chromatographed mediator, 10% anhydrous acetic acid and 70% acetone (acetic acid was not used when the modifier was 3-NNR). Depending on the desired surface coverage, Γ, either the dilution of the mediator solution with acetone was varied or the time the electrode was immersed in the mediator solution (10 s - 2 min). Finally, the electrode was washed in a buffer solution of the same compositon as was used in the measuring cell of the cyclic voltammetry set up.

The cyclic voltammetry set up for determination of the Γ consisted of a potentiostat with a sweep generator connected to a Houston XY-recorder (Omnigraphic 2000) and a measuring cell with a Pt gauze as the counter electrode and a saturated calomel electrode (SCE, Radiometer K-401) as the reference. The Γ of the adsorbed modifier was evaluated from the integrated anodic peak of a single linear scan ($E^{\circ\prime} \pm$ 200 mV at 50 mV s^{-1}), corrected for the background current.

Phosphate buffer solutions of various pHs (2-11) were prepared by mixing two filtered (Millipore, Art. HAWPO4700, pore size 0.45 µm) stock solutions of 0.25 M NaH_2PO_4 (Merck, Art. 6346) and of 0.25 M Na_3PO_4 (Kebo-Lab, Sweden, Art. 1.3278). Citrate buffer solutions (pH 2-6) were prepared in the same way from 0.25 M citric acid (Merck, Art. 244) and 0.25 M tri-sodium citrate (Merck, Art. 6448). The pH was measured with a combined pH-electrode (Radiometer, GK2421C) connected to a pH-meter (Radiometer, model PHM 64), calibrated with standard solutions of pH 3, 7 and 9 (Merck, Art. 9434, 9439 and 9461). All electrochemical measurements were performed in deareated buffer solutions, at 23 ± 1 °C.

The formal potential, $E^{\circ\prime}$, of the adsorbed mediators was evaluated by taking the mean value of the anodic and cathodic peak potentials [50]. The variation of the $E^{\circ\prime}$-value with pH was investigated in the cell mentioned above, by varying the pH of the contacting buffer solution successively by the addition of the corresponding acid or base and recording cyclic voltammograms with a BAS 100-A Electrochemical Analyzer at each pH. The cyclic voltammograms were obtained with a single sweep starting in the cathodic direction and cycled at least ± 100 mV around the particular $E^{\circ\prime}$ at a rate of 50 mV s^{-1}. The pH of the contacting solution was continuously followed by the pH-electrode. The $E^{\circ\prime}$-value of dissolved Meldola Blue was determined with the use of a hanging mercury drop electrode (HMDE, Metrohm mod. E410).

Rotating disk electrode (Tacussel, mod. EDI) experiments were made in a cell initially containing 12 ml of a deareated buffer solution at pH 7.0. The rotational speed was varied between 50 and 200 rad s^{-1}. The background currents were less than 0.1 µA and any corrections could therefore be omitted. A Pt wire encircling the cell was used as the counter electrode and a SCE equipped with a Luggin capillary was used as the reference. The NADH content in the cell was varied by injecting various volumes (50-200 µl) of NADH stock solutions to the buffer.

The flow injection system consisted of a peristaltic pump (Gilson Minipuls 2), a pneumatically operated injection valve (Cheminert, type SVA) and a flow-through amperometric cell of the confined wall-jet type [38] under three electrode potentiostatic control using a Princeton Applied Research (model 174A) instrument. The applied potential was 0 mV versus an Ag/AgCl (0.1 M KCl) reference electrode, with a Pt wire as the counter electrode. The outlet jet-electrode distance was set to 1.8 mm [38]. A knotted micro-line tubing (Cole Parmer, i.d. 0.51 mm, volume 100 µl) was used as the connector between the injector and the inlet of the amperometric cell. All other connections were made of Teflon tubings (i.d. 0.5 mm).

All measurements were made at a carrier flow rate of 0.85 ml min^{-1}. Samples of NADH, dissolved in the same buffer solution as the carrier, were either injected with a 50 µl injection-loop with the responses read as the peak currents of the recordings, or continuosly pumped through the system with the recordings read as the steady-state currents.

1,4-Dihydronicotinamide adenine dinucleotide (NADH) was obtained from Sigma Chemical Co. (Cat. No. N-8129). The concentration of the coenzyme solutions was calculated from spectrophotometric assays at 340 nm using a molar absorptivity of 6220 $(M\ cm)^{-1}$.

RESULTS AND DISCUSSION

Formal potential and acid-base properties of the mediators

The redox reaction in aqueous solutions for phenazine, phenothiazine and phenoxazine derivatives occurs by the participation of two electrons [51]. The total number of protons that also participates in the redox process as well as the formal potential, $E^{o'}$, of a compound, may vary in accordance with functional groups in the aromatic skeleton [51]. Depending on the number of protons taking part in the redox process, the $E^{o'}$ will move with -90 mV/pH ($3H^+$), -60 mV/pH ($2H^+$), or -30 mV/pH ($1H^+$). A change of the slope, $\Delta E^{o'}/\Delta pH$, when pH is increased indicates a proton dissociation. A change in the slope value, e.g from -60 to -30, is caused by the reduced form (pK_r) and an opposite change, i.e from -30 to -60, by the oxidized form (pK_o) [52]. When derivatives of these structures are adsorbed on graphite the same basic redox

reaction with the participation of two electrons seems to hold true [25,26,30].

An initial investigation was made by cyclic voltammetry of graphite electrodes chemically modified with compounds (I-X) in 0.25 M phosphate buffer at pH 7 with no soluble mediator present in the solution. For each electrode, only a single electrochemical active compound was present on the surface as seen from the cyclic voltammograms (-700 to +300 mV vs SCE), except in the case of 3-NNR where the presence of NR could be detected. After some cycles of the 3-NNR CME at pH 3.5, the NR peak disappeared. All of the CMEs showed the typical behaviours of an electrochemical reversible redox reaction of an irreversibly surface immobilized redox species [53,54]; i.e., with constancy of the surface coverage on repeated cycling, with the anodic and the cathodic peaks almost mirror-images of each other, and with a moderate peak potential separation of 10-50 mV at surface coverages between of 0.4 to 5 nmole cm^{-2}, all at a sweep rate of 50 mV s^{-1}.

The variation of the formal potential, E°', with pH of the adsorbed parent compounds (I-III) and the adsorbed derivatives (VI-X) on graphite was measured in 0.25 M phosphate buffer in the pH range 2-11, by both varying the pH from the acid to the alkaline region and vice versa. MB and NB have earlier been studied at this laboratory under equal conditions [25,29]. The E°' for Nile Red and 3-benzoyl-Nile Blue were determined only at pH 7.0 and the values -475 and -220 mV vs SCE, respectively, were found.

The variation of E°' with pH resulted for each of the three compounds NR, TBO and BCB in one linear segment in the acid region with slopes of -77, -73 and -79 mV/pH, respectively, and one linear segment in the more alkaline region with slopes of -50, -32, and -33 mV/pH, respectively. From the intersection of the two linear segments the pK_r-values were obtained, see Table 2. In the case of TBO and BCB a sliding change of E°' with pH was noticed in the vicinity of the pK_r. A slope of -74 mV/pH was found when the experiment was repeated with BCB in 0.25 M citrate buffer solutions in the pH range 2-6, which indicates that the buffer capacities of the 0.25 M phosphate buffer solutions should be sufficient.

Some additional noteworthy observations were made in the investigation of the compounds (I-III) consisting of three aromatic rings. For TBO and BCB a decrease in the surface coverage was observed on repeated

TABLE 2. *Formal potentials, $E^{o'}$, versus SCE at pH 7.0, and pK_a-values of the reduced (pK_r) and oxidized (pK_o) forms of the compounds (I-V) in aqueous buffer solutions [51] and adsorbed on graphite. The $\Delta E^{o'}$- and ΔpK_r-values refer to the change from the soluble to the adsorbed state of the compound (assuming that the pKr_2 in solution and the pK_r on graphite can be ascribed to the dialkylamino group).*

	in aqueous solution				*on graphite*			
Compound	$E^{o'}$/mV	pK_{r1}	pK_{r2}	pK_o	$E^{o'}$/mV	pK_r	$\Delta E^{o'}$/mV	ΔpK_r
NR (I)	-565	5.3	6.2	6.8	-630	4.6	-65	-1.6
TBO (II)	-210	4.8	5.4	11.0	-285	4.2	-75	-1.2
BCB (III)	-195	4.6	6.3	10.7	-340	5.0	-145	-1.3
NB (IV)	-360	3.9	6.9	9.7	-420	5.3	-60	-1.6
MB (V)	-110*	-	-	-	-175	5.0	-65	-

**determined with cyclic voltammetry and HMDE*

cycling at lower pHs, mainly seen as a decrease in the anodic peak area after a cathodic sweep. For NR the decrease was more pronounced and with noticable tailing of the reduction and oxidation peaks. An increased water solubility is expected and therefore a decrease in the surface coverage due to the restricted number of aromatic rings as well as the protonation of the reduced forms (for NR also the oxidized form) at low pHs, resulting in a net positive charge of +2 of the reduced molecules (c.f. the pK_r-values of the compounds in solution).

In the earlier studies of adsorbed MB [25] and adsorbed NB [29], both containing four aromatic rings, two linear segments were found for both compounds with slope values close to -60 and -30 mV/pH in the acid and in the more alkaline region, respectively, giving the single pK_r-values presented in Table 2. No E°'-value of dissolved MB could be found in the litterature. For a comparison of the E°'-values of dissolved and adsorbed MB a tentative value at pH 7 of MB in solution was obtained using a HMDE. The cyclic voltammograms obtained with the HMDE revealed the typical shapes of a compound where the reduced

TABLE 3. *Formal potentials, $E^{o'}$, versus SCE at pH 7.0, and conditional pK_a-values of the compounds (VI-X) adsorbed on graphite. The $\Delta E^{o'}$-values (adsorbed state) refer to the change caused by the derivatisation of the parent 3-amino-7-dialkylamino compound. The ΔpK_a-values refer to the total effect on the pK_r-value of the 7-dialkylamino group and the pK_o-value of the substituent in position 3 caused by both the derivatisation of the parent compound and a change from the soluble to the adsorbed state. 3-AMB (X) is compared with NB (IV).*

Compound	*$E^{o'}$/mV*	*pK_r*	*pK_o*	*$\Delta E^{o'}$/mV*	*ΔpK_r*	*ΔpK_o*
3-NNR (VI)	*-545*	*4.4*	*3.0*	*85*	*-1.8*	*-3.8*
3-TBO (VII)	*-135*	*4.6*	*10.3*	*150*	*-0.8*	*-0.7*
3-NBCB (VIII)	*-180*	*5.2*	*10.3*	*160*	*-1.1*	*-0.4*
3-NNB (IX)	*-220*	*4.9*	*8.2*	*200*	*-2.0*	*-1.5*
3-AMB (X)	*-360*	*3.8*	*7.3*	*60*	*-*	*-2.4*

form is adsorbed or precipitated on the electrode surface [55]. Evaluating the E°'-value by taking the mean value of the peak potential of the anodic and cathodic waves thus inherently contributes to an error, and a true value of dissolved Meldola Blue cannot be found using this method. However, as shown in Table 2 a maked difference ($\approx$ -65 mV) in the E°'-values found for dissolved and adsorbed MB reflects a strong interaction of adsorbed Meldola Blue with the graphite surface.

A comparison of compounds containing different amino substituents dissolved in both water and organic solvents shows that a dialkylamino group is more easily protonated than an amino group [56], and therefore it is reasonable to assume that the pK_{r2} in Table 2 corresponds to the dialkylamino group in position 7 of the compound. Furthermore, it is likely that the single pK_r found for the adsorbed compounds (I-III) is an average of two pK_r-values. This is supported by the observations of an increased solubility of the reduced compounds in the acid region. If this is the case, slope values around -90 mV/pH in the acid region should be the result, unless other paramenters affect the surface reaction. No explanation of the intermediate slope values of compounds (I-III) can be given at this stage. The ΔpK_r-values given in

Table 2 are based on the assumptions mentioned above, although this may not hold true for Nile Blue A.

The results of the studies of the derivatives (VI-X) are shown in Fig. 1 a-e. Since each of the five compounds can exist in four different forms, the redox reactions that occur are described by the quadratic reaction schemes. In a scheme, the oxidised forms are shown on the left side and the reduced forms on the right, with the vertical arrows on the left and right side corresponding to the pK_o and pK_r-values, respectively. The predominant redox reaction between the two pK_a values is marked by the diagonal arrows. In the graphs all linear segments are extrapolated to pH=0 and the value of the apparent standard potential, E°, for the current redox reaction is given at the ordinate. Next to the linear segments the slope values are found, and from their intersections the conditional pK_a-values are given at the abscissa. The results are summarized in Table 3.

From the investigation of compounds (I-X) some general conclusions can be made of the effect of adsorption and derivatisation on the formal potential and the acid-base properties of the mediators. By changing the state of the mediator from soluble to adsorbed a decrease in the formal potential is seen for all of the parent compounds (c.f. Table 2). This reflects a more pronounced interaction of the oxidized form with the electrode surface than of the reduced form of the adsorbed aromatic redox compounds [53]. The decrease in E°' is counterbalanced by the derivatization in position 3 (c.f. Table 3), giving as a net result an increase in the E°' of the new adsorbed species compared with the value of the dissolved parent compound. A comparison between the E°'-values of compounds (VI-X) in solution and when adsorbed could not be performed due to the low solubility of the these compounds in aqueous solution.

Fig. 1a-e. *Variation of the formal potential, E°', vs SCE, of the derivatives (VI-X) adsorbed on graphite with pH in the contacting 0.25 M phosphate buffer solution. See text above for comments of schemes and figures.*

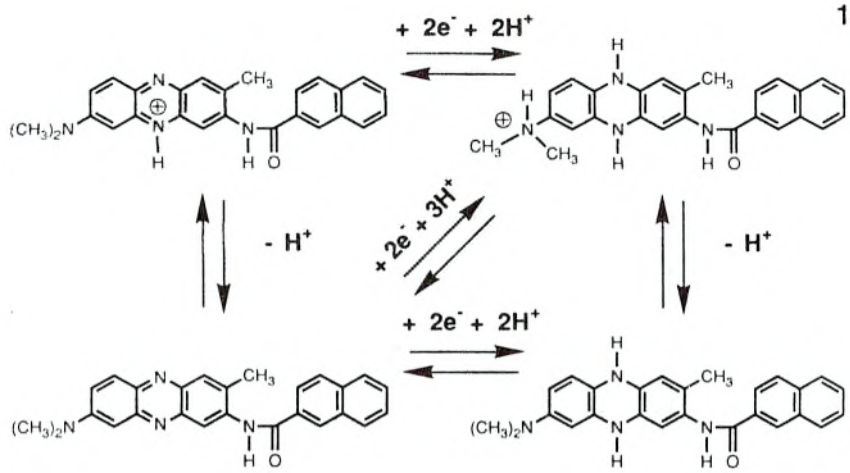

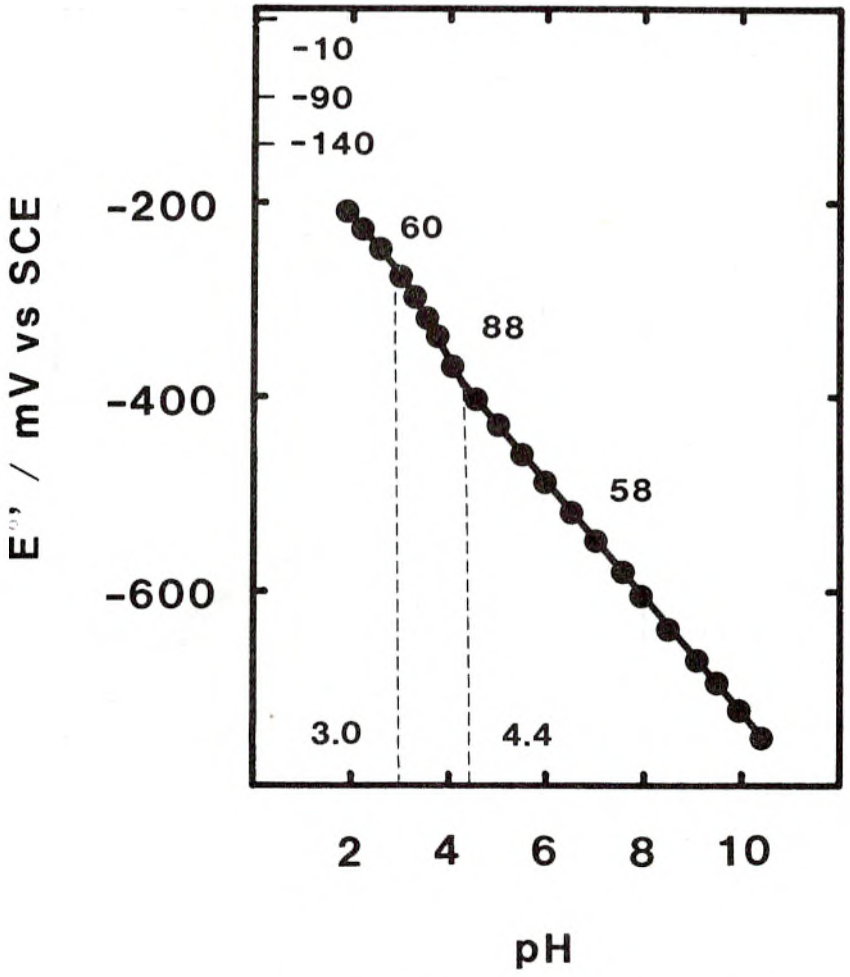

Fig. 1a. *3-ß-Naphthoyl-Neutral Red (VI)*

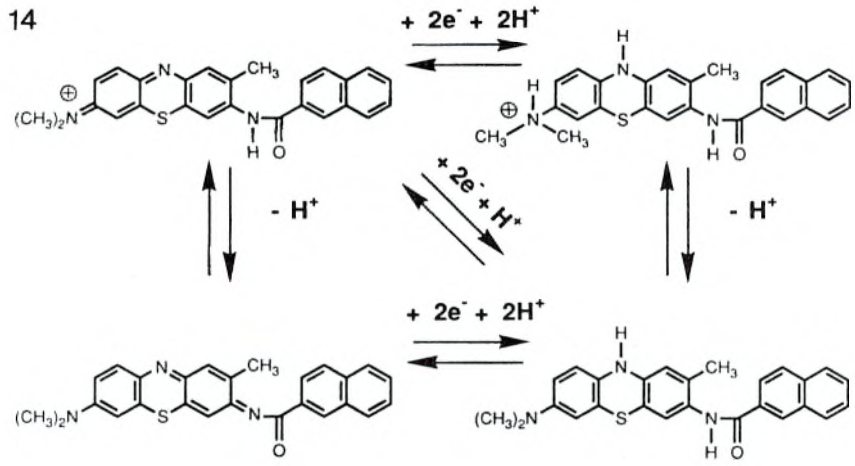

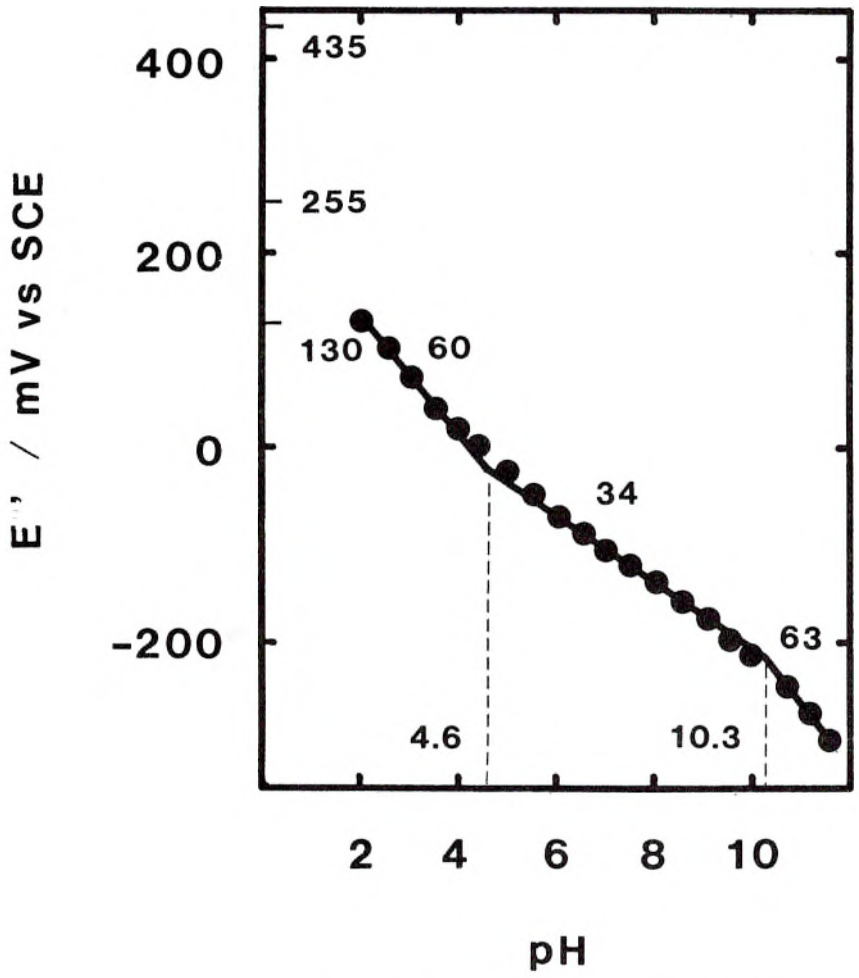

Fig. 1b. *3-ß-Naphthoyl-Toluidine Blue O (VII)*

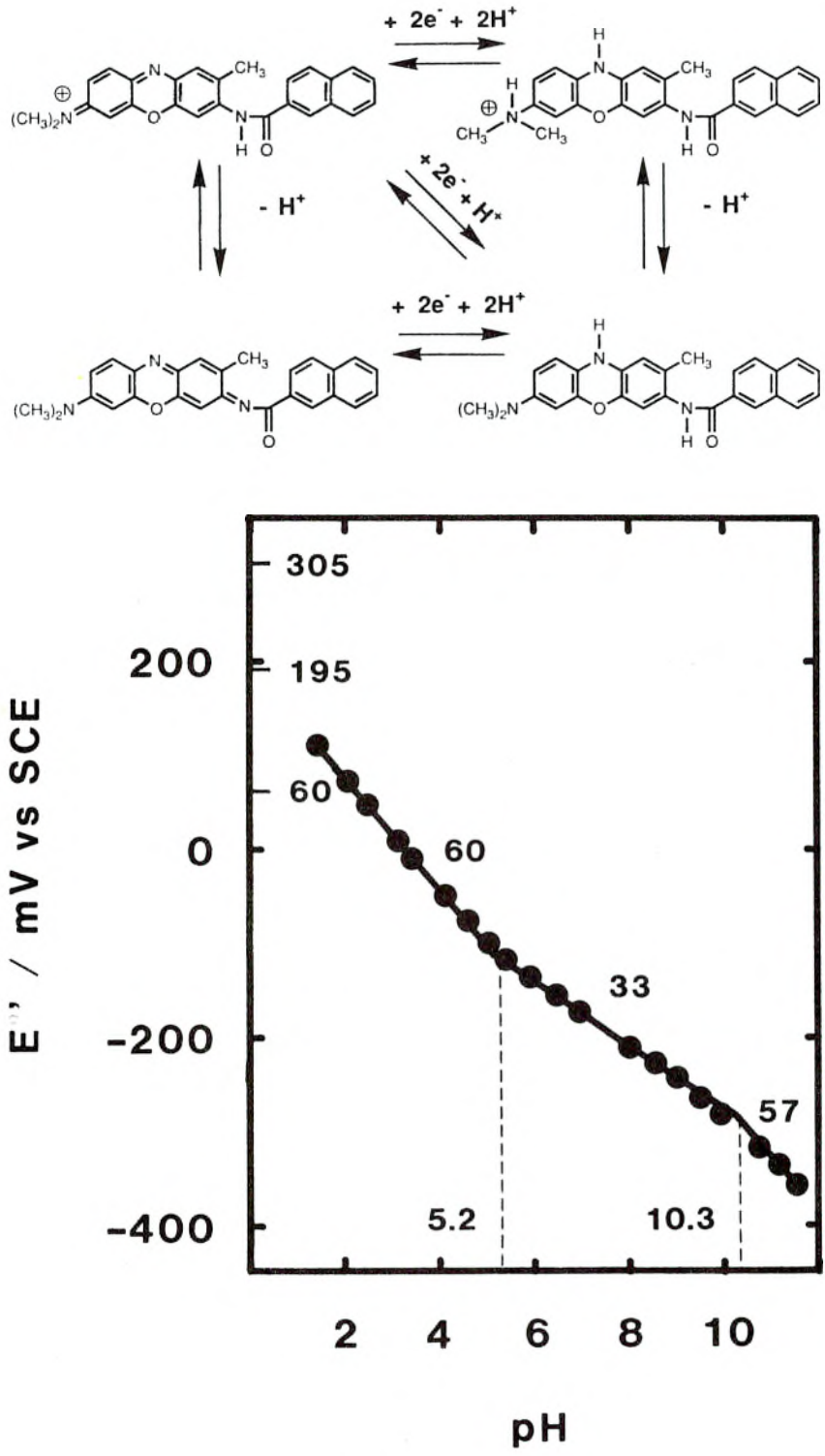

Fig. 1c. *3-β-Naphthoyl-Brilliant Cresyl Blue (VIII)*

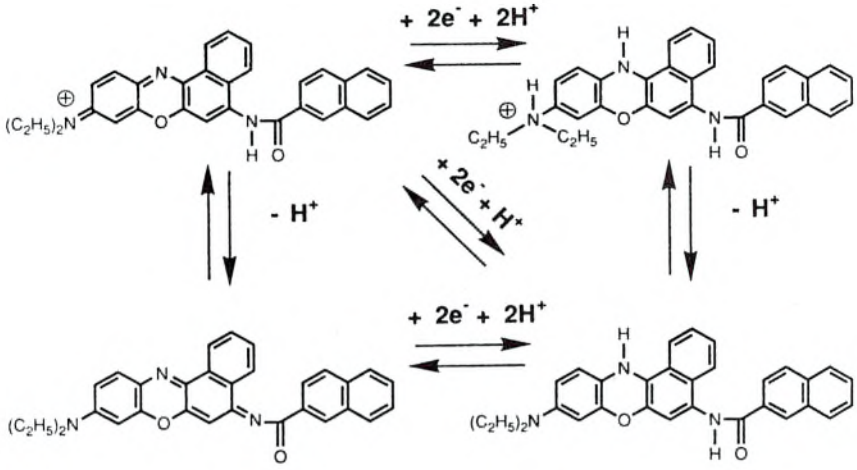

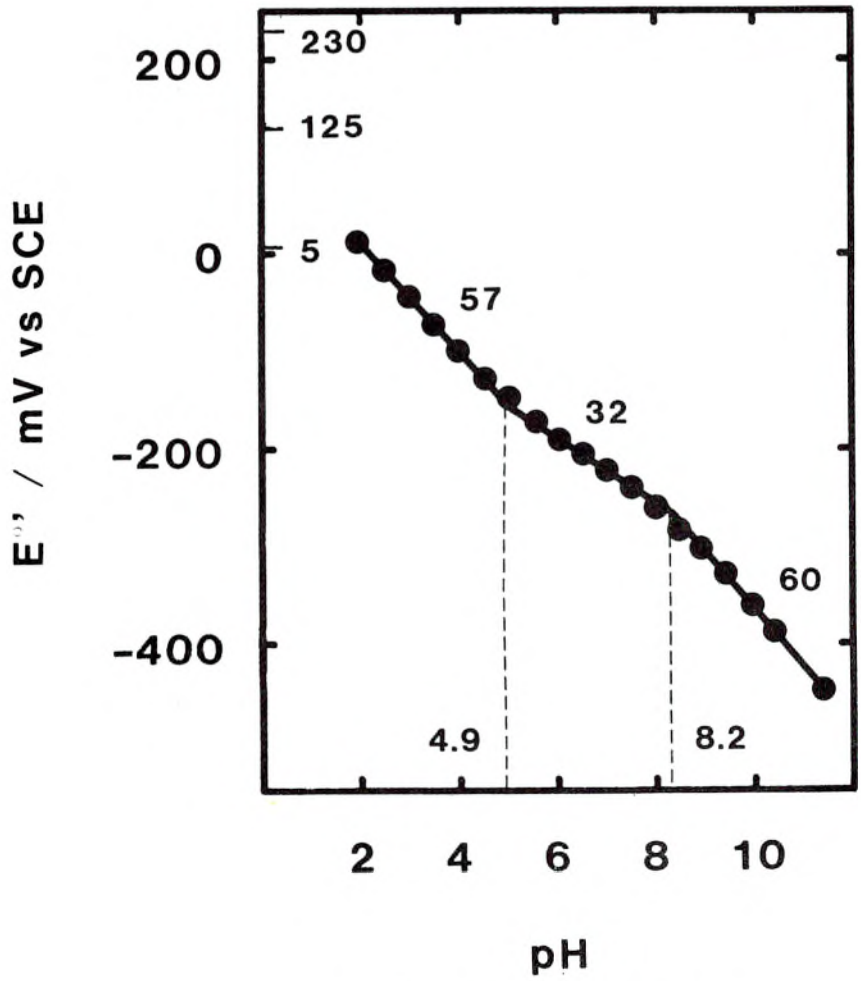

Fig. 1d. 3-β-Naphthoyl-Nile Blue A (IX)

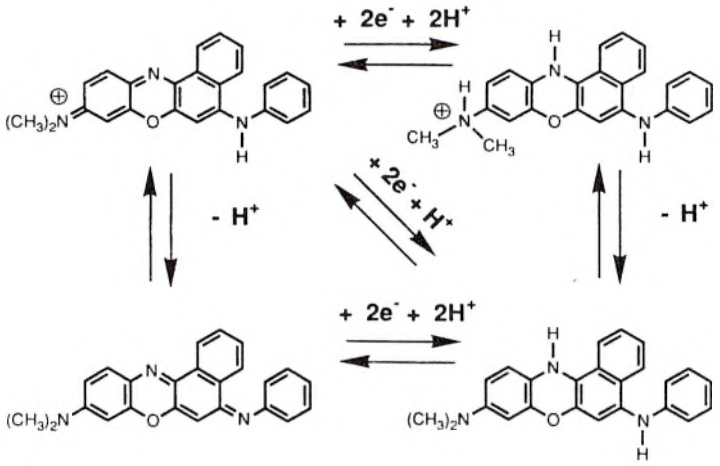

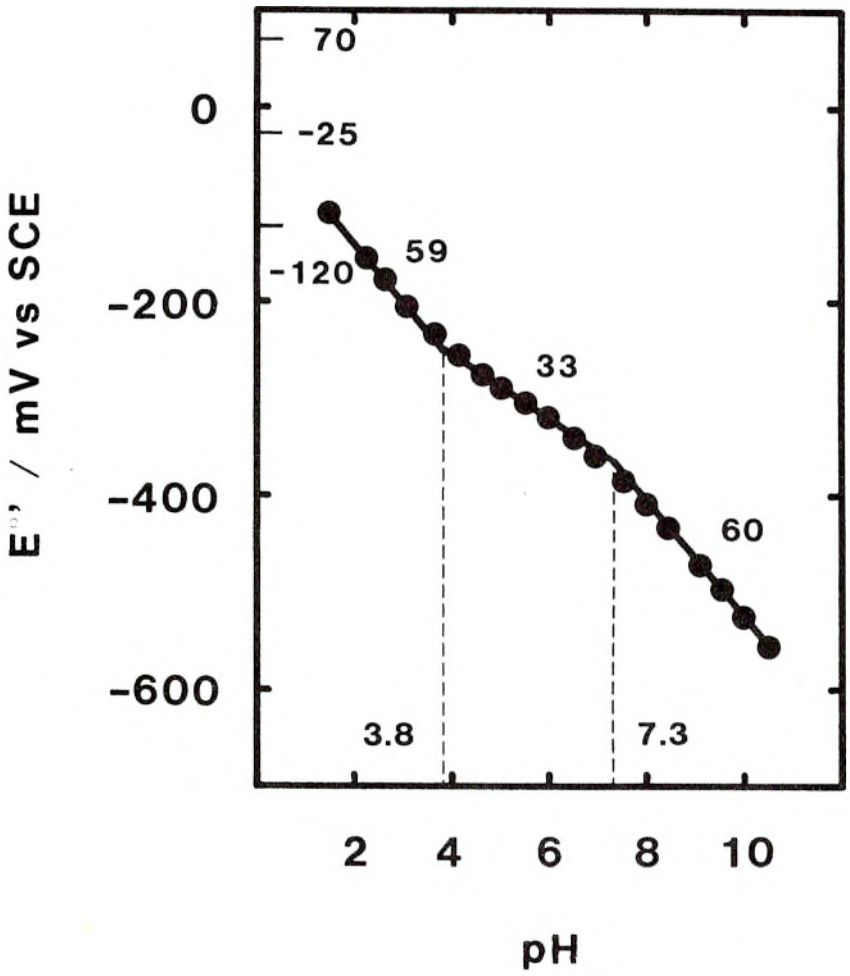

Fig. 1e. *3-Anilino-Meldola Blue (X)*

The pK_r-value of the dialkylamino group is lowered by an average value of 1.4 pH units by adsorption. In the reduced state the reciprocal action between positions 3 and 7 should be small and therefore only a minor inductive effect from the substituent in position 3 should be observed. This is indicated by the small random shift of less than 0.5 pH units of the pK_r-value of the dialkylamino group found when comparing the adsorbed parent compound with the corresponding derivative (Table 2 and 3).

In a study by Huck [57] the pK_o-values of NB when dissolved in aqueous solution and when adsorbed on graphite were found to be 10.2 and 13.0, respectively, and those of 3-NNB, 4.4 and 7.8, respectively. The experimental conditions, however, differed with respect to the buffer composition and the type of graphite material used in this report. The change of the amino group in position 3 to an amide group thus gives a drastic decrease of the pK_o-value, both in the soluble and the adsorbed state. When the state of the mediator is changed from soluble to adsorbed, the effect on the pK_o-value is the opposite of the pK_r-value, i.e an increase. From Table 3 it can be seen that the net effect of both adsorption and derivatisation of the 3-amino compounds is a decrease of the pK_o-values between 0.4 and 3.8 pH units.

Some specific effects on the $E^{o'}$- and pK_o-values caused by the incorportation of different structural elements are found by a comparison of the data obtained for the adsorbed compounds (VI-X) given in Table 3. Within the homologous series (VI-VIII), where the hetero-atom in position 5 varies, the nitrogen atom gives the compound outstanding properties considering the low $E^{o'}$- and pK_o-values, probably due to the valence number of three of the nitrogen atom, see Fig. 1a. It can also be noted that the pK_r-value of the phenoxazine derivative (VIII) is higher than for the other two homologues.

The addition of a benzene ring in the 1,2-position (c.f (VIII) and (IX)) causes a decrease in the pK_o-value. The incorporation of an aromatic ring in the structure at the 1,2 position increases the resonance stabilisation of the imino form and should promote the dissociation of the proton in the amide group. Compound (IX) containes a diethyl- instead of a dimethyl-amino group in position 7, which might have a noticeable local effect but hardly any significant inductive effect on

position 3, and therefore a minor influence on the pK_o-value. For compound (X) proton dissociation of the oxidized form occurs even more easily since the additional stabilisation through delocalisation within the planar amide group is absent. The substituent in position 3 of the 1,2-benzophenoxazinium derivatives gives decreasing pK_o-values in the order, primary amine > naphthylamide > benzylamine.

The E°' of -220 mV vs SCE at pH 7.0 found for both adsorbed 3-benzoyl-Nile Blue A and 3-NNB, suggests that the effect on the E°' is negligible whether one or two aromatic rings are coupled to the amide group. The substituent in position 3 thus gives E°'-values in the order, naphthylamide ≈ benzylamide > benzylamine > primary amine > keto (Nile Red), as seen by a comparison of the 1,2-benzophenoxazinium derivatives studied.

Electrocatalytic oxidation of NADH

Cyclic voltammograms obtained with a single scan (E°'± 300 mV at 5 mV s^{-1}) starting in the anodic direction, of graphite electrodes chemically modified with 3-NTB, 3-NBCB, 3-NNB, or 3-AMB (Γ=2-3 nmol cm^{-2}), recorded in 0.25 M phosphate buffer containing 3 mM NADH at pH 7.0 showed an electrocatalytic oxidation of NADH. No electrocatalytic activity could be traced at the 3-NNR CME. Since the pK_o of 3-NNR is 3.0, all of the 3-NNR exists as the imino form at pH 7.0 (lower left structure in the quadratic reaction scheme, Fig. 1 a). Furthermore, the E°' of 3-NNR of -545 mV vs SCE at pH 7.0 is very close to the E°' of -560 mV of the NAD+/NADH redox couple [52,58]. A small thermodynamic driving force for the electrocatalytic oxidation of NADH as well as a poor activity of the imino structure are probably the causes for the lack of electrocatalytic activity at the 3-NNR modified electrode.

It is belived that a charged paraphenylenediimine structure (the iminium form) is a more efficient catalytic structure than an uncharged (the imino form) [24,27,44-46]. In the earlier study of 3-NNB [24], a decrease in the electrocatalytic activity was observed at pHs higher than the pK_o of 3-NNB, where the uncharged imino form is the predominant

structure. A lower reaction rate between the imino form of the mediator and NADH is expected from a comparison of the rate with other related neutral mediators, both adsorbed [26] and dissolved [44-46]. Earlier electrochemical investigations have suggested an initial formation and a concurrent rate limiting decomposition of a charge transfer (CT) complex between adsorbed phenoxazine derivatives and NADH [25-29]. The existence of a complex between NADH and adsorbed Nile Blue A has been demonstrated by surface enhanced Raman scattering [59]. The mediated oxidation of NADH via electron transfer by adsorbed phenoxazine derivatives at a constant pH has been approximated with a reaction mechanism analogous to the kinetics of the Michaelis-Menten type, i.e.

$$\mathbf{NADH + M_{ox} \underset{k_{-1}}{\overset{k_{+1}}{\rightleftharpoons}} [CT\ complex] \xrightarrow{k_{+2}} NAD^+ + M_{red}} \qquad (1)$$

where M denotes the mediator. The assumed rate limiting step (k_{+2}) was considered to be chemically irreversible both for thermodynamic reasons and because the mediator is rapidly reoxidized electrochemically at an applied potential higher than the E°' of the mediator [25,26]. The overall rate coefficient, k_{obs}, was given as [25]

$$k_{obs} = k_{+2} / (K_M + [NADH]) \qquad (2)$$

with the inversed form as

$$1/k_{obs} = (K_M / k_{+2}) + ([NADH] / k_{+2}) \qquad (3)$$

and with $K_M = (k_{-1} + k_{+2}) / k_{+1}$

The k_{obs}, at a particular NADH concentration and with a particular surface coverage of the mediator, can be determined by rotating disk electrode (RDE) measurements [60,61]. The reciprocal of the catalytic current at the RDE, for a mediated catalytic reaction with a limiting chemical step, is given by a derived Koutechy-Levich equation [62]

$$\frac{1}{i_{cat}} = \frac{1}{nFAk_{obs}\,\Gamma\,[NADH]} + \frac{1}{0.620nFAv^{-1/6}D^{2/3}\,[NADH]} \cdot \frac{1}{\omega^{1/2}} \qquad (4)$$

where [NADH] is the bulk concentration (mol cm^{-2}), ω the rotational speed (rad s^{-1}), D the diffusion coefficient (cm^2 s-1), υ the hydrodynamic viscosity (cm^2 s^{-1}) and all other parameters have their usual significances.

Each of the derivatives (VII-X) were investigated with the RDE method at pH 7.0. It was assumed that the contribution of the imino form to the reaction rate could be neglected, see below. For 3-NNB and 3-AMB, the kinetic evaluations and the reported surface coverages in this section, are therefore based on a correction of the measured Γ by the factors 0.941 and 0.666, respectively, calculated with respect to the found pK_o-values.

The electrocatalytic current of the NADH oxidation increased with an increased rotational speed and showed a curvature in plots of i vs $\omega^{1/2}$ (Levich plot) for the compounds (VII-X). Strictly linear plots were obtained when eqn. (4) (Koutechy-Levich plot) was used, yielding intercepts that differed from zero for the various concentrations of NADH.

Fig. 2 shows typical plots of the reciprocal apparent k_{obs} (obtained from eqn. (4)) versus the concentration of NADH for electrodes modified with 3-NNB, 3-NTB, and 3-NBCB. A linear relation was found only at higher concentrations of NADH. By extrapolation of the linear part to the ordinate, the rate constant k_1, i.e. k_{obs} at zero concentration of NADH, was obtained. The rate constants k_{+2} and K_M were obtained from the linear part of plots according to eqn. (3). It was noted that the deviation from linearity occurred for NADH concentrations just below the calculated K_M value for each individual modified electrode. The K_M value varied between 1.2-4.5 mM among the different electrodes. In a study of two 3-AMB modified electrodes, strictly linear plots were found in the the concentration range 0.3 - 2.1 mM NADH, giving k_{+2} values of 0.75 and 0.78 s^{-1}, and K_M values of 0.24 and 0.23 mM at surface coverages of 0.40 and 0.58 nmole cm^{-2}, respectively.

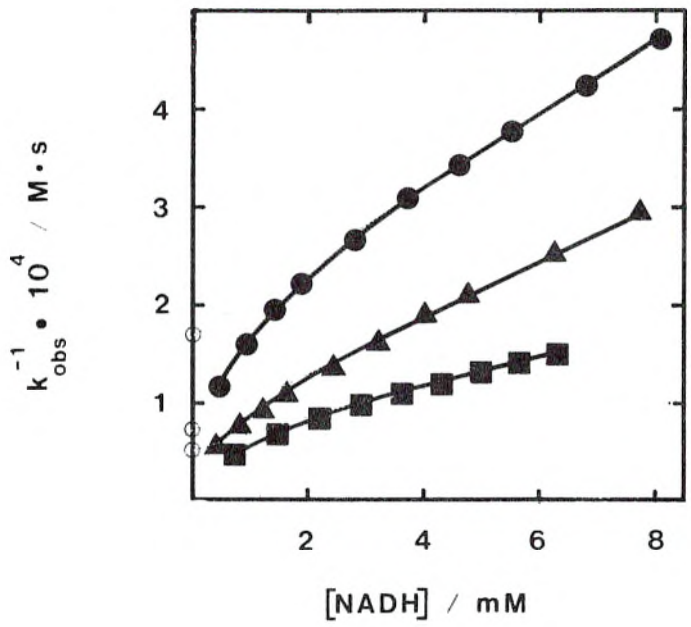

Fig. 2. *Data obtained from RDE measurements and eqn. (4) showing plots of the reciprocal apparent k_{obs} versus the concentration of NADH at pH 7.0 for electrodes modified with 3-NBCB (VIII) (●), 3-NTB (VII) (▲), and 3-NNB (IX) (■) with surface coverages of 1.4, 0.86, and 1.0 nmole cm^{-2},respectively. The reciprocal of the rate constant k_1 is obtained by extrapolation of the linear segment of a plot to zero concentration of NADH, as indicated by a dotted line.*

For different electrodes and with various coverages of 3-NTB, 3-NBCB, and 3-NNB, respectively, a general trend was observed of an increasing k_1 with a decreasing Γ for values less than 1 nmol cm^{-2}, see Fig. 3. In order to estimate a consistent rate constant, k_o, where the dependence on the surface coverage is eliminated, a linear extrapolation to a surface coverage of zero was performed for each of the compounds (VII-IX). It should be stressed that no linear relation is expected or can be confirmed at present due to the uncertanties in the measurements caused by the variation between different electrodes.

TABLE 4. *Apparent rate constants at pH 7.0 of the iminium form of the derivatives (VIII-X) adsorbed on graphite with NADH.*

Compound	$k_o 10^{-4}/(M \cdot s)^{-1}$	k_{+2}/s^{-1}
3-NTB (VII)	4	37
3-NBCB (VIII)	3	36
3-NNB (IX)	5	69
3-AMB (X)	0.3	0.76

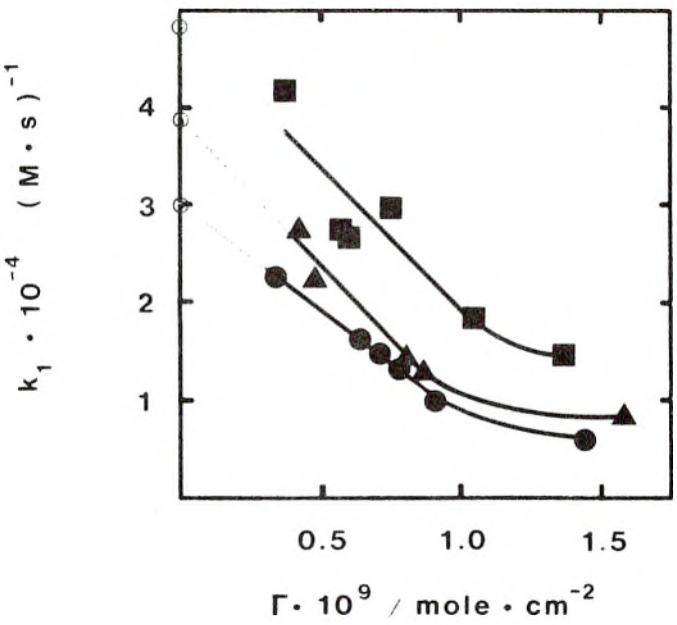

Fig. 3. *Variation of the rate constant k_1 with the surface coverage of 3-NBCB (VIII) (●), 3-NTB (VII) (▲), and 3-NNB (IX) (■) CMEs at pH 7.0. The rate constant k_o is obtained at a surface coverage of zero, as indicated by a dotted line.*

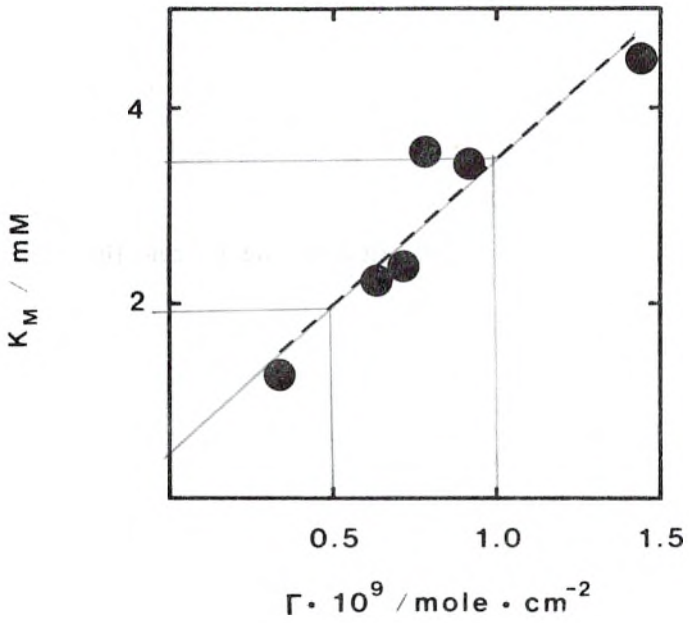

Fig. 4. *Variation of the rate constant K_M with the surface coverage at pH 7.0 of six 3-NBCB (VIII) modified electrodes.*

The obtained k_{+2} values of each of the compounds (VII-IX) showed a random variation of about ± 6 s^{-1} (SD, n=4 or 5) around an average value and no trend was observed for various surface coverages. Therefore, as illustrated in Fig. 4., the variation of k_1 with Γ can be ascribed to a variation of K_M with Γ in the approximative kinetic model given by eqns. (1) and (2).

The estimated k_o values, and the average k_{+2} values for Γ less than 1 nmol cm^{-2} are summarised in Table 4. The results confirm an increased reaction rate, although not strict, at a more oxidative $E^{o'}$ value of the mediator [27]. The high reaction rate for 3-NNB may indicate that the size of the dialkylamino group in position 7 is of great importance for the electrocatalytic activity of the paraphenylenediimine structure.

However, it can not be ruled out that the benzene ring in 3-NNB, absent in 3-NTB and 3-NBCB, may have an influence on the catalytic activity, e.g. by affecting the surface orientation of the compound [59]. A sulfur rather than an oxygen atom in position 5 of the mediator seems to give a slight increase of the E°'-value and of the reaction rate with NADH. An overall reaction rate of 10 $(M\ s)^{-1}$ between NADH and Nile Blue A adsorbed on graphite has previously been reported [27]. By comparing adsorbed NB, 3-NNB, and 3-AMB, a drastic effect of the catalytic properties of the mediators can be seen, where the substituent in position 3 results in an increase of both the E°' and the reaction rate with NADH in the order amine < benzylamino < naphthamido.

The influence of pH on the electrocatalytic oxidation of NADH

The influences of pH on the electrocatalytic oxidation of NADH at electrodes modified with compounds (VII-X) were investigated in a flow system. The same flow system as in a recent study of the NADH sensor properties of 3-NTB CMEs was used [30], where the electrodes were mounted in a flow-through amperometric cell of the confined wall-jet type [38]. The dispersion coefficient [63] was 1.3 at a flow rate of 0.85 ml min^{-1} and with an injection volume of 50 µl, allowing a sample throughput of 150 h^{-1}.

The variation of the response at a constant pH and flow rate for different values of Γ at two different NADH concentrations with a 3-NBCB CME mounted in the flow system is shown in Fig. 5. As can be seen, the response to NADH approaches a constant level once the coverage has reached a certain value. This is predicted by the overall reaction mechanism given by eqn. (1) [25,30]. The lower curve was obtained for an NADH concentration of 1.8 mM, and the lower sensitivity at this NADH concentration should indicate that the linear range has been exceeded. An upper linear limit of 2 mM at pH 7 was found for 3-NTB [30], and a lower upper linear limit for 3-NBCB than for 3-NTB is expected when comparing their k_o-values shown in Table 4. Only a minor variation of the sensitivity at small coverages is observed, and a decrease of Γ from the virtually independent region to 1 nmole cm^{-2} would result in a maximum loss of sensitivity of 8%.

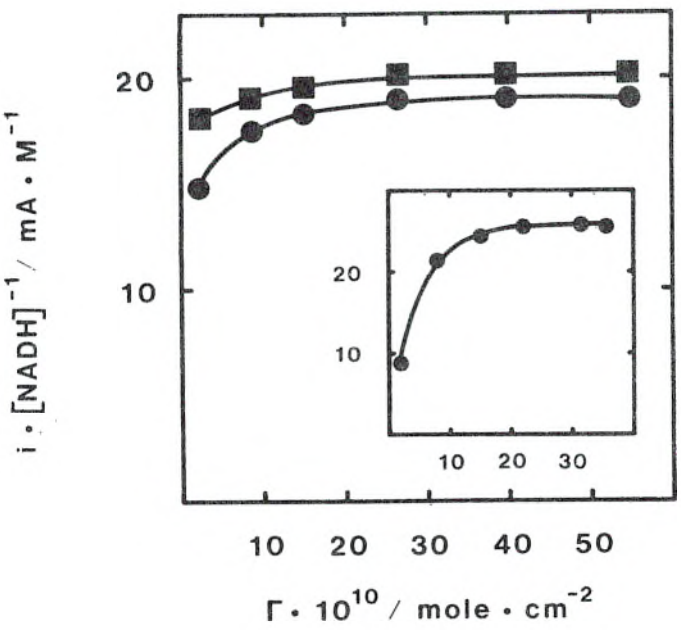

Fig. 5. Steady state mesurements in the flow system showing the dependence of the NADH sensitivity of a 3-NBCB (VIII) CME with surface coverage for 0.18 mM (■) and 1.8 mM (●) NADH solutions at pH 7.0. Flow rate 0.85 ml min^{-1}; applied potential + 50 mV vs SCE. The inserted figure shows the dependence at the RDE for a 3-NTB (VII) CME at pH 7.0 in a 3.6 mM NADH solution. Rotational speed 100 rad s^{-1}; applied potential 0 mV vs SCE.

With the CME mounted in the flow-through cell the mass transfer of NADH to the electrode surface cannot be predicted since the flow characteristics are not fully known [38]. It is expected, however, that the mass transfer of solution is not so efficient compared with the RDE. For low values of Γ, the more pronounced dependence of the sensitivity on Γ at the RDE is illustrated in the smaller inserted figure in Fig. 5.

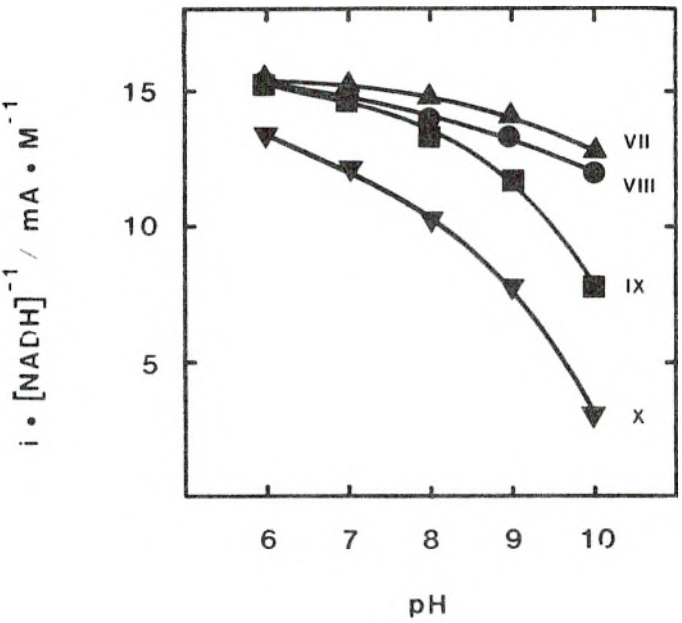

Fig. 6. Variation of the NADH sensitivity of 3-NTB (VII) (▲), 3-NBCB (VIII) (●), 3-NNB (IX) (■), and 3-AMB (X) (▼) CMEs as seen by injecting 50 µl samples of 0.4 mM NADH solutions at different pHs. Conditions as in Fig. 5., average surface coverages are given in Table 5.

The influence of pH on the reaction rate with NADH for the absorbed compounds (VII-X) is depicted in Fig. 6. The investigation of the sensitivity of the CME started at pH 6, and each value given in Fig. 6 is based on the average value of four injections (RSD 0.3-0.6%), registered with an interval of 60 s. The values at pH 9 for 3-AMB, and at pH 10, for 3-AMB and 3-NNB, are, however, based on two injections only since a decrease in the current response was observed for the second injection. The observed difference in the response values between two consecutive injections was at most 6%.

In the earlier study of adsorbed 3-NTB [30], a variation between different electrodes of ± 1 mA M^{-1} (SD, n=4) at pH 7 was found, and an almost mass transfer limited current response was obtained at pH 6. A comparison of the sensitivity between compounds (VII-IX) is thus unreliable at pH 6 and 7, but it can be concluded that they all result in an almost mass transfer limited response seen from the merging curves at pH 6. This is not the case for 3-AMB although a surprisingly high sensitivity is obtained at pH 7 despite a relatively low k_o value.

For all of the compounds (VII-X) a decrease in the reaction rate with NADH at more alkaline pHs is observed. The decrease is more pronounced for the compounds (IX-X), based on a 1,2-benzo-phenoxazine. A major dependence due to a decrease in the total amount of adsorbed mediator can be ruled out since the final Γ for all the electrodes were more than 3 nmole cm^{-2} determined after the measurements. As seen from Fig. 5, even a small amount of the iminium form on the electrode surface would give a relatively high sensitivity. However, a correlation of the decrease in the sensitivity with pH to the pK_o value of each compound can be seen from Table 5. The results suggest that an increased proportion of the less catalytically active imino form at the CME should be the main reason for the decrease in the sensitivity with an increase in pH.

The influence of pH can be considered as dualistic since it affects both the structure and the E°' of the mediator. For the imino form, E°' will vary with -60 mV/pH compared with -30 mV/pH for the iminium form (c.f. Fig. 1b-e) while the variation of the E°' of the NAD^+/NADH redox couple will be -30 mV/pH [58] throughout the investigated pH range. An increase of pH is therefore also expected to cause a decrease in the overall reaction rate for the imino form due to a decrease in the potential difference between the two redox couples and thereby a decrease in the thermodynamic driving force. A dependence on the catalytic activity with pH has also been observed for Meldola Blue [27,38], although no imino form can exist within the structure. Additional mechanisms might be inherent in the curves, but their influences should be of minor importance as reflected by the relatively low pH dependence found for 3-NTB and 3-NBCB, see Fig. 6.

TABLE 5. *A comparison of the relative NADH sensitivity (pH9/pH6) and the amount of imino form present at pH 9.0 between electrodes modified with compounds (VII-X). Data from Fig. 6.*

Compound	%sensitivity pH 9 / pH 6	pK_o	%imino form at pH 9	Average Γ nmole·cm^{-2}
3-NTB (III)	91	10.3	5	5.0
3-NBCB (VIII)	86	10.3	5	4.3
3-NNB (IX)	77	8.2	85	4.7
3-AMB (X)	23	7.3	98	8.9

The chemical and the electrochemical stabilities of the adsorbed phenoxazine derivatives (VIII-X) were investigated by subjecting the CMEs to 30 minutes of continuous cycling ($E^{o'}$ ± 300 mV at 50 mV s^{-1}) in the voltammetric assembly at pH 9.0. This resulted in a variation of less than 2% of the coverage for all of the compounds. Despite the stability of the modified electrodes in buffer solutions with no NADH present, a decrease in the response with time was observed at pH 9 with the CMEs mounted in the flow system at steady state measurements with 0.4 mM NADH, see Fig. 7 and Table 6. In the determination of the final Γ with cyclic voltammetry a peak broadening was observed (also noticed in the RDE measurements) after the electrodes had been exposed to NADH, but no new peaks appeared in the range of -700 to +200 mV vs SCE.

Adsorption of NAD^+ at glassy carbon electrodes occurs at potentials more positive than 0 mV vs SCE and a desorption has been indicated when a potential of 0 mV is applied [7]. When NADH is oxidized at a CME, a peak broadening can be caused by interactions between adsorbed mediator molecules and adsorbed NADH related products [54]. However, the small variation of the NADH response with time for the 3-NBCB CME in Fig. 7 excludes any severe fouling of this CME.

Furthermore, a 3-NTB CME stored one month in a quiet buffer at pH 7.0 showed a pronounced peak broadening after one week, although it was not exposed to NADH [30]. An escape of the modifier from the surface into the pores of the electrode was suggested as one possible reason for the peak broadening.

Some additional investigations with 3-NNB and 3-AMB CMEs were made. No significant change in the initial response to NADH was observed at pH 9 for 3-NNB and 3-AMB electrodes in the flow-through cell after being first subjected to 30 minutes of cyclic voltammetry. An increased deactivation rate of the response to NADH at pH 10 and 11, compared with the rate at pH 9, was noticed. When pH was changed back to 9, a lower response than the initial one was found, indicating that the deactivation of the CMEs was irreversible. A repeated experiment with 3-AMB was performed at pH 9, this time in the injection mode, with an injection frequency of one per minute. A lag period of 30 minutes with the electrode only facing a flowing buffer was introduced after 15 injections. The current response of the succeeding injection equalled the last injection preceding the lag period, followed by a continued decrease in the response for another 14 injections. A total decrease in the sensitivity of 30% was found after the 30 injections.

These observations together with the data shown in Tables 5 and 6, suggest that the diminished electrocatalytic activities for the CMEs may be ascribed to the occurrence of a side-reaction between the imino form of the mediator and the cofactor. The electrochemical activity of the mediator is retained reflected by cyclic voltammogram, with only a minor change in the $E^{\circ\prime}$, whereas the electrocatalytic properties are largely lost. The deactivation is clearly more severe for the compound with a benzylamino than for compounds with a naphthoylamide group in position 3, where the structure rather than the amount of the imino form present at the electrode surface appears to be of greater importance (c.f. Table 5). For 3-NNB and 3-AMB consisting of six rings the Γ remained essentially constant compared with 3-NBCB having five rings where a decrease of 39% is found. Both desorption due to an increased water solubility of a possible coupling product with the cofactor, or an electrochemical inactive product may be the reason for this.

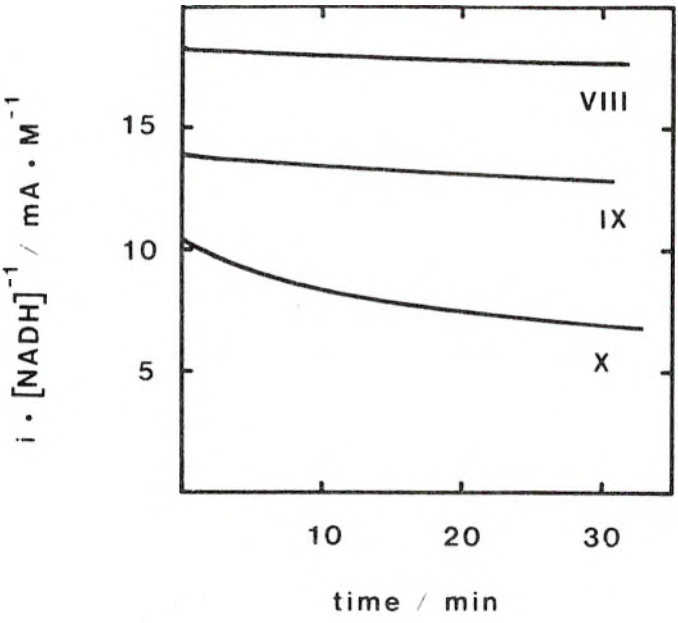

Fig. 7. *Steady state measurements showing the change in the NADH sensitivity of 3-NBCB (VIII), 3-NNB (IX), and 3-AMB (X) CMEs with time for 0.4 mM NADH solutions at pH 9.0. Conditions as in Fig. 5., initial and final surface coverages are given in Table 6.*

TABLE 6. *The stability of electrodes modified with the phenoxazine derivatives 3-NBCB (VIII), 3-NNB (IX), and 3-AMB (X). Data from Fig. 7.*

Compound	*Γ(initial)/ nmole·cm^{-2}*	*Γ(final)/ nmole·cm^{-2}*	*Decrease in sensitivity % after 30 min*
3-NBCB (VIII)	*1.8*	*1.1*	*3*
3-NNB (IX)	*1.8*	*1.7*	*7*
3-AMB (X)	*1.6*	*1.6*	*34*

A side reaction resulting in a coupling product which more easily desorbs should to a higher extent prevent fouling of the electrode surface and covering of neighbouring active mediator molecules, and thereby cause a less decrease in the sensitivity.

For CMEs based on immobilized ortho-quinones a deactivation of the electrocatalytic properties was demonstrated to occur in the presence of NADH [13,14,16,18]. Ortho-quinones are also active for the electrocatalytic oxidation of ascorbic acid. In the presence of this compound no deactivation was observed [13,16]. In one study [18] it was proposed that a side-reaction in the electrocatalytic oxidation of NADH could take place through a coupling reaction between the presumed intermediate NAD· radical and a semiquinone. The probability of the occurrence of a side-reaction for a single mediator molecule, resulting in a blocking of the electrode surface, was estimated to be one per 1100 electrocatalytic cycles [18]. A charge transfer reaction within a complex between NADH and ortho- or para-quinones has been considered as possible in aqueous solutions [64], and the formation of a CT complex between p-benzoquinone derivatives and an NADH model compound has been observed in organic solvents [65]. A formation of a radical ion pair by an electron transfer within a CT complex may be a route for side-reactions for both quinones and neutral phenoxazine derivatives.

The observed deactivation of mediators incorporating the quinone and in this study the imino structure, suggests that the iminium structure, with a positive charge initially present, may stabilise the transition state of such a complex and may also prevent a formation of a radical ion pair. The presence of a strong base may also have a significant effect on the overall kinetics and thus cause a difference in the stability of the imino and the iminium form of the mediator in the presence of NADH [66].

So far, mechanisms and improvements in the electrocatalytic oxidation of NADH have been studied on a basis of successful and improved catalysis rather than on a deactivation of the catalytic properties of the mediator. Further investigations of the deactivation reactions between the imino form of 3,7-diamino derivatives of phenoxazines and allied structures, are of great interest to elucidate at which position in the mediator a reaction occurs.

CONCLUSIONS

A change of an amino substituent in position 3 for a substituted amine of the 7-dialkylamino derivatives of phenoxazines and phenothiazines increases the E°' of the resulting compound which gives a higher reaction rate with NADH. The increase in the reaction rate is to some extent counteracted by a decrease in the pK_o-value of the new derivative compared with the parent compound, leading to a decrease in the reaction rate at more alkaline pHs through the formation of the less catalytic active imino form. The imino structure of the mediators also seems to be the least stable part of the CME, seen as an initial deactivation of the electrocatalytic properties of the CME in the presence of the cofactor. A preliminary indication of a higher reaction rate with a diethylamino rather than a dimethylamino group in position 7 is observed. The variation of the response with pH for 3,7-diamino derivatives with the electrocatalytic structure incorporated in an aromatic system consisting of three rings, instead of four ring, gives the advantage of a less pronounced variation in the response with pH. The disadvantage is a less stable adsorption layer. The phenazine structure studied, unsubstituted in position 5, is a less suited structure for NADH catalysis, mainly due to low E°' and pK_o values. This study suggests that a general improvment can be made, e.g. by the incorporation at position 3 of an electron attracting structure which lacks acid-base properties, whereby the formation of an imino structure within the mediator can be prevented.

ACKNOWLEDGEMENT

The authors thank Mr. Christer Grönsterwall, Carnegie Medicin, for the loan of the BAS 100-A Electrochemical Analyzer. Financial support from the Swedish Board for Technical Development (STU) and the National Energy Administration (STEV) is gratefully acknowledged.

REFERENCES

1 J. N. Burnette and A. L. Underwood, *Biochemistry*, 4 (1965) 2060.

2 W. J. Blaedel and R.G. Haas, *Anal. Chem.*, 42 (1970) 918.

3 P. Leduc and D. Thevenot, *Bioelectrochem. Bioenerg.*, 1 (1974) 96.

4 W. J. Blaedel and R. A. Jenkins, *Anal. Chem.*, 46 (1974) 1952.

5 M. Aizawa, R. N. Coughlin and M. Charles, *Biochim. Biophys. Acta*, 385 (1975) 362.

6 R. D. Braun, K. S. V. Santhanam and P. J. Elving, *J. Am. Chem. Soc.*, 97 (1975) 2591.

7 J. Moiroux and P. J. Elving, *Anal. Chem.*, 50 (1978) 1056.

8 J. Moiroux and P. J. Elving, *Anal. Chem.*, 51 (1979) 346.

9 H. Jaegfeldt, *J. Electroanal. Chem.*, 110 (1980) 295.

10 W. T. Bresnahan and P. J. Elving, *J. Am. Chem. Soc.*, 102 (1981) 2379.

11 P. J. Elving, W. T. Bresnahan, J. Moiroux and Z. Samec, *Bioelectrochem. Bioenerg.*, 9 (1982) 365.

12 R. L. Blankespoor and L. L. Miller, *J. Electroanal. Chem.*, 171 (1984) 231.

13 D. C.-S. Tse and T. Kuwana, *Anal. Chem.*, 50 (1978) 1315.

14 C. Degrand and L. L. Miller, *J. Am. Chem. Soc.*, 102 (1980) 5728.

15 H. Jaegfeldt, A. B. C. Torstensson, L. G. O. Gorton and G. Johansson, *Anal. Chem.*, 53 (1981) 1979.

16 C. Ueda, D. C.-S. Tse and T. Kuwana, *Anal. Chem.*, 54 (1982) 850.

17 M. Fukui, A. Kitani, C. Degrand and L. L. Miller, *J. Am. Chem. Soc.*, 104 (1982) 28.

18 H. Jaegfeldt, T. Kuwana and G. Johansson, *J. Am. Chem. Soc.*, 105 (1983) 1805.

19 L. L. Miller, B. Zinger and C. Degrand, *J. Electroanal. Chem.*, 178 (1984) 87.

20 H. Huck and H.-L. Schmidt, *Angew. Chem.*, 93 (1981) 421.

21 K. Ravichandran and R. P. Baldwin, *Anal. Chem.*, 55 (1983) 1586.

22 A. Torstensson and L. Gorton, *J. Electroanal. Chem.*, 130 (1981) 199.

23 Y. Kimura and K. Niki, *Anal. Sci.*, 1 (1985) 271.

24 H. Huck, *Fresenius' Z. Anal. Chem.*, 313 (1982) 548.

25 L. Gorton, A. Torstensson, H. Jaegfeldt and G. Johansson, *J. Electroanal. Chem.*, 161 (1984) 103.

26 L. Gorton, G. Johansson and A. Torstensson, *J. Electroanal. Chem.*, 196 (1985) 81.

27 L. Gorton, *J. Chem. Soc.*, Faraday Trans., I, 82 (1986) 1245.

28 B. Persson, L. Gorton and G. Johansson, in J.-L. Aucouturier, J.-S. Cauhapé, M. Destriau, P. Hagenmuller, C. Lucat, F. Ménil, J. Portier and J. Salardenne (Eds.), *Proc. "2nd Int. Meeting on Chemical Sensors"*, Imprimerie Biscaye, Bordeaux, (1986) p. 584.

29 L. Gorton, B. Persson, M. Polasek and G. Johansson, *Proceedings of ElectroFinnAnalysis Conference*, Plenum Publishing Co., 1988, in press.

30 B. Persson, *J. Electroanal. Chem.*, in press.

31 J. J. Kulys, *Enzyme Microb. Technol.*, 3 (1981) 344.

32 W. J. Albery and P. N. Bartlett, *J. Chem. Soc., Chem. Commun.*, (1984) 234.

33 K. McKenna, S. E. Boyette and A. Brajter-Toth, *Anal. Chim. Acta.*, 206 (1988) 75.

34 B. F. Y. Yon Hin and C. R. Lowe, *Anal. Chem.*, 59 (1987) 2111.

35 C. P. Andrieux and J. M. Savéant, *J. Electroanal. Chem.*, 93 (1978) 163.

36 R. W. Murray, A. G. Ewing and R. A. Durst, *Anal. Chem.*, 59 (1987) 379A.

37 A. Schelter-Graf, H.-L. Schmidt and H. Huck, *Anal. Chim. Acta*, 163 (1984) 299.

38 R. Appelqvist, G. Marko-Varga, L. Gorton, A. Torstensson and G. Johansson, *Anal. Chim. Acta*, 169 (1985) 237.

39 L. Gorton and A. Hedlund, *Anal. Chim. Acta*, 213 (1988) 91.

40 M. Polasek, L. Gorton, R. Appelqvist, G. Marko-Varga and G.Johansson, *paper in doctoral Thesis*, Roger Appelqvist, University of Lund, 1987.

41 M. Kotoucek and J. Tomásová and S. Durcáková, *Collect. Czech. Chem. Commun.*, 34 (1969) 212.

42 M. Kotoucek and J. Zavadilová, *Collect. Czech. Chem. Commun.*, 37 (1972) 3212.

43 J. F. Thorpe, *J. Chem. Soc.*, 91 (1907) 324.

44 A. Kitani and L. L. Miller, *J. Am. Chem. Soc.*, 103 (1981) 7636.

45 A. Kitani, Y.-H. So and L. L. Miller, *J. Am. Chem. Soc.*, 103 (1981) 7636.

46 J. Grodkowski, F. Neta, B. W. Carlson and L. Miller, *J. Phys. Chem.*, 87 (1983) 3135.

47 R. Nietzki and A. Bossi, **Ber.**, 25 (1892) 2994.

48 V. Stuzka and Z. Stránsky, *Acta Univ. Palacki. Olomuc. Fac. Rerum Nat.*, 21 (1966) 251.

49 M. L. Crossley, R. J. Turner, C. M. Hoffman, P. F. Dreisbach and R. P. Parker, *J. Am. Chem. Soc.*, 74 (1952) 578.

50 E. Laviron, *J. Electroanal. Chem.*, 52 (1974) 355.

51 J. M. Ottaway, in E. Bishop (Ed.), *Indicators*, Pergamon Press, Oxford, 1972, 490-509.

52 W. M. Clark, *Oxidation - Reduction Potentials of Organic Systems*, Wiliams and Wilkins, Baltimore, 1960.

53 E. Laviron in A. J. Bard (Ed.), *Electroanalytical Chemistry*, Vol. 12, Marcel Dekker, New York, 1982, pp. 53-157.

54 R. W. Murray in A. J. Bard (Ed.), *Electroanalytical Chemistry*, Vol. 13, Marcel Dekker, New York, 1984, pp. 191-368.

55 A. J. Bard and L. R. Faulkner in *Electrochemical Methods, Fundamentals and Applications*, Wiley, New York, 1980, p. 525.

56 H. K. Hall, Jr., *J. Phys. Chem.*, 60 (1956) 63.

57 H. Huck, *Ber. Bunsenges. Phys. Chem.*, 87 (1983) 945.

58 H. K. Chenault and G. M. Whitesides, *Appl. Biochem. Biotechnol.*, 14 (1987) 147.

59 Ni Fan, H. Feng, L. Gorton and T. M. Cotton, *Langmuir*, 6(1) (1990) 66.

60 C. P. Andrieux, J. M. Dumas-Bouchiat and J. M. Savéant, *J. Electroanal. Chem.*, 114 (1980) 159.

61 C. P. Andrieux, J. M. Dumas-Bouchiat and J. M. Savéant, *J. Electroanal. Chem.*, 123 (1981) 171.

62 R. W. Murray, *Phil. Trans. R. Soc. Lond.*, A 302 (1981) 253.

63 J. Ruzicka and E. H. Hansen, in P. J. Elving and J. D. Winefordner (Eds.), *Flow Injection Analysis*, Wiley, New York, 1981, pp. 15-17.

64 B. W. Carlson and L. L. Miller, *J. Am. Chem. Soc.*, 107 (1985) 479.

65 S. Fukuzumi, N. Nishizawa and T. Tanaka, *J. Org. Chem.*, 49 (1984) 3571.

66 S. Fukuzumi, Y. Kondo and T. Tanaka, *J. Chem. Soc. Perkin Trans. II*, (1984) 673.

V

AN AMPEROMETRIC GLUCOSE ELECTRODE BASED ON CARBON PASTE, CHEMICALLY MODIFIED WITH GLUCOSE DEHYDROGENASE, NICOTINAMIDE ADENINE DINUCLEOTIDE AND A PHENOXAZINE MEDIATOR, COATED WITH A POLY(ESTER-SULFONIC ACID) CATION EXCHANGER.

Gudrun Bremle, Björn Persson and Lo Gorton,
Dept. of Analytical Chemistry, P.O.Box 124, S-221 00 Lund, Sweden.

Abstract

An amperometric glucose electrode is described based on carbon paste chemically modified with glucose dehydrogenase, nicotinamide adenine dinucleotide and a mediator, Meldola Blue. The surface of the chemically modified carbon paste electrode (CMCPE) is protected by the deposition of a poly(ester sulfonic acid) cation exchanger to form a membrane, that prevents the aqueous soluble species from dissolving out of the CMCPE. The CMCPE was investigated in the FIA mode. Linear calibration curves for glucose were obtained between 100 μM and 20 mM glucose at +100 mV vs Ag/AgCl. The sample throughput was 40 h^{-1}. The electrodes remained stable for about two weeks.

Introduction.

Glucose dehydrogenase (GDH) is a redox enzyme that has only been used in a few instances for the construction of amperometric glucose sensors [1-11]. The enzyme depends on the soluble cofactor nicotinamide adenine dinucleotide (NAD^+) for activity, which thus has to be added to the analytical system. This is obviously a drawback when constructing a compact biosensor based on this enzyme. Several attempts have been made to overcome this problem common to all dehydrogenases, e.g. by the immobilization of the nicotinamide cofactor to the dehydrogenase [12,13], to another macromolecule [14,15], to the electrode surface [16,17] or by co-immobilizing the cofactor and the enzyme to the same support [18,19].

Another problem with dehydrogenase based amperometric sensors is the irreversible electrochemical behaviour of both redox forms of the cofactor (NAD^+ and NADH) [20]. GDH catalyses the oxidation of the β-form of D-glucose in the presence of NAD^+ whereby an equivalent amount of NADH is produced. The formal potential, E°', at pH 7 of the NAD^+/NADH redox couple is -560 mV vs SCE [20], which in principle should make it possible to detect the NADH amperometrically at 0 mV, where most common interfering compounds are neither oxidized nor reduced. The electrochemical oxidation of NADH suffers, however, from a very large overvoltage as well as from fouling reactions [20]. NADH is very fastidious in its choice of structures with which it rapidly donates its two electron charge. There exist a few groups of substances, mediators, which rapidly and selectively oxidize NADH [21]. By immobilizing such structures on electrode surfaces to form chemically modified electrodes, efficient electrocatalytic oxidation of NADH can be accomplished below 0 mV [21].

The interest in GDH instead of the commonly used glucose

oxidase for the making of glucose sensors is rationalized partly because oxygen is not involved in and does not disturb the enzyme cycle and partly because of the chemically modified electrodes at which the NADH can be measured at 0 mV. Another reason is that GDH belongs to the large group of dehydrogenase enzymes that all depend on the same cofactor for activity. If the problems connected with the construction of a compact amperometric enzyme electrode based on GDH could be solved, it would open up new possibilities for the construction of biosensors for other substrates based on other dehydrogenases and possibly also for sensors that can be used in complex media.

There has recently been a great interest in making reagentless enzyme electrodes based on redox enzymes where the enzyme is mixed into a carbon paste electrode also containing a mediator to facilitate the electron transfer from the cofactor to the electrode proper [22-26]. Most of these chemically modified carbon paste electrodes (CMCPE) are based on other types of redox enzymes than dehydrogenases. In this paper we describe a carbon paste electrode into which GDH, NAD^+, as well as a mediator, Meldola Blue [21,27], are mixed. The electrode surface is protected by the deposition of a poly(ester-sulfonic acid) cation exchanger that is dried directly onto the electrode surface to form a membrane. This membrane prevents the aqueous soluble species in the paste from dissolving out into the contacting solution and also prevents macromolecular and small negatively charged interfering compounds from reaching the chemically modified carbon paste [24,28,29].

Experimental

The following chemicals were used in this study:

Glucose dehydrogenase, EC 1.1.1.47 from Bacillus megaterium,

was obtained from Merck (cat. no. 13732, 220 U mg^{-1}) as a lyophilized powder. Nicotinamide adenine dinucleotide, NAD^+, and 1,4-dihydronicotinamide adenine dinucleotide, NADH, were obtained from Merck (cat. no. 24542) and from Sigma (cat. no. N-8129), respectively. D-Glucose was obtained from BDH (cat. no. 10117). A 1.0 M stock solution was prepared by dissolving an appropriate amount in the 0.25 M phosphate buffer. Mutarotational equilibrium between the α- and the β-forms was reached by allowing the solution to stand for 12 h before use. L(+)-Ascorbic acid was obtained from Merck (cat. no. 127). 7-dimethylamino-1,2-benzophenoxazinium chloride, Meldola Blue, MB, was obtained from Boehringer Mannheim (cat. no. 258 504) and used as received. Graphite powder was obtained from Fluka (cat. no. 50870) and carbon black (Ketjen Black, EC-600 JD, Akzo Chemie, the Netherlands) was kindly provided by Mr. W. Larsen, Akzo Zout Chemie Svenska AB, Göteborg, Sweden. Paraffin oil was obtained from Fluka (cat. no. 76235). The poly(ester-sulfonic acid) cation-exchanger (Eastman AQ-29D, Eastman Chemical Products, Publ. no. GN-375, 1987) was obtained dissolved in water (30 w/v %) as a gift from Dr. W. Waeny, Eastman Chemical Int. AG, Zug, Switzerland.

Preparation of carbon paste, CP, and chemically modified carbon paste, CMCP.

Two CPs were made by either using the graphite powder or the Ketjen black. The first CP was prepared in the following way: to 100 mg of graphite powder (used as received) an aliquot of 40 μl of paraffin oil was taken. The mixture was thoroughly mortered together to form a uniform paste. The second CP was prepared in the following way: Ketjen black was first thorougly mortered to become a fine powder. To 100 mg of this fraction 440 μl of paraffin oil were taken and the mixture was then thoroughly mortered to form a uniform paste.

Five different ways were examined to prepare mediator modified carbon pastes. These were; adorption of MB onto the surface of the carbon paste electrode from an aqueous solution of the modifier, mixing the dry MB powder directly into the paste, and adding MB to the carbon powder when dissolved in a solvent and letting the solvent evaporate before the addition of the paraffin oil. The solvents used were acetone, ethanol, and water.

Enzyme and cofactor CMCPs were made by mixing various amounts of GDH and NAD^+ with the graphite and the Ketjen black pastes, where MB was added as a dry powder to the paste, see under Results and Discussion. After preparation these pastes were store at 4°C until use.

Making electrodes

Plastic syringe holders (1.0 ml syringe, Brunswick 81/79J03 with a tip of 7.0 mm o.d. and 1.8 mm i.d.) were packed with about 0.1 ml of CP in the end of the holder leaving about 3 to 4 mm in the syringe top empty to be filled with the CMCP to produce the final electrode. Electrical contact was made by inserting a gold wire in the CP. After the tip of the syringe had been filled with CMCP, the end was rubbed gently on glass to produce a flat shining electrode surface with an area of about 0.024 cm^2. The outer end-parts of the plastic syringe were polished with fine emery paper (Tufbak Durite, P1200) to promote adherence of the Eastman AQ-29D coating. This coating was obtained by dipping the electrode into a 0.5% (w/v) solution prepared by proper dilution of the 30% stock solution with water. The amount of the 0.5% solution that remained on the electrode was estimated to be about 5 μl. Between dippings, the electrodes were allowed to dry for at least 20 min at room temperature with the electrode surface hanging down. After the last dipping the electrode was allowed to dry for at least 1 h

before use.

Some experiments were made with MB adsorbed from an aqueous solution on the surface (0.0731 cm^2) of the flat circular end of a solid graphite rod (RW 001, Ringsdorff Werke, GmbH) [27] and with soluble MB using a hanging mercury drop electrode, HMDE (Metrohm, Mod. E410)

Electrochemical measurement of MB modified carbon paste.

Cyclic voltammetry of MB modified carbon paste electrodes was employed using a Pt gauze as the counter electrode and a saturated calomel electrode, SCE, as the reference. The amount of electrochemically active mediator was evaluated by integration of the voltammetric waves corrected for the background current. The formal potential, E°', of the mediator was evaluated by taking the mean value of the anodic and cathodic peak potentials of a cyclic voltammogram [30,31]. The supporting electrolyte for these experiments was a 0.25 M phosphate buffer at pH 7.0. Some experiments were made with MB adsorbed on the solid graphite electrode and with dissolved MB using the HMDE.

Experiments with enzyme and cofactor modified carbon paste.

Batch experiments

The enzyme and cofactor modified carbon paste electrode covered with the membrane was dipped into a thoroughly stirred solution (25.0 ml) consisting of 0.25 M phosphate buffer at pH 7.0. The electrode was connected to a potentiostat (Princeton Applied Research, Mod. 174A) using a Pt foil as the counter and a SCE as the reference electrode. Successive additions of 200 μl of a 1.0 M D-glucose solution were added and the responses were registered on a chart recorder as steady state currents.

FIA equipment

The flow injection system consisted of a peristaltic pump, Gilson Minipuls 2, a pneumatically operated valve, Cheminert, type SVA, and a flow through amperometric cell of the wall-jet type [32] under three electrode potentiostatic control using a Princeton Applied Reserch, mod. 174A, instrument. A Pt-wire and an Ag/AgCl electrode (0.1 M KCl) served as the counter and the reference electrodes in the cell. The tip of the syringe containing the CP was pressfitted into a Teflon holder that was inserted into the flow through cell. The outlet jet-electrode distance was set to 1.8 mm [32,33]. A knotted micro-line tubing (Cole Parmer, i.d. 0.51 mm, volume 100 μl) was used as the connector between the injector and the amperometric cell. All other connections were made of Teflon tubing, i.d. 0.5 mm. The carrier used was a 0.25 M phosphate buffer, at pH 7.0, pumped with a flow rate of 0.85 ml min^{-1}. The carrier was degassed by applying a reduced pressure to the solution for a few minutes to prevent microbubbles to appear in the flow system. Samples dissolved in the same buffer were injected with a 50 μl loop if not otherwise stated.

Results and Discussion

Deposition of the mediator to carbon paste and electrochemistry of mediator modified carbon paste.

In previous investigations of the electocatalytic effect of adsorbed Meldola Blue [27] and other adsorbed phenothiazine and phenoxazine derivatives on solid graphite electrodes [33,34] it was concluded that the response to NADH became independent of the amount of adsorbed mediator once the surface coverage exceeded a certain value. Efforts were therefore taken to add the mediator to the carbon paste in a way that a high electrochemical response of the mediator, as seen with cyclic

voltammetry, could be obtained. The investigation was performed by a comparison of the electrochemical response of the mediator with the technique used to deposite the mediator to the CP, see Experimental section. The highest electrochemical response was obtained with the mediator added as a dry powder. With the mediator first dissolved in ethanol a high electrochemical response was also registered. When dissolved in either water or aceton much lower electrochemical responses were obtained. The lowest response was obtained when MB was adsorbed on the surface of the carbon paste electrode. The same results were obtained for CPs based on either graphite or Ketjen black. It was thus concluded that the mediator should be added as a dry powder to the carbon paste and all results reported below were obtained with the mediator added in this way.

Fig. 1 shows four different cyclic voltammograms of MB all registered in 0.25 M phosphate buffer at pH 7.0. Fig. 1**a** reflects the characteristics of adsorbed MB on a graphite surface [27, Fig. 1**b** those of dissolved MB (0.5 mM) in the buffer solution when using the HMDE, Fig. 1**c** those of MB when added as a dry powder to the CP (4 mg per 100 mg graphite powder), and Fig. 1d those of the MB modified CP electrode also covered with six layers of the Eastman AQ 29D membrane.

As can be seen all cyclic voltammograms clearly show the oxidation and reduction waves of MB. This is in accordance with an electrochemical reaction previously shown for MB at this pH [27];

$$MBH \Longleftrightarrow MB^{+} + H^{+} + 2e^{-} \qquad (1)$$

where MBH and MB^{+} denote the reduced and the oxidized forms of MB, respectively. An approximate value of the formal potential, E°', of the mediator can be obtained by taking the mean value of the peak potentials of the oxidation and reduction waves

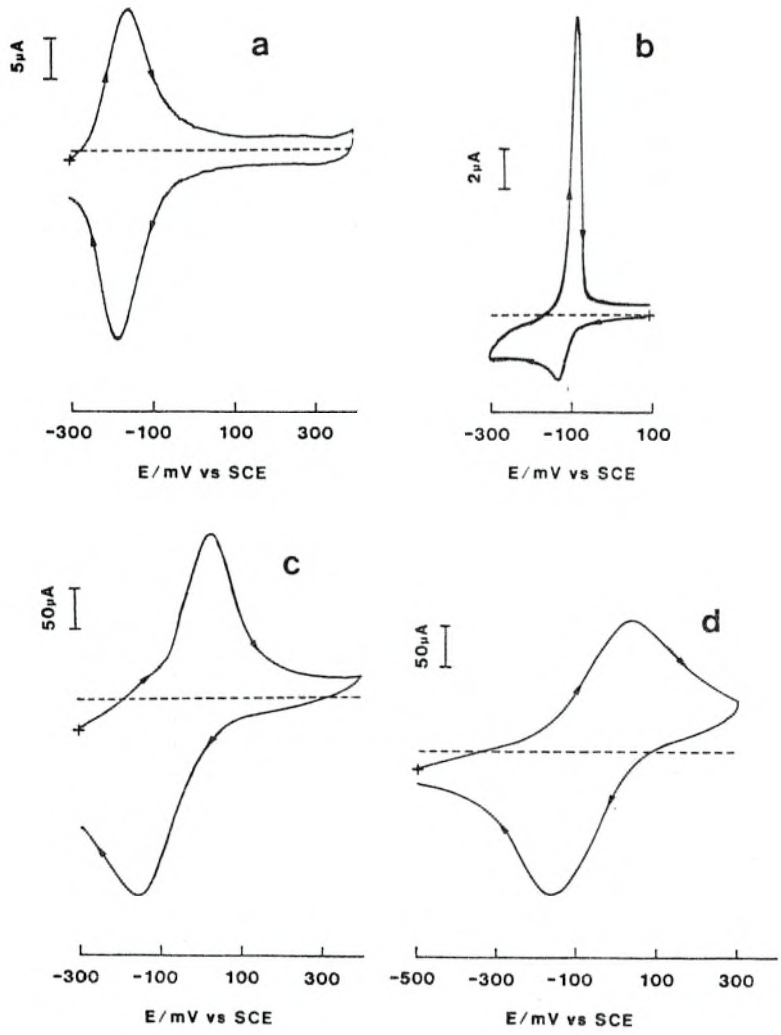

Fig. 1. Cyclic voltammograms (CV) of **a**/ adsorbed MB (6 10^{-9} mol cm^{-2}) on a solid graphite rod, **b**/ dissolved MB (0.5 mM) using a HMDE, **c**/ MB mixed dry into a graphite paste (see #1 in Table 1), and **d**/ as in **c**/ but covered with six layers of the poly(ester sulphonic acid) cation exchanger.
All CVs were recorded with a sweep rate of 50 mV s^{-1} and in a 0.25 M phosphate buffer (pH 7.0) as the supporting electrolyte. (+) denotes the starting potential and (——) zero current.

[30,31]. The E°'-value of MB adsorbed on solid graphite, Fig. 1a, was previously found to be -175 mV vs SCE at pH 7.0 [27]. No literature data of the E°'-value of dissolved MB was available but a tentative value could be obtained by registration of cyclic voltammograms of dissolved MB using the HMDE. The cyclic voltammograms obtained for dissolved MB revealed the typical shape of a redox species where the oxidized form is soluble and where the reduced form is precipitated on the electrode surface because of its low solubility in aqueous solutions [31]. The E°'-value for MB in solution was evaluated to be -110 mV vs SCE at pH 7.0, which is in accordance with previous data when comparing the E°'-values of adsorbed and dissolved phenoxazine derivatives [34]. Both the anodic and the cathodic peak potentials of MB in the CMCP are more positive than those of adsorbed MB on solid graphite. The mean E°'-value of MB in the CMCP at this pH was -70 mV vs SCE indicating yet another E°'-value of MB. The reason for a higher value than in solution may be that the reduced form of MB may be soluble in the paraffin oil of the CMCP which should move the E°' to a more positive value [30], see also below.

The voltammograms of the CMCP revealed much higher amounts of electrochemically active MB compared with the highest values reported for adsorbed MB on solid graphite [27]. The area of the CMCPE exposed to the contacting buffer is about one third of that of the solid graphite rod. The voltammograms indicate that about 20 to 30 times more electrochemically active MB can be deposited in the CMCP as compared with the amount of adsorbed MB on a solid graphite electrode. The shapes of the anodic and the cathodic waves are different and not mirror images of each other. The anodic wave indicates the oxidation of a species immobilised or precipitated on the electrode surface. The estimated integrated areas under the peaks of a single cyclic voltammogram are within the same order of magnitude with a slightly larger value for the area under the

reduction wave.

It was noticed that the current of the voltammetric waves first became higher on successive scans of the CMCPE immediately after exposure to the contacting buffer. The peak potential of the oxidation wave varied somewhat with the size of the current being more positive for higher currents. The peak potential of the reduction wave remained, however, constant throughout the experiments. The E°'-value given above (-70 mV) is therefore only an approximative value. The voltammograms then became slightly lower on successive scans probably because of dissolution of MB from the CMCP out into the buffer. It was also noticed when the CMCPE was stored in buffer that the solution in the close vicinity of the electrode surface became slightly coloured by dissolving MB. The variation between the peak current and the sweep rate of the scan does neither follow a linear relationship with the square root of the sweep rate nor with the sweep rate but rather something in between. The peak separation of the CMCPE is rather large, ≈100 to 150 mV, in contrast to adsorbed MB [27] and dissolved MB. The reason for this is not fully clear. One explanation could be that both immobilised and dissolved MB contribute to the obtained voltammograms. Other reasons may be a restriction in the charge transfer process due to the high surface concentration of the mediator.

A cyclic voltammogram of a CMCPE covered with six layers of the Eastman AQ 29D polymer is shown in Fig. 1d. The high electrochemical response reveal that the MB in the CMCP is in contact with the buffer solution. The peak potential values remain virtually the same after the addition of the membrane but the shape of the anodic wave becomes quite different, now more a mirror image of the cathodic wave. For some electrodes the area under the waves increased whereas for other electrodes the area decreased after the membrane deposition. On successive

scans the voltammograms were almost completely identical indicating that the membrane prevents leakage of mediator from the CMCP. Only a very weak colouring of the contacting solution was noticed after storage of the membrane covered electrode for several days in buffer. However, the membrane soon became strongly coloured and it is expected that the negative charges within the membrane should attract the positively charged oxidized form of the mediator [28,29]. There is no evidence that the entrapped mediator in the membrane is electrochemically active. Very similar results (not shown) to those mentioned above were obtained when Ketjen black was used instead of the graphite powder. The only exception was that no colouring of the buffer was noticed on storing these membrane covered electrodes, probably indicating a stronger affinity of MB to Ketjen black than to graphite.

Fig. 2 shows a cyclic voltammogram of a graphite CMCPE (no membrane) in pure buffer (Fig. 2**a**) and with NADH (10.7 mM, Fig. 2**b**) added to the buffer. Compared with the cyclic voltammogram in Fig. 2**a**, the anodic wave is increased and the cathodic wave is decreased. When NADH from the contacting buffer reaches the electrode surface it will react with the oxidised form of the mediator, MB^+. First a complex will be formed which will rapidly decompose into NAD^+ and the reduced form of the mediator, MBH [21,27]. The reduced form of the mediator will be electrochemically reoxidised if the applied potential is more positive than the E°'-value of the MB^+/MBH redox couple.

$$NADH + MB^+ \Longleftrightarrow \text{complex} \longrightarrow NAD^+ + MBH \qquad (2)$$

$$MBH \longrightarrow MB^+ + H^+ + 2e^- \qquad (3)$$

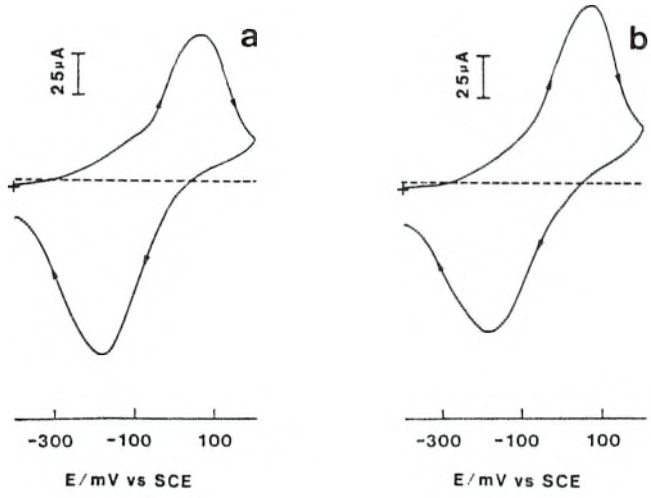

Fig. 2. Cyclic voltammograms of graphite paste electrodes (# 1 in Table 1) **a**/ without and **b**/ with NADH (10.7 mM) in the contacting solution. Electrochemical conditions, see Fig. 1.

Enzyme and cofactor modified carbon paste.

When GDH and NAD^+ are added to the MB modified carbon paste all necessary chemicals are present within the paste to obtain a response to dissolved glucose at low applied potentials. It was concluded from the experiments described above that an applied potential of +100 mV should be sufficient to rapidly reoxidise the reduced form of the mediator, reaction (3), Fig. 2**b**, expected to be formed in the presence of glucose and not to be rate limiting to the overall reaction kinetics. All electrodes were covered with the membrane to prevent dissolution of aqueous soluble species in the paste into the buffer. The reaction scheme is outlined in Fig. 3.

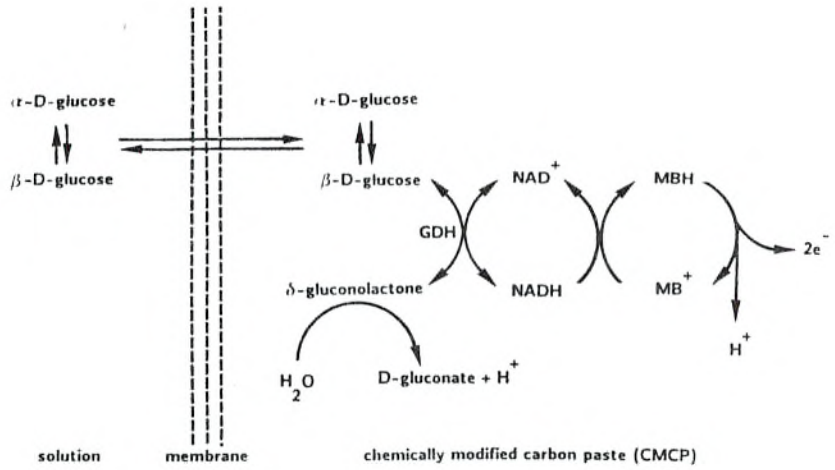

Fig. 3. Reaction sequence within the membrane coated CMCPE, for further details see text.

Glucose from the solution will pass the membrane, where the β-D-form will be enzymatically oxidised in the presence of NAD^+ to form δ-gluconolactone and NADH. The enzymatic reaction is chemically reversible but is counteracted by the irreversible addition of water to the lactone, driving the enzymatic reaction to the product side. The NADH formed will be reoxidised by MB^+ to form MBH, reaction (2), which in turn is electrochemically reoxidised at the applied potential. This reaction sequence will also counteract the reversible nature of the enzyme reaction.

Fig. 4a shows a set of calibration curves obtained from batch experiments (see Experimental section) of four electrodes equally prepared from the same batch of CMCP and covered with three layers of the membrane. The composition of the CMCP was according to #1 given in Table 1. The main information given in the figure is that the system works. Both GDH and NAD^+ are active when mixed into the carbon paste and the NADH formed in the enzymatic reaction can be electrocatalytically oxidised as expected from the results given in Fig. 2b. However, the variation in the response between the electrodes is rather large. Several explanations for this may be given; the carbon paste is not homogeneously mixed, the actual electrode area may vary after filling the tip of the syringes with the enzyme-cofactor paste, the deposition of the membrane is not reproducibly done. Fig. 4b shows the calibration curves of the same set of electrodes when further covered with three additional layers of the membrane. The electrodes covered with three layers of the membrane gave as expected higher responses (≈ 10 times) compared with electrodes covered with six layers of the membrane as a result of an increased mass transfer resistance. The higher response of the thrice coated electrodes results in calibration curves starting to deviate from linearity at lower glucose concentrations than the calibration curves obtained for electrodes covered with six layers. When plotting the calibration data as response current versus response current divided by the glucose concentration (electrochemical Eadie-Hofstee plot [35]), the apparent Michaelis-Menten constant, K_M^{app}, can be calculated from the slope of the linear part of the plot [24,35]. Fig. 5 shows the typical result of such an Eadie-Hofstee plot for glucose concentrations between 5 and 70 mM and with an electrode with six membrane layers. Both the enzymatic reaction and the reaction between the mediator and NADH obey kinetics described by the Michaelis-Menten equation [27]. The K_M for free GDH was previously determined to be 3.0 mM [36] (0.1 M phosphate buffer

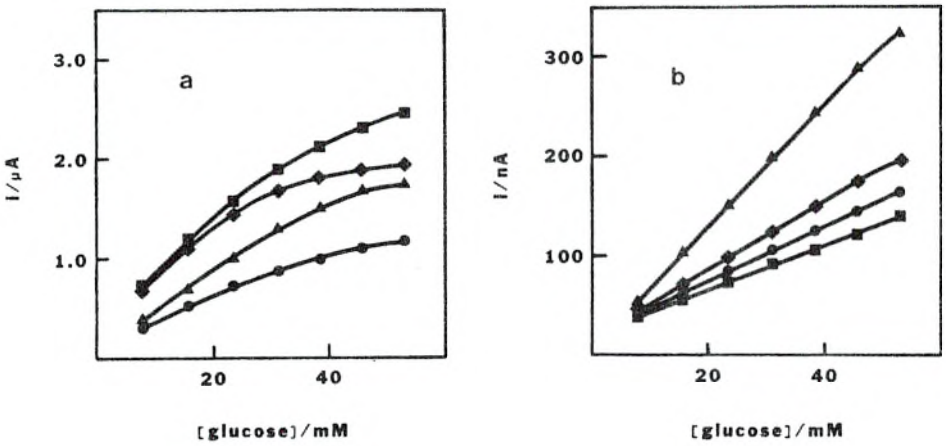

Fig. 4. Calibration curves obtained from batch experiments of four (-■-, -◆-, -▲-, and -●-) equally prepared electrodes (#1 in Table 1) after being covered with three layers (**a**/) and with six layers (**b**/) of the polymer.

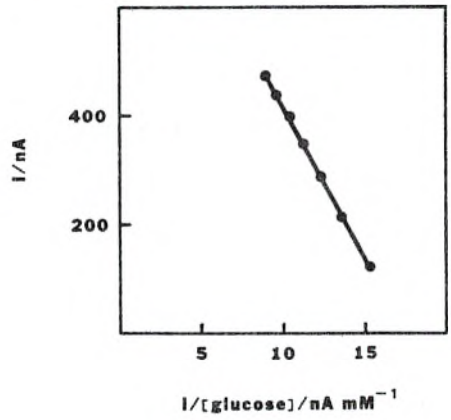

Fig. 5. Electrochemical Eadie-Hofstee plot of a CMCPE (#1 in Table 1) covered six times with the polymer. For experimental conditions, see Fig. 4 and text.

at pH 7.6) and the K_M for the reaction between MB and NADH at pH 7.0 to be 1.1 mM [27]. The K_M^{app} values increased between six and seven times when the electrodes were further covered with the membrane from three to six layers. The kinetics of the enzymatic reaction or the reoxidation of the reduced cofactor within the CMCP are not expected to vary with the number of membrane layers. The only possible explanation to the increased value of K_M^{app} when increasing the number of membrane layers is therefore an increased mass transfer resistance for glucose to reach the CMCP. Typical values for electrodes covered three times with the membrane were between 20 and 50 mM and accordingly, values between 120 and 350 mM were obtained for electrodes covered six times. If the glucose concentration is less than 0.1 K_M^{app} linear calibration curves are then expected.

The stability of the thrice covered electrodes revealed, however, a decrease in the response to glucose between subsequent measurements whereas the response of the six times covered electrodes remained virtually unchanged. When the six layered electrodes were stored between days in buffer the initial background currents were negative, large, and decreased only slowly (up to 1 h) before a steady baseline was reached. When stored dry the initial background current was positive and very small which allowed measurements within 1 min. Most of the electrodes showed a somewhat increased glucose response after storage. To obtain stable electrodes it was thus concluded that the electrodes should be covered six times with the coating and that they should be stored dry overnight. Fig. 6 shows the calibration curves obtained with the same electrode coated six times after 1, 8, and 16 days and stored dry.

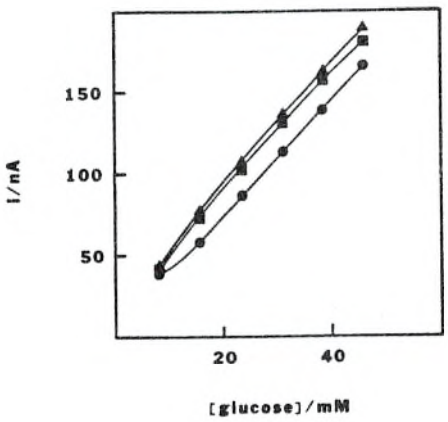

Fig. 6. Calibration curves obtained for the same CMCPE (#1 in Table 1) six times covered with the polymer, (-●-) 1 day, (-▲-) 8 days, and (-■-) 16 days after preparation.

Four different mixtures of enzyme and cofactor carbon pastes, Table 1, were prepared and analysed for their glucose response and stability between experiments.

Table 1. The contents of the four enzyme and cofactor modified carbon pastes.

#	amount of carbon/mg	amount of paraffin oil/µl	amount of MB/mg	amount of GDH/mg	amount NAD^+/mg
1	100 (graphite)	40	3.7	8.0 (1770 U)	51.7
2	100 (Ketjen black)	440	4.4	8.5 (1880 U)	50.8
3	100 (graphite)	40	3.9	8.6 (1890 U)	75.4
4	100 (graphite)	40	3.6	17.0 (3740 U)	51.1

Comparisons were made between the carbon materials, between the amounts of cofactor and enzyme, between the number of membrane coatings (3 or 6 times with the 0.5% polymer solution), and between storage conditions (in 0.25 M phosphate buffer at 4°C or dry at 4°C) to obtain electrodes that showed a long term stability to allow further investigations in the FIA mode (see below). No experiments were made with uncovered electrodes based on the experience of previous work with a carbon paste containing only one aqueous soluble component (glucose oxidase) [24], which revealed a much prolonged stability of the electrode when covered with the membrane. The pastes investigated here all contain three aqueous soluble compounds, the mediator, GDH, and NAD^+, and therefore stability of uncovered electrodes was not expected. Five or six electrodes of each batch were identically prepared and tested for their glucose responses.

Electrodes based on graphite (#1) gave responses about ten times larger than electrodes based on Ketjen black (#2) containing similar amounts of GDH, MB, and NAD^+. To make a paste of the graphite powder only 40 µl of the paraffin oil needed to be added to 100 mg of the powder, whereas ten times more were needed for the Ketjen black. The more pronounced organic nature of the Ketjen black paste might therefore decrease the activity of the enzyme in this preparation compared with the paste based on the graphite powder. Because of the lower glucose response of the Ketjen black paste electrodes, it was concluded that Ketjen black was a less suitable carbon material for this purpose and all further experiments were performed with carbon pastes based on graphite.

When the NAD^+ content of the carbon paste was increased from 51.7 mg (#1) to 75.4 mg per 100 mg of graphite (#3) no significant increase in the response to glucose was noticed

indicating that the amount of NAD^+ in the paste (#1) does not set a limit to the response. When the GDH content was increased from 1770 U (#1) to 3740 U (#4) per 100 mg of graphite a very drastic increase (≈ 10 times) in the glucose response was observed. The membrane of these electrodes soon became, however, bulky and for some of the electrodes the membrane even bursted. A high content of aqueous soluble species in the carbon paste unable to pass the membrane is expected to cause osmosis leading to such a high pressure on the inside of the membrane causing eventual rupture. The final conclusion was that electrodes prepared from batch #1 covered six times with the membrane and stored dry overnight were the most stable and reliable glucose electrodes and should suit as electrodes for introduction into a FIA system.

FIA measurements.

Fig. 7 shows the response to 5 mM glucose for five different injection volumes. The FIA peaks show that the electrode rapidly responds to the incoming sample plug but there is a marked tailing of the peaks. A larger volume gives as expected a higher response but will also decrease the sample throughput. The same FIA system with an injection volume of 50 μl was previously investigated using solid electrodes and the disperion factor [37] was determined to be 1.3 [33]. Comparing the responses for 50 and 400 μl injections reveal a response ratio of 2.3 without reaching a steady state response for the larger injection volume. This clearly shows the influence of the membrane on the response of the electrode. The response is also much lower than that obtained for solid graphite electrode where the surface was modified with adsorbed mediator and GDH [3]. As a compromise between response and sample throughput an injection volume of 50 μl was chosen.

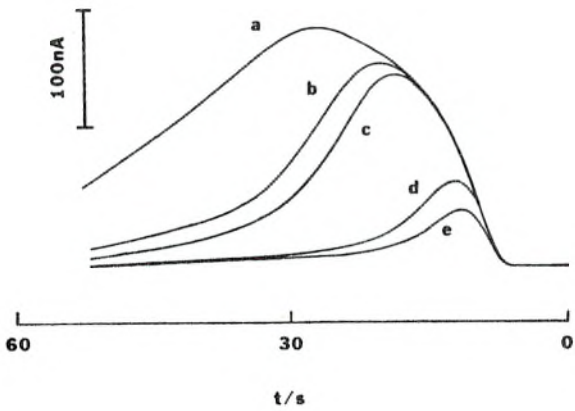

Fig. 7. FIA peaks obtained for 5 mM glucose with a CMCPE (#1 in Table 1) six times covered with the polymer and with different injection volumes; a/ 400, b/ 200, c/ 160, d/ 50, and e/ 25 μl. For experimental conditions, see text.

Fig. 8a shows a series of FIA peaks obtained within the linear concentrations. The products formed on the inside of the membrane except NADH are D-gluconate and protons. The D-gluconate is negatively charged and will face a negatively charged barrier when diffusing out of the membrane. A slight decrease in pH is therefore expected on the inside of the membrane as a result of the enzymatic reaction which should contribute to an increased tailing of the peaks. Other reasons for the tailing may be that the enzymatic and electrochemical reactions occur not only just inside of the membrane but also further within the paste. With an injection volume of 50 μl a sample throughput of about 40 h^{-1} can be obtained. Fig. 8b shows the reproducibility for continuous injections of 5 mM glucose over a period of 90 min. The figure also shows the slight baseline drift that was typical for these electrodes. The linear dynamic response range is set by the actual electrode. As was shown above the variation of the response

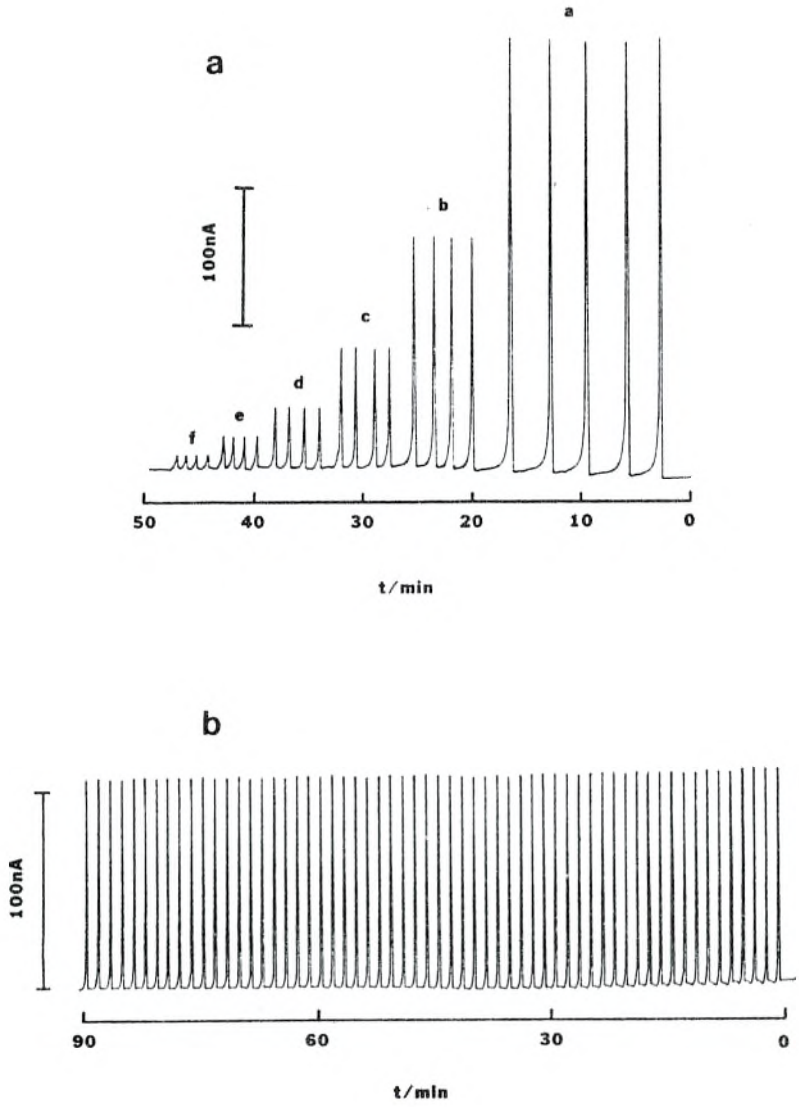

Fig. 8. FIA recordings (50 μl) of a 20 days old CMCPE (#1 in Table 1) six times covered with the polymer, in **a**/ of six different glucose concentrations (a/ 10, b/ 5, c/ 2.5, d/ 1.25, e/ 0.625, and f/ 0.312 mM) and in **b**/ of continuous injections of 5 mM glucose.

between electrodes is rather large. The lower limit of the calibration curve was about 150 μM and the upper limit about 20 mM. The lowest detection limit obtained was 80 μM (twice the background noise). The background current was in the order of 10 to 20 nA.

The variation of the response with the applied potential is depicted in Fig. 9. The response increases somewhat when the applied potential is decreased from +100 mV to +50 mV. A step wise decrease in potential with 50 mV results in a decreased response down to -100 mV and a further decrease to -150 results in a total loss of response. When reversing the direction of the potential change the response current only appears after the potential has been made more positive than -50 mV. No explanation can be given at this stage to why the response remains nill going from -150 to -100 mV.

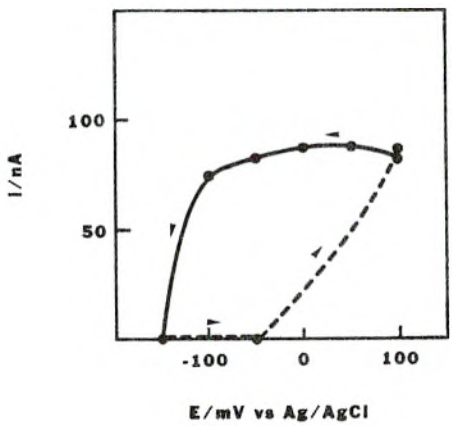

Fig. 9. Variation of the FIA response (50 μl) to 5 mM glucose with the applied potential of a CMCPE (#1 in Table 1) six times coated with the polymer. The arrows indicate the direction of the change of potential, starting at +100 mV.

A separate experiment was performed to see the exclusion effect of the membrane to ascorbic acid, a negatively charged and a low molecular weight substrate easily oxidisable at low potentials at carbon electrodes [38]. Fig. 10 shows the variation of the response to 1 mM L(+)-ascorbate at a naked graphite paste electrode as a function of the applied potential as well as at an electrode covered with six layers of the membrane. Even at low potentials (-100 mV) a response to ascorbate is obtained. An increase in the applied potential results in an increased response, but not even at +300 mV maximum response is not reached revealing the irreversible nature of the electrochemical oxidation of ascorbate [38]. Fig. 10 also shows the variation of the same electrode when covered with six layers of the membrane clearly denoting the exclusion effect of the membrane.

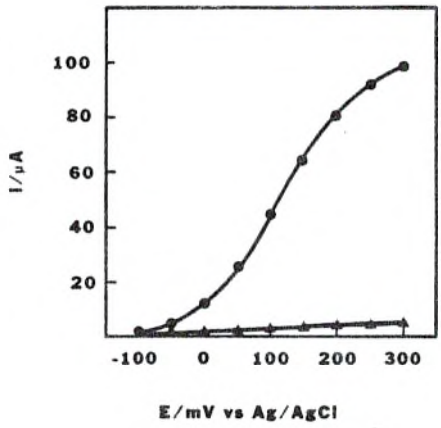

Fig. 10. Variation of the FIA response (50 μl) to 1 mM L(+)-ascorbate of an uncovered (-●-) and of a six times polymer covered carbon paste electrode (-▲-). The composition of the carbon paste was 40 μl paraffin oil to 100 mg of graphite powder. For FIA conditions, see text.

Conclusion

A dehydrogenase is shown to be immobilised with retained activity together with its necessary cofactor and a mediator within a graphite paste electrode. The enzyme catalysed reaction can be followed amperometrically within a potential range that governs a selective detection. Graphite has been reported to catalytically decompose the cofactor [39] but with this paste no decrease in the response to glucose could be traced within a few weeks that could be correlated to a decomposition of the cofactor and hence a decrease in the content of active cofactor in the paste. This might be the result of a high loading of the cofactor or that the catalytically active sites of the graphite might be blocked by a small amount of the cofactor, by the mixing with paraffin oil, enzyme, or mediator. The mediator used, Meldola Blue, is in its oxidised form water soluble and is irreversibly decomposed at pHs higher than 7. There are other mediators [33,34] that are stable under alkaline conditions and exhibit a more irreversible adsorption on graphite than Meldola Blue. The reasons why Meldola Blue was chosen for this first study of a phenoxazine CMCPE were that it is commercially available, documented in a previous glucose sensor investigation [3], and also to make possible a future comparison of the behaviours of CMCPEs based on less water soluble mediators and sensors thereof.

Acknowledgement

The authors thank the National Energy Administartion (STEV) and the Swedish Board for Technical Development (STU) for financial support. The authors also thank Dr. W. Waeny, Eastman Chemical Int. AG, Zug, Switzerland, and Mr. W. Larsen, Akzo Zout Chemie Svenska AB, Göteborg, Sweden, for the gifts of the Eastman AQ 29D preparation and of the Ketjen Black, respectively.

References

1. N. Cenas, J. Rozgaite and J. Kulys, *Biotechnol. Bioeng., 26* (1984) 551.
2. F. Schubert, D. Kirstein, K. L. Schroeder and F. W. Scheller, *Anal. Chim. Acta, 169* (1985) 391.
3. G. Marko-Varga, R. Appelqvist and L. Gorton, *Anal. Chim. Acta, 179* (1986) 371.
4. J. Kulys, V. V. Sorochinskii and R. Vidziunaite, *Biosensors, 2* (1986) 135.
5. G. Palleschi, *Anal. Lett., 2* (1986) 135.
6. G. Palleschi, G. G. Guilbault, G. J. Lubrano and M. A. Nabi Rahni, *Anal. Chim. Acta, 192* (1987) 339.
7. W. J. Albery, P. N. Bartlett and A. E. G. Cass, *Phil. Trans. R. Soc. London, B, 316* (1987) 107.
8. J. Kulys, N. Cenas and J. Kanapieniene, *Stud. Biophys., 119* (1987) 175.
9. G. Palleschi, *NATO ASI Ser., Ser. C, 226 (Anal. Uses Immobilized Biol. Comp. Detect., Med. Ind. Uses)* (1988), 83.
10. M. Polasek, L. Gorton, R. Appelqvist, G. Marko-Varga and G. Johansson, paper in R. Appelqvist Doctoral Thesis, University of Lund, 1987.
11. T. Buch-Rasmussen, Thesis, Danish Technical University, 1989.
12. M. O. Månsson, P. O. Larsson and K. Mosbach, *Eur. J. Biochem., 86* (1978) 455.
13. M. Lindberg, P. O. Larsson and K. Mosbach, *Eur. J. Biochem., 40* (1973) 187.
14. B. Dolabdjian, G. Grenner, P. Kirch and H.-L. Schmidt, *Enzyme Eng., 4* (1978) 399.
15 A. F. Bückmann, M.-R. Kula, R. Wichman and C. Wandrey, *J. Appl. Biochem., 3* (1981) 301.
16. T. Yao and S. Musha, *Anal. Chim. Acta, 110* (1979) 203.
17. W. J. Blaedel and R. A. Jenkins, *Anal. Chem., 48* (1976) 1240.
18. S. Yabuki, H. Shinohara, Y. Ikariyama and M. Aizawa, *J. Electroanal. Chem., 277* (1990) 179.
19. M. J. Batchelor, M. J. Green and C. L. Sketch,*Anal. Chim. Acta, 221* (1989) 289.
20. H. K. Chenault and G. M. Whitesides, *Appl. Biochem. Biotechnol., 14* (1987) 147.
21. L. Gorton, *J. Chem. Soc., Faraday Trans., I, 86* (1986) 1245.
22. T. Ikeda, H. Hamada, K. Miki and M. Senda, *Agric. Biol. Chem., 49* (1985) 541.
23. P. D. Hale, T. Inagaki, H. I. Karan, Y. Okamoto and T. A. Skotheim, *J. Am. Chem. Soc., 111* (1989) 3482.
24. L. Gorton, H. I. Karan, P. D. Hale, T. Inagaki, Y. Okamoto and T. A. Skotheim, *Anal. Chim. Acta, 228* (1990) 23.
25. P. D. Hale, T. Inagaki, H. S. Lee, H. I. Karan, Y. Okamoto and T. A. Skotheim, *Anal. Chim. Acta, 228* (1990) 31.
26. J. Wang, L.-H. Wu, Z. Lu, R. Li and J. Sanchez, *Anal. Chim. Acta, 228* (1990) 251.

27. L. Gorton, A. Torstensson, H. Jaegfeldt and G. Johansson, *J. Electroanal. Chem., 161* (1984) 103.
28. J. Wang and T. Golden, *Anal. Chem., 61* (1989) 1397.
29. J. Wang and Z. Lu, *J. Electroanal. Chem., 266* (1989) 287.
30. E. Laviron, in *Electroanalytical Chemistry, Vol. 12*, A. J. Bard, ed., Marcel Dekker, New York, 1982, pp. 53-157.
31. A. J. Bard and L. R. Faulkner, in *Electrochemical Methods, Fundamentals and Applications*, Wiley & Sons, New York, 1980.
32. R. Appelqvist, G. Marko-Varga, L. Gorton, A. Torstensson and G. Johansson, *Anal. Chim. Acta, 169* (1985) 237.
33. B. Persson, *J. Electroanal. Chem.*, in press.
34. B. Persson and L. Gorton, *J. Electroanal. Chem.*, accepted.
35. R. A. Kamin and G. S. Wilson, *Anal. Chem., 52* (1980) 1198.
36. P. V. Sundaram, B. Blumenberg and W. Hinsch, *Clin. Chem., 25* (1979) 1436.
37. J. Ruzicka and E. H. Hansen, in *Flow Injection Analysis, 2nd Ed.*, J. D. Winefordner and I. M. Kolthoff, eds., Wiley & Sons, New York, 1988, p. 23.
38. I.-F. Hu and T. Kuwana, *Anal. Chem., 58* (1986) 3235.
39. T. C. Wallace and R. W. Coughlin, *Biotechnol. Bioeng., 20* (178) 403.

VI

Biofuel anode based on D-glucose dehydrogenase, nicotinamide adenine dinucleotide and a modified electrode

Björn Persson, Lo Gorton, Gillis Johansson and Arne Torstensson

Department of Analytical Chemistry, University of Lund, PO Box 124, S-221 00 Lund, Sweden

(Received 1 April 1985)

A biofuel cell anode has been made from a modified graphite electrode and immobilized D-glucose dehydrogenase [β-D-glucose:NAD(P)$^+$ 1-oxidoreductase, EC 1.1.1.47] so that energy could be drawn from the conversion of D-glucose to D-gluconic acid. An equivalent amount of dihydronicotinamide adenine dinucleotide (NADH) was formed from NAD$^+$ and reduced the surface groups of the modified electrode. Reoxidationn of the latter produced the electrons necessary for a power output from the cell. Electrode modification was made by adsorption of N,N-*dimethyl-7-amino 1,2-benzophenoxazinium onto the graphite. A current density of 0.2 mA cm^{-2} at a cell voltage of ~0.8 V was obtained for more than 8 h with a simulated oxygen cathode. The internal resistance in the cell, in particular in the separator, appeared to be the main current-limiting factor.*

Keywords: Electrode; biofuel anode, D-glucose dehydrogenase; nicotinamide adenine dinucleotide

Introduction

The possible advantages of biofuel cells have been recognized for a long time, but the number of such fuel cells described so far is small.[1,2] The main obstacle has been the slowness of charge transport from the substrate to the anode, both when microorganisms and isolated redox enzymes have been used. When redox enzymes are used, energy is first transferred to a coenzyme or to a prosthetic group and then to an electrode. The electron transfer is slow either because the prosthetic group is embedded in the enzyme and is less accessible for interaction with an electrode reaction, or because the overvoltage of the coenzyme reaction at the electrode is high. Addition of a mediator which reacts with the microorganism, with the coenzyme or with the prosthetic group and then with the electrode provides a much easier route for charge transfer. *N*-Methyl and *N*-ethyl phenazinium ions, Methylene Blue, tetramethyl phenylenediamine and 2,6-dichlorophenol indophenol have been shown to mediate electron transfer in reactions involving alcohols, D-glucose or xanthine as substrates.[3–10]

The present work deals with energy transfer from D-glucose to a graphite electrode via a NAD$^+$/NADH dependent enzyme, D-glucose dehydrogenase [GDH, β-D-glucose: NAD(P)$^+$ 1-oxidoreductase, EC 1.1.1.47]. Direct oxidation of NADH requires a potential of +550 to +800 mV vs. SCE at pH 7.0, depending on the electrode material, i.e. an overpotential of ~1 V. The direct oxidation may result in electrode fouling, resulting in still higher overvoltages.[11] Mediated oxidation, on the other hand, will take place close to the formal potentials ($E^{0'}$) of the mediators, which are −165 mV and −210 mV for the *N*-methyl and *N*-ethyl phenazinium ions, respectively,[12] and −175 mV for *N,N*-dimethyl-7-amino-1,2-benzophenoxazinium ion, Meldola Blue (MB$^+$),[13] all vs. SCE at pH 7.0. A spontaneous reaction is therefore expected when the bioanode with mediator is coupled to an oxygen cathode with a potential of +560 mV. The alkyl phenazinium ions are very unstable and light-sensitive, whereas Meldola Blue is fairly stable, especially at pH values <7.0. Meldola Blue adsorbs irreversibly on graphite to form a modified electrode, with a high reaction rate with NADH.[14] The advantages of using mediators immobilized on electrode surfaces have recently been reviewed.[14,15]

The reduced coenzyme will be produced by the reaction:

$$\beta\text{-D-glucose} + \text{NAD}^+ + \text{H}_2\text{O} \xrightarrow{\text{GDH}} \text{D-gluconate} + \text{NADH} + \text{H}^+ \quad (1)$$

The reaction between the mediator and the reduced coenzyme involves the formation of a charge-transfer complex which decomposes to NAD$^+$ and the reduced mediator (MBH) in a rate-limiting step:[13]

$$\text{NADH} + \text{MB}^+ \rightleftharpoons (\text{NADH}\cdot\text{MB}^+) \quad (2)$$

$$(\text{NADH}\cdot\text{MB}^+) \rightarrow \text{NAD}^+ + \text{MBH} \quad (3)$$

MBH is oxidized electrochemically:

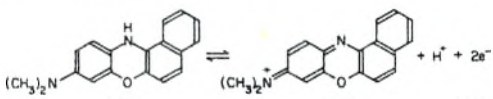

(4)

The reaction is, in fact, more involved than the scheme shown in equations (2)–(4) above; it is known that rate increases in a complex way when pH decreases.[16]

If the sequence described above is used in a biofuel cell with the enzyme immobilized in a reactor and with a modified electrode, the overall reaction will be:

$$\beta\text{-D-glucose} + \text{H}_2\text{O} \rightarrow \text{D-gluconate} + \text{H}^+ + \text{energy} \quad (5)$$

0141–0229/85/110549–04 $03.00

Materials and methods

A three-compartment glass cell with ceramic sintered porous glass discs as separators was used throughout (see *Figure 1*). The anode compartment was filled with 30 ml solution, which was deaerated by nitrogen bubbling. The anode was a graphite disc, external diam. 46 mm, thickness 7 mm (Ringsdorff-Werke GmbH, RW-0711). The bottom circular surface, of area 16 cm^2, was polished on wet, fine emery paper and then covered with mediator. The circumferential surface was covered with a Teflon tape.

Modification was made by dipping the electrode into an ethanol–phosphate buffer (50:50 v/v), pH 4.0, containing 1 mmol l^{-1} of the chromatographically purified Meldola Blue. The electrode was washed and the surface coverage was determined from a cyclic voltammogram as described previously.[13] The electrode was rotated at 740 rev min^{-1} during fuel cell operation.

The real cathode, a Pt gauze in line with the intermediate chamber in the cell, was the working electrode of a potentiostatic circuit. The electrode reaction was the reduction of water to hydrogen, which occurs at negative potentials. A variable series voltage displaced the potential of point P (V_2) to +560 mV (*Figure 1*) vs. SCE, i.e. to the same potential as that of an ideal oxygen electrode. The modified electrode will therefore 'see' the Pt gauze as an ideal oxygen cathode. The local potentiostatic voltage was set so that the current (A_2) in the local loop was at least 1 mA larger than the expected maximum biofuel cell current. The current through the Pt gauze cathode was thus kept constant but the proportion of the current carried by the local auxiliary anode diminished as the biofuel cell current increased. Time dependent pH changes in the chamber resulted in some drift of the current setting. The cell current and the cell voltage were read from the ammeter (A_1) and voltmeter (V_1), respectively, when the biofuel cell was loaded with the resistor (R).

D-Glucose dehydrogenase (GDH), from *Bacillus megaterium* (Merck, catalogue no. 13732) was immobilized on porous glass (CPG-10, 80–120 mesh, pore size 700 Å) using glutaraldehyde.[17] It was put into a Teflon reactor, int. diam. 6.0 mm, volume 600 µl. Liquid was pumped through the reactor with a peristaltic pump (≈13 ml min^{-1}). Liquid was also pumped through a spectrophotometer (LKB, model 2151) set at 372 nm. Due to the high NADH concentration, it was necessary to select a wavelength towards one end of the absorption curve.

The anode compartment initially contained 80 mmol l^{-1} D-glucose in 30 ml 0.25 M phosphate buffer, pH 7.0, and various concentrations of 1,4-dihydronicotinamide adenine dinucleotide (NADH) (Sigma Chemical Co., catalogue no. N.8129). The intermediary and cathode (11 ml) compartments were filled with 0.37 M phosphate buffer, pH 7.0.

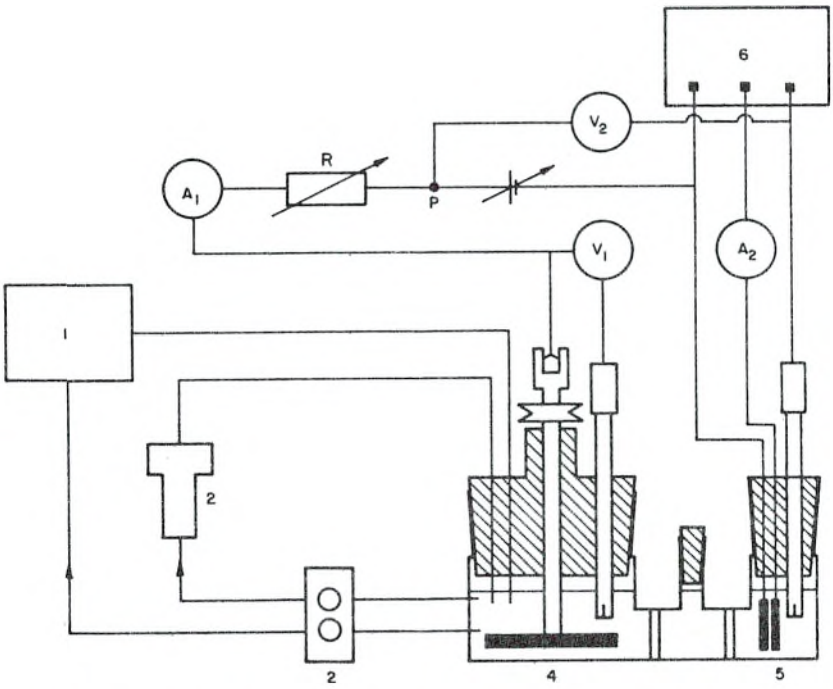

Figure 1 Diagram of the biofuel cell. 1, Flow-through spectophotometer for NADH-monitoring; 2, enzyme reactor; 3, peristaltic pump; 4, anode half-cell; 5, cathode half-cell with a simulated oxygen electrode controlled by the potentiostat; 6, V_1 and V_2 read the anode potential and the potential of point P vs. SCE, respectively; A_1 and A_2 read the currents in the biofuel cell and the simulated oxygen circuit, respectively

Results

The operating conditions of the biofuel cell were selected so that the coenzyme would be mainly present in the reduced form, i.e. the enzyme reactor should have a high conversion capacity compared to the rate of the electrochemical reactions in equations (2)–(4). Separate experiments showed that the enzyme reactor could convert NAD^+ to NADH with essentially 100% efficiency at 13 ml min^{-1} when the D-glucose concentration was 50 mmol l^{-1}. Since D-glucose was present at a concentration of 80–65 mmol l^{-1} in the anolyte, a completely reduced coenzyme will be continuously pumped back to the anode compartment. The NAD^+/NADH ratio reached ~0.06 for a biofuel cell current of 3 mA, which is an indication that the combined rate of pumping and enzymatic reaction [equation (1)] was high compared to the rate of electron transfer at the modified electrode.

The cell currents of the loaded biofuel cell were independent of the rotational speed of the anode in the range 440–2500 rev min^{-1}. This indicated that the mass transfer of NADH up to the surface of the modified electrode was faster than the cell reaction. The cell current became almost independent of the NADH concentration if it was ⩾0.30 mmol l^{-1} when the cell current was 1.1 mA. The internal resistance of the biofuel cell was close to 200 ohm, however, and this limited the maximum cell current to ~4 mA.

The anode potential at very low resistive loadings depends on the NAD^+/NADH ratio (see *Figure 2*). The anode potential with the fictive reaction

$$NADH + MB^+ \rightleftharpoons MBH + NAD^+ \qquad (6)$$

should be equal to the $E^{0'}$ at pH 7 of the NAD^+/NADH couple, i.e. −560 mV at NAD^+/NADH = 1. Comparison with the experimental value (−255 mV) shows that the potential at a net current close to zero (305 mV) is less than that. The actual loss with load is still larger.

The anode potential versus the cell current is shown in *Figure 3* for two different runs. The external load resistor was only 5 ohms at the highest current shown, indicating current limitation by internal resistances in the cell. The power output (*Figure 4*) was calculated from the current times the cell potential (i.e. 560 mV is added to the potentials shown in *Figure 3*). The usual maximum was not reached because of the high internal resistance.

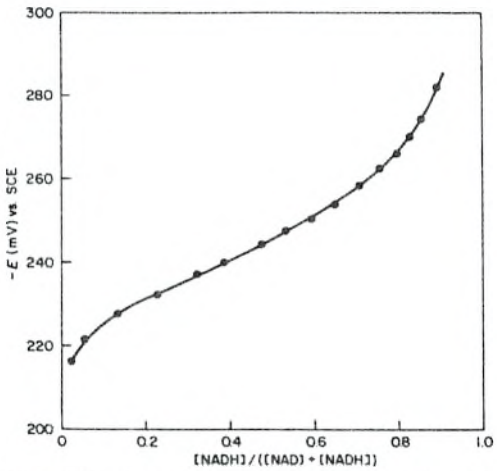

Figure 2 Variation of anode potential with the fraction of reduced coenzyme. Total coenzyme concentration 0.84 mmol l^{-1}, surface coverage 1.4 nmol cm^{-2}, external load 10 MΩ

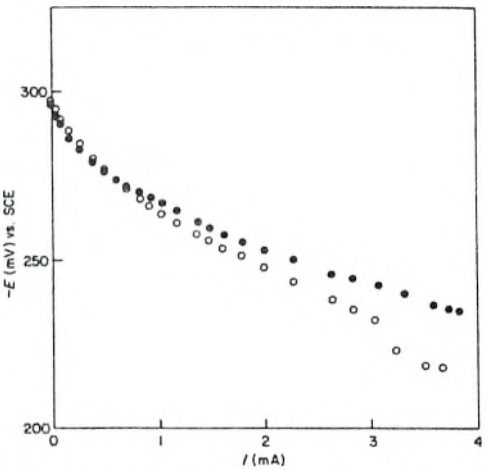

Figure 3 Anode potential versus current output of the cell. ●, Coverage 1.8 nmol cm^{-2}, coenzyme concentration 0.83 mmol l^{-1}; ○, coverage 1.7 nmol cm^{-2}, coenzyme concentration 0.74 mmol l^{-1}

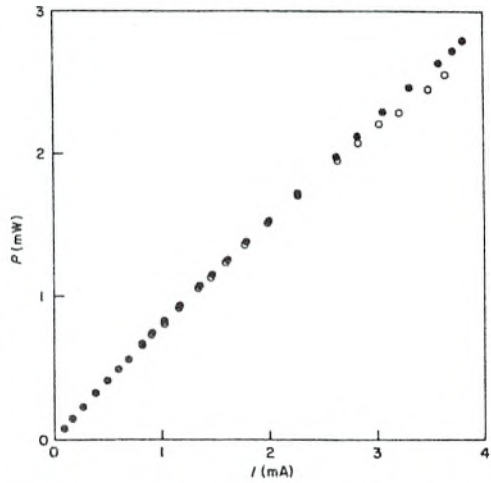

Figure 4 Power output for various loading currents. Conditions as for *Figure 3*

Figure 5 shows a recording of the currents versus time for a constant load resistor. The coverage on the anode decreased from 1.2 to 0.4 nmol cm^{-2} during the experiment (a monolayer of Meldola Blue is thought to be present at ~ 1 nmol cm^{-2}).[13] The decrease in coverage had little effect, but if the experiment had been continued the reaction rate and thus the current would certainly have been diminished. The anode potential increased from −120 mV at the start to −40 mV at the end of the experimental period, and altogether 0.5 out of a total of 2.8 mmol D-glucose in the cell was consumed.

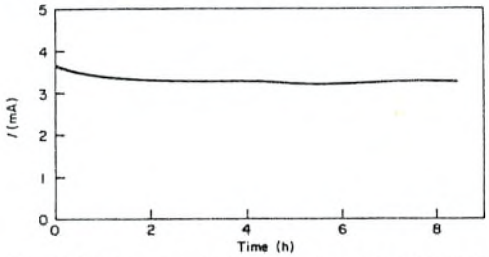

Figure 5 Current output of fuel cell with an external load of 10 ohms. Initial surface coverage was 1.2 nmol cm^{-2} and initial concentrations of coenzyme and D-glucose were 0.75 and 79 mmol l^{-1}, respectively

Discussion

The result presented above shows that a regenerative biofuel cell can be made with a NADH-dependent redox enzyme and a modified electrode. The fuel cell supplied electricity derived from the oxidation of D-glucose over several hours. The cell uses an immobilized enzyme which is stable for months, but the mediator has to be renewed after a number of hours.

Although the mediator is the least stable component of the described fuel cell, it is more satisfactory than most other mediators which have been studied. The stability increases as the pH decreases but at the expense of an increased rate of decomposition of NADH. Further studies are necessary to find still more favourable conditions. The convenience of electrode modification and the low $E^{0'}$ of the mediator as well as the relatively fast rate of reaction of the mediator with NADH are distinct advantages. The total amount of mediator is so small that it corresponds to mediator concentrations in the submicromolar range, had it been desorbed into the solution. It is therefore unlikely that soluble mediator plays any important role in the fuel cell reaction.

The internal resistance was found to be the main limiting factor and a different cell design is, therefore, called for. The anode current density of the present cell could not be increased above 0.2 mA cm^{-2} because the anode area was larger than the area of the separators. Future designs should therefore incorporate either a low-resistance membrane or a cathode which is compatible with the anolyte composition.

Acknowledgements

This work was supported by grants from the Swedish Natural Science Research Council.

References

1 Lewis, K. *Bacteriol. Rev.* 1966, **30**, 101–113
2 Wingard, L. B., Jr., Shaw, C. H. and Castner, J. F. *Enzyme Microb. Technol.* 1982, **4**, 137–142
3 Bennetto, H. P., Stirling, J. L., Tanaka, K. and Vega, C. A. *Biotechnol. Bioeng.* 1983, **25**, 559–568
4 Ardeleanu, I., Marguineanu, D.-G. and Vais, H. *Bioelectrochem. Bioenergy* 1983, **11**, 273–277
5 Roller, S. D., Bennetto, H. P., Delaney, G. M., Mason, J. R., Stirling, J. L. and Thurston, C. F. *J. Chem. Technol. Biotechnol.* 1984, **34B**, 3–12
6 Delaney, G. M., Bennetto, H. P., Mason, J. R., Roller, S. D., Stirling, J. L. and Thurston, C. F. *J. Chem. Technol. Biotechnol.* 1984, **34B**, 13–27
7 Yahiro, A. T., Lee, S. M. and Kimble, D.O. *Biochim. Biophys. Acta* 1964, **88**, 375–383
8 Kulys, J. J. and Malinauskas, A. A. *J. Anal. Chem. USSR* 1979, **34**(4), 603–606
9 Davis, G. and Hill, H. A. O. *Enzyme Microb. Technol.* 1983, **5**, 383–388
10 Laane, C., Pronk, W., Franssen, M. and Veeger, C. *Enzyme Microb. Technol.* 1984, **6**, 165–168
11 Moiroux, J. and Elving, J. P. *Anal. Chem.* 1979, **51**, 346–350
12 Torstensson, A. and Gorton, L. *J. Electroanal. Chem.* 1981, **130**, 199–207
13 Gorton, L., Torstensson, A. Jaegfeldt, H. and Johansson, G. *J. Electroanal. Chem.* 1984, **161**, 103–120
14 Murray, R. W. in *Electroanalytical Chemistry* (Bard, A. J., ed), Marcel Dekker, New York, 1983, vol. 13, pp. 191–368
15 Guadalupe, A. R. and Abruna, H. D. *Anal. Chem.* 1985, **57**, 142–149
16 Appelqvist, R., Marko-Varga, G., Gorton, L., Torstensson, A. and Johansson, G. *Anal. Chim. Acta* 1985, **169**, 237–248
17 Johansson, G. and Ogren, L. *Anal. Chim. Acta* 1976, **84**, 23–29

VII

Sveta Priyomova

Bioelectrochemistry and Bioenergetics, 16 (1986) 479–483
A section of *J. Electroanal. Chem.*, and constituting Vol. 212 (1986)
Elsevier Sequoia S.A., Lausanne – Printed in The Netherlands

949 — BIOFUEL ANODE FOR CELL REACTIONS INVOLVING NICOTINAMIDE ADENINE DINUCLEOTIDE AS A CHARGE CARRIER *

BJÖRN PERSSON, LO GORTON and GILLIS JOHANSSON

Department of Analytical Chemistry, University of Lund, P.O. Box 124, S-221 00 Lund (Sweden)

(Manuscript received March 22nd 1986)

SUMMARY

Biofuel cell anodes with porous graphitic materials were modified by adsorption of a mediator (*N*,*N*-dimethyl-7-amino-1,2-benzophenoxazine, Meldola Blue) for oxidation of the dihydronicotinamide adenine dinucleotide. Electrodes made from reticulated vitreous carbon were already heavily polarized at current densities less than 1 mA cm^{-2}, mainly because of the low surface coverage with mediator. Graphite felt electrodes adsorbed the mediator so well that current densities up to about 10 mA cm^{-2} could be supported. The cell resistances rather than the catalytic activity were then limiting the current.

INTRODUCTION

It was shown recently [1] that the catalytic oxidation of NADH at modified electrodes could be utilized in the anode reaction of a biofuel cell deriving energy from the oxidation of glucose. The general anode scheme can be written

$$\text{Substrate} + NAD^+ + H_2O \xrightarrow[\text{genase}]{\text{dehydro-}} \text{Product} + NADH + H^+ \quad (1)$$

$$NADH + MB^+ \rightarrow NAD^+ + MBH \quad (2)$$

$$MBH \rightarrow MB^+ + H^+ + 2\,e^- \quad (3)$$

The enzyme, which for glucose is glucose dehydrogenase, can be immobilized on a porous support outside the cell. The redox energy will then be transferred to the anode via the soluble carrier NADH which is recycled through equation (2). The mediator, which so far has been Meldola Blue, MB^+, forms a charge-transfer complex with NADH which decomposes to NAD^+ and the reduced form in a rate-limiting step [2,3]. The mediator is adsorbed on a graphitic material and it can

* Contribution presented at the VIIIth International Symposium on Bioelectrochemistry and Bioenergetics, Bologna, June 24th–29th 1985.

0302-4598/86/$03.50

therefore be reoxidized very efficiently in a fast electrochemical step, equation (3). The overall reaction of such a half-cell will then be

$$\beta\text{-D-glucose} + H_2O \rightarrow \text{D-gluconate} + H^+ + \text{energy} \quad (4)$$

The efficiency of a biofuel cell depends on the control of the same type of factors as for conventional fuel cells, namely the efficiency of the catalytic reaction, the size and form of the electrodes, the mass transfer, and the cell resistance. The special aspect to be considered for a biofuel cell is the electron transfer between an enzymatically catalyzed reaction and the anode material. The previous work [1] reported that up to 0.2 mA cm^{-2} could be obtained by mediated electron transfer from the soluble energy carrier NADH. The catalyst was adsorbed on a solid graphite which was known to bind the mediator well. Further progress is possible either by modifying the mediators so that they will bind to a wider range of materials or by finding graphites that will bind the existing mediator. Both approaches have been pursued in parallel and this work reports on the use of two porous materials, one of which performs very well.

EXPERIMENTAL

A two-compartment Perspex cell with a cation-exchange membrane separator (BDH No. 55165-2 U) was used throughout (Fig. 1). The membrane area and the resistance were 0.78 cm^2 and 5 ohm respectively. The cathode compartment contained a simulated oxygen electrode [1] with a current-independent voltage of +560 mV *versus* s.c.e. The anode was made of Graphite Felt (Sigri Elektrographit GmbH, D-8901 Meitingen, type GFA-5). The material was cut into circular disks, diam. 10 mm, which were compacted into the anode compartment so that an electrical contact with a platinum wire was obtained. A porous electrode was thus obtained, the length of which was 15 mm. Two reference electrodes with Luggin capillaries were used for potential measurements in the anode compartment (Fig. 1). The distance between the front of the anode and the membrane was 10 mm.

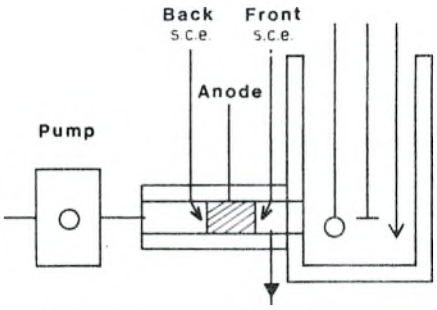

Fig. 1. Cell arrangement consisting of a porous anode, an ion exchange membrane separator and a simulated oxygen cathode in a separate compartment. The anolyte was pumped with a flow rate of 8 cm^3 min^{-1}.

The anolyte consisted of 0.25 *M* deoxygenated phosphate buffer, pH 7.0, which contained 0.67 m*M* dihydronicotinamide adenine dinucleotide (NADH) (Sigma cat. No. N8129). The anolyte was pumped through the porous electrode at a flow rate of 8.0 cm^3 min^{-1} and was collected from an outlet near the membrane for a spectrophotometric assay of NADH. A normal biofuel cell operation involves regeneration of the NADH in a reactor containing an immobilized enzyme and recirculation of the anolyte, as reported before [1], but an open-loop experiment was selected for this study because of its more straightforward answers.

Some experiments were also done with an anode material consisting of a 20 mm long piece of Reticulated Vitreous Carbon, RVC (Energy Res. and Gener., Inc., Oakland, CA, type RVC 2–1-100-S).

The anode was modified by flushing a 1 m*M* solution of N,N-dimethyl-7-amino-1,2-benzophenoxazinium ions, Meldola Blue (Boehringer Mannheim GmbH) through the cell for a couple of minutes, followed by a rinsing with buffer.

RESULTS AND DISCUSSION

The properties of the biofuel anode were evaluated by loading the complete electrochemical cell with external resistors between 100 kΩ and 5 Ω, see Fig. 2. The voltages at the front end of the anode decreased to a fairly constant level before the maximum current, 7.4 mA, was reached with an external resistance of 5 Ω. The voltage at the back of the anode drops very little as the current increases, however.

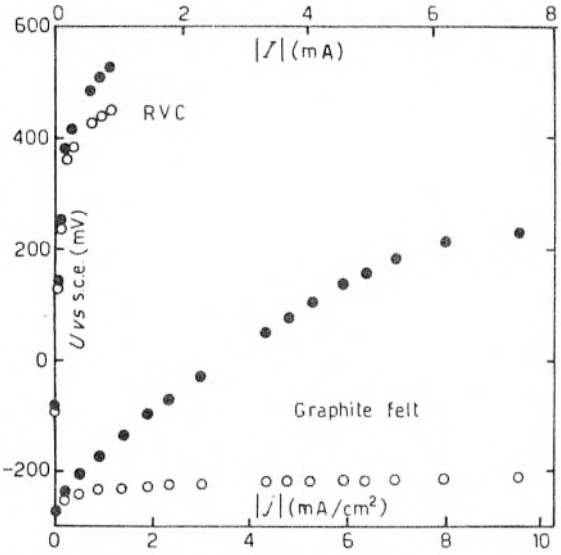

Fig. 2. Loading characteristics *U versus* |*I*| (mA) and *versus* |*j*| (mA cm^{-2}) of the anode halfcell as measured at the front (●) and the back (○) of the anode.

This indicates that the anode is highly polarized at the front end, while the polarization and the current density are low at the back of the anode.

The resistance within the graphite felt was estimated to be at most 10 Ω between any point and the platinum wire. The solid graphite material should therefore have approximately the same potential everywhere. The solution|electrode potential will therefore change by more than 400 mV over the length of the anode; as mentioned above, this is due to the large electrode polarization at the front end, where most of the NADH is oxidized.

The anode potential levels out at +250 mV, rather than at +560 mV, when the external circuit approaches a short circuit. The reason is of course internal resistances in the cell. The voltage drop over the solution resistance from the front end of the anode to the simulated oxygen cathode should therefore be more than 300 mV.

The NADH concentration in the solution flowing through the anode drops by 43% at the highest current. The effect of concentration polarization should therefore be small compared with the effect of the voltage drop in the electrolyte in the pores. This was also verified by increasing the flow rate by 50%; the front-end electrode potential decreased only by a few mV at a cell current of 6.2 mA. The part of the anode farthest away from the cathode is hardly utilized at all. The conclusion is that the current output from the cell is limited to about the same degree by the voltage drop in the electrolyte between the electrodes and by the polarization of the anode. The latter is in turn caused to a large degree by the voltage drop in the pores.

Figure 2 also demonstrates some experiments with the RVC anode material. It can be seen that the cell voltage drops very rapidly and that both ends of the anode are affected to about the same degree. The solution resistances, both between the anode and the cathode, and within the pores, play an insignificant role compared to the polarization of the electrode material.

The surface coverage of the RVC was estimated as 0.1 nmole as compared to 2 nmole for the graphite felt anode. The estimates are very uncertain, particularly for the RVC where quinone groups give significant currents even in the absence of mediator. The low surface coverage results in fewer catalytic sites and the cell voltage will therefore drop at low currents. Other explanations, *e.g.* influences from the RVC material itself, cannot be ruled out, however. Various surface treatments of the RVC, *e.g.* anodic oxidation or plasma etching did not improve the electrode performance significantly.

Previous work [1] has shown that a reactor with immobilized glucose dehydrogenase with a volume of 600 mm^3 was able to keep the nicotinamide coenzyme almost completely in the reduced form at a cell current of 4 mA and with a glucose concentration of at least 50 m*M*. The same reactor would certainly be able to regenerate NADH at the maximum current used in this work, namely 7.4 mA, and thus to couple the reaction to the glucose oxidation as an energy source. No demonstration of this was included because it is obvious that resistances rather than the rate of the enzymatic reaction are the limiting factors.

The present cell provides two main advantages over that described previously,

namely a low-resistance separator, and a high-area anode. The high area of the porous graphite makes it unnecessary to rotate the electrode in order to speed up the mass transfer and a simpler and more convenient cell is thus obtained. The gross geometrical area viewing the cathode is 0.78 cm^2 as compared with 16 cm^2 in the cell described previously. The maximum current is nevertheless about twice as large, which implies that the gross current density was increased almost 50 times. These results indicate that the electrolyte resistances in the solution and within the porous electrode are the limiting factors. The mediated electron transfer from NADH to the graphite, which is the new element, should be able to provide even higher current densities, provided that the resistances are lowered by an appropriate cell design.

ACKNOWLEDGEMENT

This work was supported by grants from the Swedish Natural Research Council.

REFERENCES

1 B. Persson, L. Gorton, G. Johansson and A. Torstensson, Enzyme Microbiol. Technol., 7 (1985) 549.
2 L. Gorton, A. Torstensson, H. Jaegfeldt and G. Johansson, J. Electroanal. Chem., 161 (1984) 103.
3 L. Gorton, J. Chem. Soc., Faraday Trans. 1, 82 (1986) 1245.

Lunds Universitet
Reprocentralen 1990